博士論文

Non-radial Oscillations of Magnetized Neutron Stars
(磁場を持つ中性子星の非動径振動)

浅 井　秀 貴

平成 27 年

ABSTRACT

We investigate the properties of non-axisymmetric oscillations of uniformly rotating and magnetized stars with purely toroidal magnetic field and of non-rotating magnetized stars with purely poloidal magnetic field, where we use polytropes as background models for the modal analyses. For the oscillations of rotating stars magnetized with purely toroidal magnetic field, we consider the effects of stellar deformation due to the magnetic field. Since separation of variables is not possible for magnetized or rotating stars, we employ series expansions of a finite length for the perturbations in terms of spherical harmonic functions. Solving the oscillation equations as a boundary and eigenvalues problem, we obtain magnetically modified normal modes such as g-, f-, p-, r-, and inertial modes for magnetized stars having purely toroidal fields. In the lowest order, the deviation of the frequencies from those of non-magnetized stars is proportional to the square of the characteristic Alfvén frequency. We also find the high-frequency modes such as f- and p-modes are strongly affected by the stellar deformation, although the low-frequency modes such as g-, r-, and inertial modes are hardly affected by the deformation. For the stars magnetized with purely poloidal fields, we find two kinds of discrete magnetic modes, that is, stable (oscillatory) magnetic modes and unstable (monotonically growing) magnetic modes. For isentropic stellar models, the frequency and growth rate of the magnetic modes are exactly proportional to the strength of magnetic field $B_{\rm S}$ measured at the stellar surface. The frequency and growth rate are affected by buoyant force in the interior of the star, and unstable magnetic modes are stabilized by stable stratification.

CONTENTS

1 Introduction

Neutron stars are classified as a compact object, the central density of which exceeds nuclear density ($\rho_n \sim 2.8 \times 10^{14}$ g cm^{-3}). They are born as a results of type II (gravitational collapse-type) supernova explosion of massive ($\sim 8M_\odot - 15M_\odot$) stars. The typical radius R and mass M of neutron stars are $R \sim 10$ km and $M \sim 1.4M_\odot$, and they are thought to have strong magnetic fields exceeding about 10^{12} G at the surface.

The interior of neutron stars is divided into a thin atmosphere, a solid crust (the outer crust and inner crust), and a fluid core (the outer core and inner core). The thin atmosphere of a neutron star is made of a hot plasma, and thermal radiations are thought to come through or from this region (see e.g., Zalvin & Pavlov 2002). Below the thin atmosphere extends the outer crust down to the neutron drip density $\rho = \rho_{\rm ND} \approx 4 \times 10^{11}$ g cm^{-3}, at which neutrons drip out from atomic nuclei to form a neutron fluid outside the nuclei. Typical thickness of the outer crust is estimated several hundred meters. The outer crust is composed of degenerate electrons e^- and positively charged ions, which may be characterized by the atomic number Z and mass number A. In the crust region, ions are crystalized by phase transition to form a Coulomb lattice. The inner crust extends in the density region $\rho_{\rm ND} \lesssim \rho \lesssim \rho_n/2$, and its thickness is about 1 km. In this region, matters are thought to be composed of free electrons, free neutrons, and neutron rich-atomic nuclei. We note that inverse β-decay dominates β-decay in such a quite high density region, and the number of neutrons in atomic nuclei increases because of neutronization due to inverse β-decay. At the bottom of the inner crust, atomic nuclei are dissolved because of extremely high density and a lattice structure is destroyed, which causes the transition from the crustal layer to a fluid core. The outer core extends in the density range $\rho_n/2 \lesssim \rho \lesssim 2\rho_n$, and is composed of neutrons, protons, electrons, and muons (named $npe\mu$ composition), and the number of neutrons dominates that of other particles. All the fermions are strongly degenerate. In the inner core in which $\rho \gtrsim 2\rho_n$, the composition of the matter in this region is not well understood. In the inner crust and the fluid outer core, neutrons and protons are thought to become superfluid and superconductor.

Rotating magnetized neutron stars can be a pulsar. Pulsars are classified, by energy sources responsible for producing observed pulses, into rotation powered, accretion powered, and magnetically powered pulsars. Radio pulsars belong to rotation powered pulsar and they are usually called simply 'Pulsar'. Most of observed pulsars are rotation powered radio pulsars, the number of which amounts to about 1700 as of 2006. Since radio pulsars emits electromagnetic radiation by transforming a fraction of rotational energy of the neutron star to electromagnetic energy, the rotation velocity of radio pulsars becomes slower with time. This is the reason why radio pulsars are classified as 'rotation powered pulsar'. We note that typical spin periods of radio pulsars are several ten milliseconds, but there are pulsars rotating at much shorter periods $P \leq$ (10 milliseconds), which are called millisecond pulsars.

Rotating and magnetized neutron stars in binary systems appear as accretion powered pulsars, and they emit X-ray radiation and X-ray pulses. The energy source of the X-ray emission is gravitational energy released during mass accretion to the neutron star from the companion star. Such neutron stars are called X-ray pulsars. Although binary X-ray sources have two categories called High Mass X-ray Binaries (HMXBs) and Low Mass X-ray Binaries (LMXBs),

X-ray pulsars belong to the former. For HMXBs, the companion stars are mostly massive ($M_2 \geq 10M_\odot$) O-B stars, while for LMXBs they are mostly dwarf stars ($M_2 \leq M_\odot$), where M_2 means the mass of the companion star. There are ∼100 LMXBs and ∼40 HMXBs discovered as of 2006.

Magnetically powered pulsars are thought to have extremely strong magnetic fields ($B \gtrsim 10^{14} - 10^{15}$ G), and to emit X-ray and/or gamma-ray emissions consuming a part of the huge magnetic energy as an energy source. These strongly magnetized neutron stars are called magnetars. Magnetars consist of two subgroups of neutron star objects: Anomalous X-ray Pulsars (AXPs) and Soft Gamma-ray Repeaters (SGRs). SGRs are characterized by the fact that they emit short recurrent X/γ-ray bursts in timescales of one second or less. Some SGRs have experienced quite rare events called giant X/γ-ray flares. The energy scale released by the giant flares is much larger than that of short bursts (flares). The SGR's rotation periods are found in the range of 2-11 seconds, which are much longer than those of radio pulsars (∼ several ten milliseconds). Observed luminosities of soft X ray-flares of magnetars are $L_{\rm X} \sim 10^{35}$ erg s^{-1}, which exceeds the energy generated by spin down of the magnetars. Thus, it is difficult to explain the magnetar's γ-ray radiations in terms of the emission mechanism assumed for normal radio pulsars. Further, there are no evidences that SGRs are in binary systems. From magnetar spin down rates, their magnetic field strength have been estimated about $10^{14} - 10^{15}$ G. These are background for us to think that magnetars are neutron stars having extremely strong magnetic fields and emit γ-ray bursts expending a part of the vast magnetic energy (Magnetar hypothesis; e.g., Duncan & Thompson 1992). According to early theoretical works, Duncan & Thonmpson (1992) suggested that if a neutron star born from a type II supernova explosion has sufficiently rapid rotation speeds at the birth, it is possible to generate very strong magnetic fields exceeding 10^{15} G by transforming a part of the kinetic (rotational) energy of the star into a magnetic energy. Further, since magnetic field lines thread the solid crust region near the stellar surface, there is a possibility that star-quakes taking place in the solid crust induce short X/γ-ray bursts, and giant flares might be caused by a large scale restructuring of the magnetic fields.

AXPs are neutron stars thought to possess extremely strong magnetic fields as SGRs do, and they emit X-ray radiation and pulses. Their spin periods and luminosities are estimated $P \sim 6$ s-12 s and $L_{\rm X} \sim 10^{33} - 10^{35}$ erg s^{-1}, respectively. The emission mechanism of AXPs is different from that of X-ray pulsars, because there are no evidences that AXPs are in binary systems. AXPs sometimes show sudden brightening, which gradually dims out within a few months. This is the reason why they are called 'Anomalous'.

Only four SGRs are known as of today and some of them are in our galaxy and the Large Magellanic Cloud. As described above, some SGRs are known to have experienced burst events called giant flare. Giant flares are so rare that there have so far been only three known giant flares: March 5, 1979 by SGR 0526-66, August 27, 1998 by SGR 1900+14, and December 27, 2004 by SGR 1806-20. We note that the giant flare detected in December 27, 2004 has the largest energy scale among the three. Obtaining observation data of the SGR giant flares, some researchers analyzed the light curves of the giant flares in detail. As a result, they found Quasi Periodic oscillations (QPOs) in the tail of the X-ray light curves of the giant flares. Israel et al. (2005) first identified QPO frequencies found in the X-ray light curves of the giant flare of SGR 1806-20 at 18, 30, and 92.5 Hz. Strohmayer & Watts (2006) identified additional QPO

frequencies at 150, 625, and 1840 Hz. Analyzing archival data of SGR 1900+14, Strohmayer & Watts (2005) have succeeded in identifying QPOs in the X-ray giant flare observed in 1998. QPOs frequencies now identified in the giant flares from two SGRs are 18, 30, 92.5, 150, 625, and 1840 Hz for SGR 1806-20 (Israel et al. 2005; Strohmayer & Watts 2006; Watts & Strohmayer 2006), and 28, 53.5, 84, and 155 Hz for SGR 1900+14 (Strohmayer & Watts 2005). Using Baysian statistics, Hambaryan et al. (2011) have reanalyzed the data for SGR 1806-20 to identify QPO frequencies at 16.9, 21.4, 36.8, 59.0, 61.3, and 116.3 Hz. For the giant flare in 1979 from SGR 0526-66, Watts (2011) mentioned in her review paper a report of a QPO at $\sim$43 Hz, but she also suggested the difficulty in the frequency analysis in the impulsive phase of the burst. We note that it is worth mentioning a promising recent attempt to find QPOs in short recurrent bursts in SGRs. Huppenkothen et al. (2014) have succeeded in identifying candidate signals at 93, 127, and 260 Hz from J1550-5418, where they used Baysian statistics for the analysis.

Since the discovery of magnetar QPOs, many researchers have suggested that the QPOs might be associated with global oscillations of neutron stars. Using oscillation modes of the magnetars it is expected that we can get information concerning the inner structure of the stars employing the method of aster-seismology. It is interesting to investigate the magnetar QPOs by analyzing the oscillation modes, not only for astronomy, but also for physics. For example, birefringence of light in vacuum by strong magnetic fields: light velocity varies depending on polarization in the same way as calcite for $B > B_{\rm cr}$, where $B_{\rm cr} = m_e^2 c^3/e \sim 4.4 \times 10^{13}$ G is the critical magnetic field, and m_e denotes the electron mass, c is the light velocity, and e denotes the elementary charge of electron. Other examples are division of photons caused by interaction with strong magnetic fields, and dependence of scattering cross-section of photons and electrons on magnetic fields. It is mostly impossible to inspect these physical events in the laboratory on earth, but understanding magnetar structures, it might be possible to inspect those phenomena.

A variety of oscillation modes are possible for neutron stars (see e.g., McDermott et al. 1988). For example, we may expect g-, f-, and p-modes, whose restoring forces are buoyant force and pressure force, respectively. p-modes are high frequency modes and their frequency increases as the number of radial nodes of the eigenfunction increases, while g-modes are low frequency modes and their frequency decreases as the number of radial nodes of eigenfunction increases. We usually find node less f-modes between the g- and p-modes. Since neutron stars have a solid crust, we may expect additional two kinds of shear modes: spheroidal shear s-modes and toroidal shear t-modes. These modes are supported by shear stress of the solid crust. If neutron stars are rotating, rotational modes such as inertial mode and r-mode are also possible, where the restoring force for the rotational modes is the Coriolis force. For strongly magnetized neutron stars, we may expect that magnetic modes such as Alfvén modes can play a role in the stars.

Duncan (1998) is the first who proposed the possibility of investigating magnetars using oscillation modes as a probe. He suggested that star-quakes frequently arising in SGRs are able to excite crustal toroidal modes and that in some burst emissions frequencies of the toroidal modes might be observationally identified. Therefore, the discovery of the QPOs in the X-ray light curve of SGR 1806-20 is a trigger for us to investigate magnetar QPOs theoretically. In the early studies of magnetar QPOs, most authors assumed crustal modes confined to the solid crust region as Duncan (1998) first assumed. Israel et al. (2005) suggested that the QPOs might be induced by seismic crustal vibrations, associated with low order-l (harmonic degree) torsional

modes because theoretical estimations of the crustal mode frequencies overlap with the observed QPOs (e.g., Strohmayer & Watts 2005, 2006; Watts & Strohmayer 2006). For example, Piro (2005) and Lee (2007) calculated toroidal modes modified by the magnetic field, although they ignored the effects of the fluid core on the modal properties. For $B \gtrsim 10^{15}$ G, since the magnetic pressure dominates shear modulus in most of the solid crust region, crustal toroidal modes are not necessarily decoupled from oscillation modes in the fluid core, if the fluid core and solid crust are magnetically connected with each other by magnetic fields. Since it is conceivable that extremely strong magnetic fields of magnetars thread both the fluid and solid crust regions, in order to determine the oscillation spectra of magnetars, we have to consider both of the regions as cavities for oscillation modes. Employing a toy model, Glampedakis, Samuelsson, & Andersson (2006) calculated global discrete modes propagating in both the fluid core and solid crust connected by magnetic field lines, and they found that global oscillation modes are easy to be excited such that both the fluid core and the solid crust oscillate in concert. Levin (2006, 2007) also calculated global modes using another toy model. He suggested that Alfvén modes in the fluid core form continuous frequency spectra and the crustal toroidal modes are quickly damped by resonant absorption in the core, and hence that there exist no discrete modes in strongly magnetized stars. However, taking account of couplings between the fluid core and the solid crust by purely poloidal magnetic fields, Lee (2008) and Asai & Lee (2014) carried out normal mode calculations for axisymmetric toroidal modes and found that there exists discrete toroidal modes. van Hoven & Levin (2011, 2012) adopted spectral method to calculate the global oscillation modes, and they found that discrete modes can be excited when the oscillation frequencies are in the gaps between continuous frequency bands. Sotani et al. (2007) calculate normal modes for general relativistic magnetized neutron stars assuming a weak magnetic field limit.

It is not easy for us to calculate and analyze the oscillation modes of magnetized stars, the governing equations of which are in principle given by partial differential equations. The reasons for the difficulty may be that separation of variables between radial coordinate and angular coordinates is not possible to express the perturbations, and that the fact that there possibly exist continuous frequency bands in the frequency spectra makes modal analysis much more difficult (see e.g., Goedbloed & Poedts 2004). In normal mode analyses, as discussed in this paper, it is customary to employ series expansions of finite lengths to represent the perturbations and to reduce the partial differential equations to a finite set of coupled ordinary linear differential equations for the expansion coefficients. However, this manipulation could be very complicated when one tries to formulate the oscillation equations and to numerically analyze the oscillation spectra for various magnetic field configurations. Such difficulty has been a reason why most of the authors employ MHD simulations to investigate the oscillations of magnetized neutron stars (e.g., Sotani, Kokkotas & Stergioulas 2008a; Cerdá-Durán et al. 2009; Colaiuda & Kokkotas 2011, 2012; Gabler et al. 2011, 2012, 2013a,b; Lander et al. 2010; Passamonti & Lander 2013, 2014).

As a matter of fact, we do not have any good knowledge about magnetic configurations in strognly magnetized neutron stars (e.g., Thompson & Duncan 1993, 1996; Thompson, Lyuitikov & Kulkarni 2002). As shown by core-collapse supernova MHD simulations (e.g., Kotake, Sato & Takahashi 2006), if the fluid core is rotating differentially, toroidal magnetic fields can be easily amplified by the winding up of the initial seed poloidal fields even if there are no initial

toroidal magnetic fields. Thus, it is desirable to carry out modal analyses for various magnetic field configurations. Most frequently employed configurations for modal analyses are so far those given by purely poloidal magnetic fields (e.g., Lee 2007, 2008; Sotani et al. 2007, 2008a; Cerdá-Durán et al. 2009; Colaiuda & Kokkotas 2011; Gabler et al. 2011, 2012; Passamonti & Lander 2013, 2014; Asai & Lee 2014). Only a few studies of normal modes of magnetized stars have been devoted to purely toroidal magnetic fields (e.g., Lander et al. 2010; Passamonti & Lander 2013) and to mixed-poloidal and toroidal magnetic fields (e.g., Colaiuda & Kokkotas 2012; Gabler et al. 2013a).

Most of the numerical studies of the oscillations of magnetized stars have been devoted to axisymmetric ($m = 0$) oscillation (especially, toroidal) modes for the case of purely poloidal magnetic field configurations, where m denotes the azimuthal index of the perturbations (e.g., Glampedakis, Samuelsson & Andersson 2006; Levin 2006, 2007; Lee 2008; Asai & Lee 2014; van Hoven & Levin 2011, 2012; Cerdá-Durán et al. 2009; Coldaiuda & Kokkotas 2011; Gabler et al. 2011, 2012; Sotani et al. 2007, 2008a). For example, Sotani et al. (2009) calculated axisymmetric ($m = 0$) polar-Alfvén oscillations (spheroidal mode) and suggested that continuous frequency spectra are not formed. Further, Colaiuda & Kokkotas (2012) employed a mixed-poloidal and toroidal magnetic field configuration to calculate axisymmetric oscillation modes to find that there exists only discrete oscillation modes and that the oscillation spectra are greatly affected by the toroidal component of the magnetic field. Gabler et al. (2013a) calculated axisymmetric oscillation modes for various magnetic field configurations (e.g., purely poloidal, purely toroidal, and mixed-poloidal and toroidal).

There are only a few studies on non-axisymmetric ($m \neq 0$) oscillation modes of magnetized stars. Using MHD simulations, Lander et al. (2010) and Passamonti & Lander (2013) investigated non-axisymmetric ($m \neq 0$) oscillation modes for magnetized stars assuming purely *toroidal* magnetic fields, while Lander & Jones (2011b) assumed purely *poloidal* magnetic fields.

In this paper, we calculate non-axisymmetric ($m \neq 0$) oscillations by employing normal mode analysis for magnetized stars both for purely toroidal magnetic field configurations and for purely poloidal magnetic field configurations. For normal mode analyses for purely toroidal magnetic field configurations (§3), we calculate magnetically modified non-radial oscillation modes such as p-, f-, g-modes. Assuming slow rotation, we also investigate inertial modes taking account of equilibrium deformation due to the magnetic fields. For purely poloidal field (§4), we analyze magnetic modes only, where we neglect the effects of both the equilibrium deformation and rotation on the modes because of their very low frequencies. For both cases, we employ polytropes as back ground neutron star models and ignore the solid crust region, that is, crustal modes.

2 Non-radial oscillations of neutron stars

We assume small amplitude oscillations to carry out normal mode analyses of neutron stars. Normal mode analyses of neutron stars can be very complicated since we have to take account of the effects of a solid crust, strong magnetic fields, rotation, and superfluidity (superconductivity). In addition, since neutron stars are general relativistic objects, we sometime need to treat the oscillations in general relativistic framework. Before we go into the results discussed in this paper, it is helpful to describe general aspects of non-radial oscillation of stars.

The oscillation modes of normal fluid stars are in general classified into p-, f-, and g-modes. p-modes are high-frequency modes and g-modes are low-frequency modes. The restoring force for the p-modes is compressibility, and the oscillation frequency increases as the number of radial nodes of the eigenfunction increases. For g-modes, on the other hand, the restoring force is buoyancy and the frequency decreases as the number of radial nodes increases. For rotating stars, there exists rotational modes such as inertial modes and r-modes, which form a subclass of inertial modes. The restoring force for rotational modes is the Coriolis force. For stars having a solid crust, there exists sound wave modes propagating in the solid region. For strongly magnetized stars, there exists Alfvén modes whose frequency is proportional to the strength of magnetic field.

2.1 normal modes of non-rotating and non-magnetic normal stars

As an example of normal mode analysis of stars, we first derive the oscillation equations of non-rotating and non-magnetic normal fluid stars in Newtonian gravity. Here, we assume adiabatic oscillations and ignore the effects of viscosity of the fluid. We treat small amplitude oscillations using linear perturbation theory. The basic equations of fluid dynamics are given by

$$\frac{\partial \rho}{\partial t} + \nabla \cdot (\rho \boldsymbol{v}) = 0, \tag{2.1}$$

$$\frac{\mathrm{d}\boldsymbol{v}}{\mathrm{d}t} = -\frac{1}{\rho}\nabla p - \nabla \Phi, \tag{2.2}$$

$$\nabla^2 \Phi = 4\pi G \rho, \tag{2.3}$$

$$\rho T \frac{\mathrm{d}s}{\mathrm{d}t} = \rho \epsilon - \nabla \cdot \boldsymbol{F}, \tag{2.4}$$

$$\boldsymbol{F}_{\mathrm{rad}} = -\lambda_{\mathrm{rad}} \nabla T, \tag{2.5}$$

where Φ is the gravitational potential, s is the specific entropy, ϵ is the energy generation rate, $\boldsymbol{F}$ is the energy flux, and $\boldsymbol{F}_{\mathrm{rad}}$ is the radiative energy flux. In general, we can write $\boldsymbol{F} = \boldsymbol{F}_{\mathrm{rad}} + \boldsymbol{F}_{\mathrm{conv}}$ ($\boldsymbol{F}_{\mathrm{conv}}$ is the convective energy flux), and

$$\frac{\mathrm{d}}{\mathrm{d}t} = \frac{\partial}{\partial t} + \boldsymbol{v} \cdot \nabla. \tag{2.6}$$

Assuming adiabatic oscillations and the Cowling approximation (ignoring perturbed gravitational potential $\delta\Phi$), we linearize the basic equations:

$$\frac{\partial \delta\rho}{\partial t} + \nabla \cdot (\delta\rho \boldsymbol{v} + \rho \delta \boldsymbol{v}) = 0, \tag{2.7}$$

$$\delta\rho \frac{\mathrm{d}\boldsymbol{v}}{\mathrm{d}t} + \rho \left(\frac{\partial \delta \boldsymbol{v}}{\partial t} + \delta \boldsymbol{v} \cdot \nabla \boldsymbol{v} + \boldsymbol{v} \cdot \nabla \delta \boldsymbol{v} \right) = -\nabla \delta p - \delta\rho \nabla \Phi, \tag{2.8}$$

$$\rho T \frac{\partial \delta s}{\partial t} + \rho T (\delta \boldsymbol{v} \cdot \nabla) s = 0, \tag{2.9}$$

where δ indicates Eulerian perturbations, and we have assumed $\mathrm{d}s/\mathrm{d}t = 0$ for adiabatic oscillations. From the thermodynamic relation

$$\Delta s = \left(\frac{\partial s}{\partial \ln \rho}\right)_p \left(\frac{\Delta\rho}{\rho} - \frac{\Delta p}{\Gamma_1 p}\right) = -\left(\frac{\Delta\rho}{\rho} - \frac{\Delta p}{\Gamma_1 p}\right)\frac{p}{\rho T}, \tag{2.10}$$

we obtain

$$\frac{\rho}{\Gamma_1 p}\left(\frac{\partial \delta p}{\partial t} + \delta\boldsymbol{v}\cdot\nabla p + \boldsymbol{v}\cdot\nabla\delta p\right) = \frac{\partial\delta\rho}{\partial t} + \delta\boldsymbol{v}\cdot\nabla\rho + \boldsymbol{v}\cdot\nabla\delta p, \tag{2.11}$$

where Δ indicates Lagrangian perturbations.

For a physical quantity f, the Eulerian δf and Lagrangian Δf perturbations are respectively defined as

$$\delta f(\boldsymbol{r}, t) = f(\boldsymbol{r}, t) - f_0(\boldsymbol{r}), \tag{2.12}$$

$$\Delta f(\boldsymbol{r}, t) = f[\boldsymbol{r} + \boldsymbol{\xi}(\boldsymbol{r}, t), t] - f_0(\boldsymbol{r}), \tag{2.13}$$

where $f(\boldsymbol{r}, t)$ is the perturbed and $f_0(\boldsymbol{r})$ is the non-perturbed quantity, and $\boldsymbol{\xi}$ is the Lagrangian displacement vector, and we have

$$\Delta f(\boldsymbol{r}, t) = \delta f(\boldsymbol{r}, t) + \boldsymbol{\xi}\cdot\nabla f_0(\boldsymbol{r}). \tag{2.14}$$

Assuming that the time dependence of the perturbations is given as $\exp(i\sigma t)$ and that the hydrostatic equilibrium structure with $\boldsymbol{v} = 0$ is spherical symmetric, we obtain

$$\delta\rho + \nabla\cdot(\rho\boldsymbol{\xi}) = 0, \tag{2.15}$$

$$-\sigma^2\boldsymbol{\xi} + \frac{1}{\rho}\nabla\delta p - \frac{\delta\rho}{\rho^2}\nabla p = 0, \tag{2.16}$$

$$\frac{\delta p}{\Gamma_1 p} + \frac{(\boldsymbol{\xi}\cdot\nabla)p}{\Gamma_1 p} = \frac{\delta\rho}{\rho} + \frac{(\boldsymbol{\xi}\cdot\nabla)\rho}{\rho}, \tag{2.17}$$

where we have used $\delta\boldsymbol{v} = i\sigma\boldsymbol{\xi}$. We note that

$$\delta\boldsymbol{v} = \Delta\boldsymbol{v} - (\boldsymbol{\xi}\cdot\nabla)\boldsymbol{v} = \partial\boldsymbol{\xi}/\partial t + (\boldsymbol{v}\cdot\nabla)\boldsymbol{\xi} - (\boldsymbol{\xi}\cdot\nabla)\boldsymbol{v}. \tag{2.18}$$

We consider the oscillations of a spherical star using spherical polar coordinates (r, θ, ϕ). For non-rotating and non-magnetized stars, separation of variables is possible to represent the perturbations using a single spherical harmonic function $Y_l^m(\theta, \phi)$. We express the displacement vector $\boldsymbol{\xi}(r, \theta, \phi)$ as

$$\boldsymbol{\xi}(r, \theta, \phi) = \xi_r(r)Y_l^m(\theta, \phi)\boldsymbol{e}_r + \xi_H(r)\nabla_H Y_l^m(\theta, \phi) + \xi_T(r)\boldsymbol{e}_r\times\nabla_H Y_l^m(\theta, \phi), \tag{2.19}$$

where

$$\nabla_H = \boldsymbol{e}_\theta\frac{\partial}{\partial\theta} + \boldsymbol{e}_\phi\frac{1}{\sin\theta}\frac{\partial}{\partial\phi}. \tag{2.20}$$

Note that

$$\boldsymbol{e}_r\cdot\nabla_H Y_l^m = \nabla_H Y_l^m\cdot(\boldsymbol{e}_r\times\nabla_H Y_l^m) = \boldsymbol{e}_r\cdot(\boldsymbol{e}_r\times\nabla_H Y_l^m) = 0. \tag{2.21}$$

The perturbations of scalar quantities are given by

$$\delta p = \delta p(r) Y_l^m(\theta, \phi), \quad \delta\rho = \delta\rho(r) Y_l^m(\theta, \phi). \tag{2.22}$$

Substituting these expressions into the linearized equation of motion, we obtain

$$\left(-\sigma^2 \xi_r + \frac{1}{\rho}\frac{\mathrm{d}\delta p}{\mathrm{d}r} - \frac{\delta\rho}{\rho^2}\frac{\mathrm{d}p}{\mathrm{d}r}\right) Y_l^m \boldsymbol{e}_r + \left(-\sigma^2 \xi_H + \frac{\delta p}{\rho r}\right) \nabla_H Y_l^m \\ -\sigma^2 \xi_T \boldsymbol{e}_r \times \nabla_H Y_l^m = 0. \tag{2.23}$$

From this equation, we can derive the following three relations:

$$-\sigma^2 \xi_r + \frac{1}{\rho}\frac{\mathrm{d}\delta p}{\mathrm{d}r} - \frac{\delta\rho}{\rho^2}\frac{\mathrm{d}p}{\mathrm{d}r} = 0, \tag{2.24}$$

$$-\sigma^2 \xi_H + \frac{\delta p}{\rho r} = 0, \tag{2.25}$$

$$\sigma^2 \xi_T = 0. \tag{2.26}$$

Therefore, we find $\xi_T = 0$ for $\sigma \neq 0$.

When the displacement vector $\boldsymbol{\xi}$ of a mode is given by

$$\boldsymbol{\xi} = \xi_r(r) Y_l^m(\theta, \phi) \boldsymbol{e}_r + \xi_H(r) \nabla_H Y_l^m(\theta, \phi) \tag{2.27}$$

the mode is called spheroidal mode, while the mode is called toroidal mode when the displacement vector is given by

$$\boldsymbol{\xi} = \xi_T(r) \boldsymbol{e}_r \times \nabla_H Y_l^m(\theta, \phi). \tag{2.28}$$

For non-rotating fluid stars, spheroidal modes and toroidal modes form separate mode groups, and $\xi_T = 0$ for $\sigma \neq 0$. For $\sigma = 0$, arbitral ξ_T is allowed, that is, toroidal modes are degenerated for $\sigma = 0$.

For modes of $\sigma^2 \neq 0$, we obtain the following oscillation equations from the above linearized equations:

$$\frac{\mathrm{d}\xi_r}{\mathrm{d}r} = \left(\frac{g}{c_s^2} - \frac{2}{r}\right)\xi_r + \left(\frac{L_l^2}{\sigma^2} - 1\right)\frac{\delta p}{\Gamma_1 p}, \tag{2.29}$$

$$\frac{\mathrm{d}\delta p}{\mathrm{d}r} = \rho(\sigma^2 - N^2)\xi_r - \frac{g}{c_s^2}\delta p, \tag{2.30}$$

where N^2 and L_l^2 are respectively the Brunt-Väisälä frequency and Lamb frequency, which are defined by

$$N^2 = -Ag, \quad L_l^2 = \frac{l(l+1)}{r^2} c_s^2. \tag{2.31}$$

Here, A is Schwartzschild discriminant defined by

$$A = \frac{\mathrm{d}\ln\rho}{\mathrm{d}r} - \frac{1}{\Gamma_1}\frac{\mathrm{d}\ln p}{\mathrm{d}r}, \tag{2.32}$$

and, g and c_s are the gravitational acceleration and adiabatic sound velocity defined by

$$g = \frac{GM_r}{r^2}, \quad c_s^2 = \frac{\Gamma_1 p}{\rho}, \quad M_r = \int_0^r 4\pi r^2 \rho \mathrm{d}r, \tag{2.33}$$

and the adiabatic exponent Γ_1 is given by

$$\Gamma_1 = \left(\frac{\partial \ln p}{\partial \ln \rho}\right)_{\rm ad}. \tag{2.34}$$

In the interior of the stars, $N^2 > 0$ ($N^2 < 0$) corresponds to radiative (convective) region. The system of coupled first order linear ordinary differential equations are solved as a boundary and eigenvalue problem for σ by imposing suitable boundary conditions at the center and the surface of the stars. We note that p-modes propagate in the regions of $\sigma^2 \gg N^2$, L_l^2, while g-modes propagate in the regions of $\sigma^2 \ll N^2$, L_l^2.

For adiabatic radial oscillations given by $\boldsymbol{\xi} = \xi_r \boldsymbol{e}_r$, we obtain the following second order linear ordinary differential equation for ξ_r:

$$\frac{\mathrm{d}}{\mathrm{d}r}\left[\Gamma_1 p \frac{1}{r^2}\frac{\mathrm{d}}{\mathrm{d}r}(r^2\xi_r)\right] - \frac{4}{r}\frac{\mathrm{d}p}{\mathrm{d}r}\xi_r + \sigma^2\rho\xi_r = 0. \tag{2.35}$$

This differential equation is also solved as boundary and eigenvalue problem for σ^2 by imposing suitable boundary conditions at the center and the surface of the stars. Modes of $\sigma^2 < 0$ indicate the dynamical instability of the equilibrium.

2.2 waves propagating in a solid crust

For solid crust regions, equation of motion is given by

$$\frac{\mathrm{d}\boldsymbol{v}}{\mathrm{d}t} = \frac{1}{\rho}\nabla\cdot\boldsymbol{\tau} - \nabla\Phi, \tag{2.36}$$

and the hydrostatic equilibrium is given by

$$\frac{1}{\rho}\nabla\cdot\boldsymbol{\tau} - \nabla\Phi = 0, \tag{2.37}$$

where $\boldsymbol{\tau}$ denotes the stress tensor and it is given by $\boldsymbol{\tau} = (\tau_{ij}) = (-p\delta_{ij})$ in equilibrium and δ_{ij} is Kronecker delta.

For waves propagating in a solid crust, the linearized equation of motion is given by

$$-\sigma^2\boldsymbol{\xi} - \frac{1}{\rho}\nabla\cdot\delta\boldsymbol{\tau} + \frac{\delta\rho}{\rho^2}\nabla\cdot\boldsymbol{\tau} = 0, \tag{2.38}$$

where the Lagrangian variation $\Delta\boldsymbol{\tau}$ is given by

$$\Delta\tau_{ij} = (\Gamma_1 p u_{ij})\delta_{ij} + 2\mu\left(u_{ij} - \frac{1}{3}u_{ll}\delta_{ij}\right), \tag{2.39}$$

and u_{ij} is the strain tensor given by

$$u_{ij} = \frac{1}{2}\left(\frac{\partial\xi_i}{\partial x_j} + \frac{\partial\xi_j}{\partial x_i}\right), \tag{2.40}$$

and $u_{ll} = u_{11} + u_{22} + u_{33} = \nabla\cdot\boldsymbol{\xi}$, and μ is the shear modulus. We note that the relation between the Lagrangian and Eulerian perturbations $\Delta\tau_{ij}$ and $\delta\tau_{ij}$ is given by

$$\Delta\tau_{ij} = \delta\tau_{ij} + \boldsymbol{\xi}\cdot\nabla\boldsymbol{\tau}. \tag{2.41}$$

Note that separation of variables is possible between radial and angular coordinates to represent the perturbations in terms of a single spherical harmonic function $Y_l^m(\theta,\phi)$ for non-rotating and non-magnetized stars even for stars having a solid crust region.

There exist spheroidal and toroidal sound wave modes propagating in the solid region.

2.3 normal modes of rotating stars

For rotating stars, equation of motion is given by

$$\frac{\mathrm{d}\boldsymbol{v}}{\mathrm{d}t} = -\frac{1}{\rho}\nabla p - \nabla\Phi - \boldsymbol{\Omega}\times\boldsymbol{v}, \tag{2.42}$$

where the angular rotation velocity $\boldsymbol{\Omega}$ of the star is along the z-axis:

$$\boldsymbol{\Omega} = (\Omega\cos\theta, -\Omega\sin\theta, 0), \tag{2.43}$$

and the equilibrium rotation velocity $\boldsymbol{v}_0$ is given by

$$\boldsymbol{v}_0 = \boldsymbol{\Omega}\times\boldsymbol{r} = (0, 0, r\Omega\sin\theta). \tag{2.44}$$

The hydrostatic balance is given by

$$\nabla p = -\rho\nabla\Phi - \rho\boldsymbol{\Omega}\times(\boldsymbol{\Omega}\times\boldsymbol{r}). \tag{2.45}$$

The second term on the right-hand-side is the centrifugal force, which deforms the equilibrium configuration.

Linearized Euler equation in the co-rotating frame of the fluid is obtained by linearizing the equation of motion of fluid dynamics:

$$-\sigma^2\boldsymbol{\xi} + 2i\sigma\boldsymbol{\Omega}\times\boldsymbol{\xi} + \frac{1}{\rho}\nabla\delta p - \frac{\delta\rho}{\rho^2}\nabla p = 0, \tag{2.46}$$

where the second term on the left-hand-side denotes the Coriolis force term, and we have used

$$\delta\boldsymbol{v} = \left(\frac{\partial}{\partial t} + \Omega\frac{\partial}{\partial\phi}\right)\boldsymbol{\xi} = (i\omega + im\Omega)\boldsymbol{\xi} = i\sigma\boldsymbol{\xi}, \tag{2.47}$$

where ω denotes the frequency observed in an inertial frame, and $\sigma = \omega + m\Omega$ the frequency in the co-rotating frame. Because of the Coriolis force term, there exists non-zero toroidal modes ξ_T even if $\sigma \neq 0$, and ξ_T is coupled with other two components (spheroidal components) ξ_r and ξ_H.

For rotating stars, there exists rotational modes such as inertial modes and r-modes, which form a subclass of inertial modes. The restoring force of rotational modes are Coriolis force and the frequencies are proportional to rotation rate Ω. r-modes are retrograde mode. For an r-mode associated with a spherical harmonic $Y_{l'}^m$ with $l' \geq |m| \neq 0$, the frequency ratio $\kappa \equiv \sigma/\Omega$ tends to $2m/[l'(l'+1)]$ in the limit of $\Omega \to 0$, where l' and m are the harmonic degree and azimuthal wavenumber, respectively. The ratio κ of inertial modes is also defined in the limit of $\Omega \to 0$, and its value depends on the azimuthal wavenumber m and on the equilibrium structure, that is, the polytropic index n when we use polytropes as background models (see e.g., Yoshida & Lee 2000a,b).

2.4 normal modes of magnetized stars

For magnetized stars, equation of motion is given by

$$\frac{\mathrm{d}\boldsymbol{v}}{\mathrm{d}t} = -\frac{1}{\rho}\nabla p - \nabla\Phi + \frac{1}{\rho}(\boldsymbol{j}\times\boldsymbol{B}), \tag{2.48}$$

where the third term of the right-hand-side denotes the Lorentz force and $\boldsymbol{j}$ is the current density. Under the MHD approximation, the Maxwell equations are given in cgs Gauss units by

$$\nabla \cdot \boldsymbol{B} = 0, \quad \nabla \times \boldsymbol{B} = 4\pi \boldsymbol{j}, \quad \nabla \times \boldsymbol{E} = -\frac{1}{c}\frac{\partial \boldsymbol{B}}{\partial t}, \quad \nabla \cdot \boldsymbol{E} = 4\pi\rho_e, \tag{2.49}$$

where ρ_e is the charge density, and we have ignored the displacement current $\partial \boldsymbol{E}/\partial t$. When we write the Ohm's law as

$$\boldsymbol{j} = \sigma_e \left(\boldsymbol{E} + \frac{\boldsymbol{v}}{c} \times \boldsymbol{B} \right), \tag{2.50}$$

where σ_e is the electric conductivity, assuming ideal MHD so that $\sigma_e \to \infty$, for a finite $\boldsymbol{j}$, we obtain

$$\boldsymbol{E} + \frac{\boldsymbol{v}}{c} \times \boldsymbol{B} = 0. \tag{2.51}$$

Using the above equations we obtain

$$\frac{\mathrm{d}\boldsymbol{v}}{\mathrm{d}t} = -\frac{1}{\rho}\nabla p - \nabla\Phi + \frac{1}{4\pi\rho}[(\nabla \times \boldsymbol{B}) \times \boldsymbol{B}], \tag{2.52}$$

and the induction equation given by

$$\frac{\partial \boldsymbol{B}}{\partial t} = \nabla \times (\boldsymbol{v} \times \boldsymbol{B}). \tag{2.53}$$

Hydrostatic equilibrium of magnetized stars is given by

$$\nabla p = -\rho\nabla\Phi + \frac{1}{4\pi}(\nabla \times \boldsymbol{B}) \times \boldsymbol{B}. \tag{2.54}$$

As in the case of rotating stars, the second term on the right-hand-side has the effect of deforming the equilibrium configuration.

Linearized Euler equation and induction equation are in the Cowling approximation given by

$$-\sigma^2\boldsymbol{\xi} + \frac{1}{\rho}\nabla\delta p - \frac{\delta\rho}{\rho^2}\nabla p - \frac{(\nabla \times \delta\boldsymbol{B}) \times \boldsymbol{B} + (\nabla \times \boldsymbol{B}) \times \delta\boldsymbol{B}}{4\pi\rho} = 0, \tag{2.55}$$

and

$$\delta\boldsymbol{B} = \nabla \times (\boldsymbol{\xi} \times \boldsymbol{B}), \tag{2.56}$$

which gives the relation between $\boldsymbol{\xi}$ and $\delta\boldsymbol{B}$. There exist non-zero toroidal components even for $\sigma \neq 0$ because of the Lorentz force term as in the case of rotating stars. In particular for non-axisymmetric ($m \neq 0$) perturbations, ξ_T is coupled with ξ_r and ξ_H.

In this paper, to calculate normal modes of magnetized stars we will assume purely toroidal or purely poloidal magnetic fields for equilibrium magnetic field configurations.

To define purely poloidal magnetic fields, we start with the Ampere's law given by

$$\nabla \times (\nabla \times \boldsymbol{A}) = 4\pi\boldsymbol{J} = -\nabla^2\boldsymbol{A}, \tag{2.57}$$

from which we obtain

$$\frac{1}{r^2}\frac{\partial}{\partial r}\left(r^2\frac{\partial A_\phi}{\partial r}\right) + \frac{1}{r^2\sin\theta}\frac{\partial}{\partial\theta}\left(\sin\theta\frac{\partial A_\phi}{\partial\theta}\right) - \frac{1}{r^2\sin^2\theta}A_\phi = -4\pi J_\phi, \tag{2.58}$$

where we have assumed that $\nabla \cdot \boldsymbol{A} = 0$ (Lorentz gauge), and that the electric current and vector potential are given as $\boldsymbol{J}(r,\theta) = [0, 0, J_\phi(r,\theta)]$ and $\boldsymbol{A}(r,\theta) = [0, 0, A_\phi(r,\theta)]$, respectively. We

carry out separation of variables between radial (r) and angular (θ) coordinates assuming the following forms

$$A_\phi(r,\theta) = rf(r)\frac{\partial}{\partial\theta}P_l(\cos\theta), \tag{2.59}$$

$$J_\phi(r,\theta) = rj(r)\frac{\partial}{\partial\theta}P_l(\cos\theta), \tag{2.60}$$

where $P_l(\cos\theta)$ denotes Legendre polynomial of order l. Therefore, we obtain

$$\frac{1}{r^2}\frac{\mathrm{d}}{\mathrm{d}r}\left[r^2\frac{\mathrm{d}}{\mathrm{d}r}(rf)\right] - \frac{l(l+1)}{r}f = -4\pi rj. \tag{2.61}$$

When we assume $l = 1$ for dipole magnetic field, the above ordinary differential equation reduces to

$$\frac{\mathrm{d}^2 f}{\mathrm{d}r^2} + \frac{4}{r}\frac{\mathrm{d}f}{\mathrm{d}r} = -4\pi j. \tag{2.62}$$

This second order ordinary differential equation is Grad-Shafranov equation.

The toroidal current density on the right-hand-side of equation (2.62) is determined by imposing integrability condition on the hydrostatic equation (2.54). The Lorentz force term is given by

$$\boldsymbol{F}_{\mathrm{L}} = \boldsymbol{J}\times\boldsymbol{B} = -(\nabla\times\boldsymbol{A})\times\boldsymbol{J} = J_\phi\left\{\left[\frac{1}{r}\frac{\partial}{\partial r}\left(rA_\phi\right)\right]\boldsymbol{e}_r + \left[\frac{1}{r\sin\theta}\frac{\partial}{\partial\theta}\left(\sin\theta A_\phi\right)\right]\boldsymbol{e}_\theta\right\}. \tag{2.63}$$

Substituting this Lorentz force term and the expansions of A_ϕ and J_ϕ for the order $l = 1$ into the hydrostatic equation (2.54), we obtain

$$\frac{\nabla p}{\rho} + \nabla\Phi - \frac{j}{4\pi\rho}\nabla\left(r^2 f\sin^2\theta\right) = 0. \tag{2.64}$$

If we assume $p = p(\rho)$ and $j = j(\rho) \propto \rho$, we can integrate the equation (2.64) to obtain the following Bernoulli equation

$$\int\frac{\mathrm{d}p}{\rho} + \Phi - \frac{c_0}{4\pi}r^2 f\sin^2\theta = C, \tag{2.65}$$

where c_0 is an arbitrary constant and C is an integral constant. This is the reason why we use the toroidal current density j given by $j(\rho) = c_0\rho$.

Purely poloidal magnetic field components are given by $\boldsymbol{B} = -\nabla\times\boldsymbol{A}$. This relation is reduced to

$$B_r = -\frac{1}{r}\frac{\partial A_\phi}{\partial\theta} - \frac{\cos\theta}{r\sin\theta}A_\phi, \quad B_\theta = \frac{\partial A_\phi}{\partial r} + \frac{1}{r}A_\phi, \quad B_\phi = 0, \tag{2.66}$$

and we obtain

$$B_r = 2f\cos\theta, \quad B_\theta = -\left(r\frac{\mathrm{d}f}{\mathrm{d}r} + 2f\right)\sin\theta, \tag{2.67}$$

where $P_1(\cos\theta) = \cos\theta$. It is clear that this magnetic field satisfies the Gauss's law $\nabla\cdot\boldsymbol{B} = 0$.

For purely toroidal magnetic fields, using integrability condition on the hydrostatic equilibrium (2.54) to obtain a Bernoulli equation, we determine purely toroidal magnetic field configurations, that is, if we assume $p = p(\rho)$, $B_r = B_\theta = 0$, and $B_\phi \propto \rho^n(r\sin\theta)^{2n-1}$, the hydrostatic equilibrium equation (2.54) can be integrated. For example, assuming $n = 1$ and $B_\phi = k\rho r\sin\theta$,

the Lorentz force term reduces to $-\nabla[B_0^2/(8\pi\rho_c)\hat{\rho}x^2\sin^2\theta]$, where $k = B_0/(\sqrt{2}\rho_c R)$ is a constant, B_0 is the parameter for the strength of magnetic fields, ρ_c is the central density of the star, and R is the stellar radius, $x = r/R$ and $\hat{\rho} = \rho/\rho_c$. We thus obtain the following Bernoulli equation

$$\int \frac{\mathrm{d}p}{\rho} + \Phi + \frac{B_0^2}{8\pi\rho_c}\hat{\rho}x^2\sin^2\theta = C, \tag{2.68}$$

where C is an integral constant. It is clear $B_\phi = k\rho r\sin\theta$ satisfies Gauss's law.

For strongly magnetized stars, in addition to g-, f-, and p-modes expected for normal fluid stars, there exists Alfvén modes whose frequency is proportional to the strength of magnetic fields. The magnetic modes appear as discrete modes or as continuous modes that form continuous frequency spectra. It is also important to note that, even without thermal mechanisms that destabilize the oscillation modes, magnetic modes can be unstable. The existence of unstable modes means that the equilibrium configuration of the stars is not stable. It is well known that stars magnetized with purely poloidal or toroidal magnetic fields are unstable, and the magnetic energy will quickly dissipated by some dissipative processes (e.g., Lasky et al. 2011; Markey & Tayler 1973; van Assche et al. 1982). For purely toroidal magnetic fields, there are two kinds of unstable modes: one is for Tayler (kink) instability, especially of $m = 1$, and another is for Parker instability of $m \neq 0$. Tayler instability arises near the polar axis by kink of the magnetic field lines, and Parker instability is caused by the magnetic buoyancy force. The growth timescales are the Alfvén timescale R/v_A, where $v_A = \sqrt{B^2/(4\pi\rho)}$ is Alfvén velocity. For purely poloidal magnetic field, the instability mode is mainly described as Tayler (kink) instability.

2.5 series expansions for the perturbations

In general, separation of variables is not possible between radial and angular coordinates to represent the perturbations for both rotating stars and magnetized stars. In this paper, to represent the perturbations we use series expansions of the perturbations in terms of spherical harmonic functions for a given $|m|$ (see §3.1.2 and 4.1.2). For example, the displacement vector $\boldsymbol{\xi}$ is expanded as

$$\boldsymbol{\xi}(r,\theta,\phi) = \sum_{l,l'\geq|m|}\left\{\left[\xi_r^{(l)}(r)\boldsymbol{e}_r + \xi_H^{(l)}(r)\nabla_H\right]Y_l^m(\theta,\phi) + \xi_T^{(l')}(r)\boldsymbol{e}_r\times\nabla_H Y_{l'}^m(\theta,\phi)\right\}, \tag{2.69}$$

where the time-dependence of the displacement $\boldsymbol{\xi}$ is given by the factor $\exp(i\sigma t)$. Then, substituting the expansions into the linearized basic equations such as (2.55), we reduces the linearized partial differential equations to a system of coupled linear ordinary differential equations for the expansion coefficients, formally given as

$$r\frac{\mathrm{d}}{\mathrm{d}r}\boldsymbol{Y} = \boldsymbol{\mathcal{C}}(r,\sigma)\boldsymbol{Y}, \tag{2.70}$$

$$\boldsymbol{Y} = \left(\xi_r^{(l=|m|)}, \xi_r^{(l=|m|+2)}, \cdots, \xi_H^{(l=|m|)}, \xi_H^{(l=|m|+2)}, \cdots, \xi_T^{(l'=|m|)}, \xi_T^{(l'=|m|+2)}, \cdots\right)^T, \tag{2.71}$$

where $\boldsymbol{\mathcal{C}}$ is the coefficient matrix. Imposing appropriate boundary conditions at the center and surface of the stars, we solve the system of differential equations as an eigenvalue problem.

2.6 oscillation frequency spectra of neutron stars

It may be instructive to mention possible oscillation modes of neutron stars. If we assume non-rotating and non-magnetized neutron stars with thermally stratified structure in the interior, we may refer to the results of modal analyses given by e.g., McDermott et al. (1988), who used for their modal analyses three-component neutron star models composed of a surface fluid ocean, a solid crust, and a fluid core. They obtained frequency spectra for a rich variety of oscillation modes, which include spheroidal g-, f, and p-modes propagating in the fluid regions, and spheroidal s- and toroidal t-modes propagating in the solid crust, which are essentially sound waves. They also found interfacial modes which have large amplitudes only at the interfaces between the fluid core and the inner crust and between the outer crust and the surface ocean.

Lee & Strohmayer (1996) calculated normal modes of slowly rotating neutron stars using the three-component models. For rotating neutron stars, there exists rotational modes in addition to the oscillation modes discussed above. The restoring force of rotational modes is the Coriolis force. Using the three-component model, r-modes are separated into the core r-modes and surface r-modes. The rotational modes have large amplitudes in the fluid regions only (fluid core and ocean), and have almost no amplitudes in the solid crust region.

If neutron stars have magnetic fields, there exist magnetic modes like Alfvén modes. If both the fluid core and solid crust are threaded by strong magnetic fields, we need to consider global oscillation modes (e.g., Lee 2008; Asai & Lee 2014). For example, Asai & Lee (2014) calculate axisymmetric ($m = 0$) toroidal modes of the magnetized neutron stars with purely poloidal magnetic field considering the core-crust coupling due to the magnetic field in general relativistic framework. They find discrete normal toroidal modes, and the frequencies of the toroidal modes form distinct mode sequences. The oscillation frequency spectra of global oscillations are quite different from those of non-magnetized stars.

In this paper, since we use polytropes as background models for modal analyses for simplicity, we ignore solid crust regions of neutron stars, that is, we do not treat crustal oscillation modes.

3 Normal modes of uniformly rotating stars magnetized with purely toroidal magnetic fields

In this section, we describe normal modes of uniformly rotating stars magnetized with purely toroidal magnetic fields. For the normal mode analyses, we take account of the effects of the deformation of equilibrium configurations due to the purely toroidal magnetic field.

3.1 method of solution

3.1.1 equilibrium model

We assume uniformly rotating polytropes for magnetized rotating stars with purely toroidal magnetic field. Equilibrium structures of the stars having purely toroidal magnetic field have been so far obtained by non-perturbative approaches in Newtonian framework by Miketinac (1973) and in general relativistic framework by Kiuchi & Yoshida (2008) or Frieben & Rezzolla

(2012). In this paper, we adopt a perturbative approch to calculate the configurations of magnetically deformed stars with purely toroidal magnetic field. According to Miketinac (1973), purely toroidal magnetic field in equilibrium stars is given by (see §2.4)

$$B_r = 0, \quad B_\theta = 0, \quad B_\phi = k\rho r \sin\theta, \tag{3.1}$$

where $k \equiv B_0/(\sqrt{2}\rho_c R)$ is a constant, B_0 is a parameter for the strength of magnetic field in the stars, ρ_c is the central density of the stars, and R is the stellar radius. Here we use spherical polar coordinates (r, θ, ϕ). The absolute value of the toroidal magnetic field is given by $|\boldsymbol{B}| = |B_\phi| = (B_0/\sqrt{2})\hat{\rho} x \sin\theta$, where $x = r/R$ and $\hat{\rho} = \rho/\rho_c$. We assume fluid velocities in equilibrium as follows:

$$v_r = 0, \quad v_\theta = 0, \quad v_\phi = \Omega r \sin\theta, \tag{3.2}$$

where Ω denotes the angular velocity of uniformly rotating stars. In this paper, we assume that the stars are deformed only by toroidal magnetic field, and we ignore the deformation due to the centrifugal force. By the assumptions (3.1) and (3.2), the induction and continuity equations are automatically satisfied and need not be considered any further. For toroidal magnetic fields (3.1), we can write the Lorentz force per unit mass as a potential force:

$$\frac{1}{4\pi\rho}(\nabla \times \boldsymbol{B}) \times \boldsymbol{B} = -\nabla\left(\frac{B_0^2}{8\pi\rho_c}\hat{\rho} x^2 \sin^2\theta\right). \tag{3.3}$$

Then, the equilibrium structures of stars are described by the hydrostatic equation, Poisson equation, and equation of state:

$$\nabla p = -\rho\nabla\Psi, \tag{3.4}$$

$$\nabla^2\Phi = 4\pi G\rho, \tag{3.5}$$

$$p = K_c\rho^{1+1/n}, \tag{3.6}$$

where n and K_c are the polytropic index and structure constant determined by the stellar mass and radius, G is the gravitational constant, Φ denotes the gravitational potential, and Ψ is the effective potential defined by

$$\Psi = \Phi + \frac{1}{3}\omega_A^2\hat{\rho} r^2[1 - P_2(\cos\theta)] - C, \tag{3.7}$$

where $\omega_A = \sqrt{B_0^2/(4\pi\rho_c R^2)}$ is the characteristic Alfvén frequency of the stars and C is a constant. $P_2(\cos\theta) = (3\cos^2\theta - 1)/2$ is Legendre polynomial $P_l(\cos\theta)$ of order $l = 2$.

Since the gravitational potential Φ is a physical quantity of order of GM/R, the ratio of the second term on the right-hand-side of equation (3.7) to Φ is given by $\bar{\omega}_A^2 \equiv \omega_A^2/\Omega_{\rm K}^2$, where $\Omega_{\rm K} = \sqrt{GM/R^3}$ is the Kepler frequency. For a neutron star with $M = 1.4M_\odot$ and $R = 10^6$ cm, we obtain $\bar{\omega}_A^2 \sim 2 \times 10^{-5}$ for $B_0 = 10^{16}$ G. Therefore, the effects of the magnetic field on equilibrium configuration are small so long as we assume $B_0 \lesssim 10^{17}$ G. In this paper, since we assume sufficiently weak magnetic fields, we can treat the deformation due to the purely toroidal magnetic fields as a small perturbation to non-magnetic stars, that is, we treat ω_A^2 as a

small parameter, compared to GM/R. In this assumption, $\hat{\rho}$ in the term proportional to $\bar{\omega}_A^2$ in equation (3.7) can be replaced by the density $\hat{\rho}_0$ of the non-magnetic stars. Thus, Ψ satisfies

$$\nabla^2\Psi = 4\pi G\rho + \frac{1}{3}\omega_A^2\left[r^2\frac{\mathrm{d}^2\hat{\rho}_0}{\mathrm{d}r^2} + 6r\frac{\mathrm{d}\hat{\rho}_0}{\mathrm{d}r} + 6\hat{\rho}_0 - \left(r^2\frac{\mathrm{d}^2\hat{\rho}_0}{\mathrm{d}r^2} + 6r\frac{\mathrm{d}\hat{\rho}_0}{\mathrm{d}r}\right)P_2(\cos\theta)\right]. \tag{3.8}$$

From equations (3.4) and (3.6), we can regard ρ as the argument of the function Ψ. If we expand $\Psi(r,\theta)$ as

$$\Psi(r,\theta) = \Psi_0(r) - 2R^2\omega_A^2[\psi_0(x) + \psi_2(x)P_2(\cos\theta)], \tag{3.9}$$

we can expand $\rho(r,\theta)$ as

$$\rho(r,\theta) = \rho_0(r) - 2R^2\omega_A^2\frac{\mathrm{d}\rho_0}{\mathrm{d}\Psi_0}[\psi_0(x) + \psi_2(x)P_2(\cos\theta)], \tag{3.10}$$

where $\Psi_0(r) = \Phi_0(r)$ and $\rho_0(r)$ denote the gravitational potential and density of the non-magnetized stars and they satisfy $\mathrm{d}p_0/\mathrm{d}r = -\rho_0\mathrm{d}\Phi_0/\mathrm{d}r = -\rho_0 GM_r/r^2$, $M_r = \int_0^r 4\pi r^2\rho_0\mathrm{d}r$, and $p_0 = K_c\rho_0^{1+1/n}$.

Substituting equations (3.9) and (3.10) to equation (3.8), we obtain

$$\begin{aligned} R^2\nabla^2[\psi_0(x) + \psi_2(x)P_2(\cos\theta)] &= 4\pi GR^2\frac{\mathrm{d}\rho_0}{\mathrm{d}\Psi_0}[\psi_0(x) + \psi_2(x)P_2(\cos\theta)] \\ &\quad + f_0(x) + f_2(x)P_2(\cos\theta), \end{aligned} \tag{3.11}$$

from which we obtain

$$\frac{1}{x^2}\frac{\mathrm{d}}{\mathrm{d}x}\left(x^2\frac{\mathrm{d}\psi_0}{\mathrm{d}x}\right) = k(x)\psi_0 + f_0(x), \tag{3.12}$$

$$\frac{1}{x^2}\frac{\mathrm{d}}{\mathrm{d}x}\left(x^2\frac{\mathrm{d}\psi_2}{\mathrm{d}x}\right) = \left[k(x) + \frac{6}{x^2}\right]\psi_2 + f_2(x), \tag{3.13}$$

where

$$f_0(x) = -\frac{1}{6}\left(r^2\frac{\mathrm{d}^2\hat{\rho}_0}{\mathrm{d}r^2} + 6r\frac{\mathrm{d}\hat{\rho}_0}{\mathrm{d}r} + 6\hat{\rho}_0\right),$$

$$f_2(x) = \frac{1}{6}\left(r^2\frac{\mathrm{d}^2\hat{\rho}_0}{\mathrm{d}r^2} + 6r\frac{\mathrm{d}\hat{\rho}_0}{\mathrm{d}r}\right), \tag{3.14}$$

$$k(x) = 4\pi GR^2\frac{\mathrm{d}\rho_0}{\mathrm{d}\Psi_0}. \tag{3.15}$$

To integrate the differential equations (3.12) and (3.13) from the center of the star, we need to impose regularity conditions at the stellar center. The regularity conditions are obtained by expanding the functions $\psi_0(x)$ and $\psi_2(x)$ around $x = 0$, that is, substituting the following expansion to equations (3.12) and (3.13).

$$\psi_j = x^s\sum_{n=0}^{\infty}(a_n^{(j)}x^n) \quad (j = 0 \text{ and } 2). \tag{3.16}$$

For $x \to 0$, since $k(x) \to k(0)$, $f_0(x) \to f_0(0)$, and $f_2(x) \to f_{20}x^2$, where $k(0)$, $f_0(0)$, and f_{20} are all constants, the exponent s gives regular solutions if $s = j$. Assuming the density is independent

of Alfvén frequency ω_A at $x = 0$, we obtain the expansion coefficient $a_0^{(0)} = 0$ for the function ψ_0. To determine the coefficient $a_0^{(2)}$ for ψ_2, we need to impose the following surface boundary condition:

$$3\psi_2(1) + \left.\frac{\mathrm{d}\psi_2}{\mathrm{d}x}\right|_{x=1} = \frac{1}{6}\left.\frac{\mathrm{d}\hat{\rho}}{\mathrm{d}x}\right|_{x=1}. \tag{3.17}$$

We describe the detail of the surface boundary condition in Appendix B.

3.1.2 perturbation equations

To calculate the oscillation modes of magnetically deformed stars, we introduce a parameter a, which is the quantity that labels the equi-potential surface of $\Psi(r,\theta)$ such that $\Psi(r,\theta) = \Psi_0(a)$, that is,

$$\Psi_0(a) = \Psi_0(r) - 2R^2\omega_A^2[\psi_0(x) + \psi_2(x)P_2(\cos\theta)]. \tag{3.18}$$

This equation defines the equi-potential surface as $r(a,\theta)$. Assuming that the deviation of the equi-potential surface $r(a,\theta)$ from the spherical surface $r = a$ is small, the function $r(a,\theta)$ is given by

$$r = a[1 + \epsilon(a,\theta)], \tag{3.19}$$

where ϵ is a quantity of order of $R^2\omega_A^2/\Psi_0(R)$. Substuting equation (3.19) to equation (3.18), we obtain $\epsilon(a,\theta)$ up to order of ω_A^2 as follows:

$$\epsilon(a,\theta) = \alpha(a) + \beta(a)P_2(\cos\theta), \tag{3.20}$$

where

$$\alpha(a) = \frac{2c_1\bar{\omega}_A^2}{x^2}\psi_0(x), \quad \beta(a) = \frac{2c_1\bar{\omega}_A^2}{x^2}\psi_2(x), \tag{3.21}$$

and $c_1 = (a/R)^3[M(a)/M]$. $M(a)$ denotes the mass in the a-constant surface and $M = M(R)$.

Hereafter, we use this parameter a instead of the radial component r of spherical coordinates. In this new coordinate system (a,θ,ϕ), the line element is given by

$$\mathrm{d}s^2 = (1+2\epsilon)(\mathrm{d}a^2 + a^2\mathrm{d}\theta^2 + a^2\sin^2\theta\mathrm{d}\phi^2) + 2a\frac{\partial\epsilon}{\partial a}\mathrm{d}a^2 + 2a\frac{\partial\epsilon}{\partial\theta}\mathrm{d}a\mathrm{d}\theta \equiv g_{ab}dx^a dx^b. \tag{3.22}$$

Then, the pressure, density, and effective potential of the magnetized stars depend only on the radial coordinate a. Note that orthogonality between the basis vectors is lost for this coordinate system.

The oscillation equations governing non-radial oscillations of magnetized rotating stars are derived by linearizing the basic equations of manetohydrodynamics. As for the effects of rotation, we only consider those of the Coriolis force and ignore those of the centrifugal force, i.e., of rotational deformation. Here, we assume the rotational and magnetic axes coincide with each other. For static and axisymmetric configurations, we can assume the perturbed quantities are proportioal to $\exp(i\omega t + im\phi)$, where ω denotes frequency observed in an inertial frame and m is the azimuthal wavenumber. Assuming adiabatic oscillations, the oscillation equations for

magnetized uniformly rotating stars in the coordinate system (a, θ, ϕ) are (see e.g., Saio 1998; Lee 1993; Yoshida & Lee 2000a):

$$-\sigma^2[(1+2\epsilon)\boldsymbol{\xi} + a\xi^a\nabla_0\epsilon + a(\boldsymbol{\xi}\cdot\nabla_0\epsilon)\boldsymbol{e}_a] = -\nabla_0\delta\Phi - \frac{1}{\rho}\nabla_0\delta p + i\sigma\boldsymbol{D}$$
$$+\frac{\delta\rho}{\rho}\left[\frac{\mathrm{d}p}{\mathrm{d}a}\boldsymbol{e}_a - \frac{1}{4\pi}(\nabla_0\times\boldsymbol{B})\times\boldsymbol{B}\right] + \frac{1}{4\pi\rho}\left[(\nabla_0\times\delta\boldsymbol{B})\times\boldsymbol{B} + (\nabla_0\times\boldsymbol{B})\times\delta\boldsymbol{B}\right], \tag{3.23}$$

$$\delta\rho + \nabla_0\cdot(\rho\boldsymbol{\xi}) + \rho\boldsymbol{\xi}\cdot\nabla_0\left(3\epsilon + a\frac{\partial\epsilon}{\partial a}\right) = 0, \tag{3.24}$$

$$\frac{\delta\rho}{\rho} = \frac{\delta p}{\Gamma_1 p} - \frac{\xi^a}{a}aA, \tag{3.25}$$

$$(\delta B)^i = \frac{1}{\sqrt{g}}\epsilon^{ijk}\frac{\partial}{\partial x^j}\left(\sqrt{g}\epsilon_{imk}\xi^j B^m\right), \tag{3.26}$$

where $\sigma = \omega + m\Omega$ denotes the frequency observed in the co-rotating frame, $\boldsymbol{\xi}(a,\theta,\phi)$ is the displacement vector, δ denotes Eulerian perturbation, ϵ_{ijk} or ϵ^{ijk} are Levi-Civita symbols, g is a determinant of metric g_{ij}, and

$$\nabla_0 = \lim_{\epsilon\to 0}\left[\boldsymbol{e}_a\frac{\partial}{\partial a} + \boldsymbol{e}_\theta\frac{1}{a}\frac{\partial}{\partial\theta} + \boldsymbol{e}_\phi\frac{1}{a\sin\theta}\frac{\partial}{\partial\phi}\right], \tag{3.27}$$

where $\boldsymbol{e}_a$, $\boldsymbol{e}_\theta$, and $\boldsymbol{e}_\phi$ are the basis vectors corresponding to a-, θ-, and ϕ-coordinates, respectively. The term $\boldsymbol{D}$ comes from the Coriolis force term and its components are given as follows (see e.g., Lee 1993; Yoshida & Lee 2000a):

$$D_a = 2\Omega\left(1+2\epsilon + a\frac{\partial\epsilon}{\partial a}\right)\sin\theta\xi^\phi,$$

$$D_\theta = 2\Omega\left(1+2\epsilon + \frac{\sin\theta}{\cos\theta}\frac{\partial\epsilon}{\partial\theta}\right)\cos\theta\xi^\phi,$$

$$D_\phi = -2\Omega\left[\left(1+2\epsilon + a\frac{\partial\epsilon}{\partial a}\right)\sin\theta\xi^a + \left(1+2\epsilon + \frac{\sin\theta}{\cos\theta}\frac{\partial\epsilon}{\partial\theta}\right)\cos\theta\xi^\theta\right]. \tag{3.28}$$

aA is Schwartzschild discriminant defined by

$$aA = \frac{\mathrm{d}\ln\rho}{\mathrm{d}\ln a} - \frac{1}{\Gamma_1}\frac{\mathrm{d}\ln p}{\mathrm{d}\ln a}, \tag{3.29}$$

where $\Gamma_1 = (\partial\ln p/\partial\ln\rho)_{\mathrm{ad}}$. In this paper, we adopt the Cowling approximation for simplicity, that is, we ignore $\delta\Phi$.

Because of the Lorentz and Coriolis forces terms in equation (3.23), separation of variables between radial coordinate (a) and angular coordinates (θ,ϕ) is not possible to represent the perturbations. Therefore, to define the perturbations we use finite length expansions in terms of spherical harmonic functions $Y_l^m(\theta,\phi)$. The displacement vector $\boldsymbol{\xi}$ is given by (see e.g., Lee 2005, 2007)

$$\xi^a = \sum_{j=1}^{j_{\max}} aS_{l_j}(a)Y_{l_j}^m(\theta,\phi), \tag{3.30}$$

$$\xi^{\theta} = \sum_{j=1}^{j_{\max}} \left[aH_{l_j}(a) \frac{\partial}{\partial \theta} Y_{l_j}^m(\theta,\phi) - iaT_{l'_j}(a) \frac{1}{\sin\theta} \frac{\partial}{\partial \phi} Y_{l'_j}^m(\theta,\phi) \right], \tag{3.31}$$

$$\xi^{\phi} = \sum_{j=1}^{j_{\max}} \left[aH_{l_j}(a) \frac{1}{\sin\theta} \frac{\partial}{\partial \phi} Y_{l_j}^m(\theta,\phi) + iaT_{l'_j}(a) \frac{\partial}{\partial \theta} Y_{l'_j}^m(\theta,\phi) \right], \tag{3.32}$$

and $\delta \boldsymbol{B}$ is given by

$$\frac{\delta B^a}{k\rho} = \sum_{j=1}^{j_{\max}} iah_{l_j}^S(a) Y_{l_j}^m(\theta,\phi), \tag{3.33}$$

$$\frac{\delta B^{\theta}}{k\rho} = \sum_{j=1}^{j_{\max}} \left[iah_{l_j}^H(a) \frac{\partial}{\partial \theta} Y_{l_j}^m(\theta,\phi) - ah_{l'_j}^T(a) \frac{1}{\sin\theta} \frac{\partial}{\partial \phi} Y_{l'_j}^m(\theta,\phi) \right], \tag{3.34}$$

$$\frac{\delta B^{\phi}}{k\rho} = \sum_{j=1}^{j_{\max}} \left[iah_{l_j}^H(a) \frac{1}{\sin\theta} \frac{\partial}{\partial \phi} Y_{l_j}^m(\theta,\phi) + ah_{l'_j}^T(a) \frac{\partial}{\partial \theta} Y_{l'_j}^m(\theta,\phi) \right], \tag{3.35}$$

where $l_j = |m| + 2(j-1)$, $l'_j = l_j + 1$ for even, and $l_j = |m| + 2j - 1$, $l'_j = l_j - 1$ for odd ($j = 1, 2, 3, ..., j_{\max}$). Eulerian perturbations of the pressure p and density ρ are

$$\delta p = \sum_{j=1}^{j_{\max}} \delta p_{l_j}(a) Y_{l_j}^m(\theta,\phi), \quad \delta\rho = \sum_{j=1}^{j_{\max}} \delta\rho_{l_j}(a) Y_{l_j}^m(\theta,\phi). \tag{3.36}$$

Substituting the expansions (3.30)-(3.36) into the perturbed equations (3.23)-(3.26), we obtain a system of coupled linear ordinary differential equations for the expansion coefficients $S_{l_j}(a)$ and $\delta p_{l_j}(a)$. These equations are called the oscillation equations and integrated within the interior of the magnetized uniformly rotating stars, see the details given in Appendix A.

To carry out modal analyses of magnetized and uniformly rotation neutron stars, we use polytropes of the indices $n = 1$, 1.5, and 3. In Figure 1, we give contour plots of the distributions of the density and magnetic fields for the three polytropes. As the polytropic index n increases, the distributions of the density and magnetic fields tend to be confined into the deep interior. The mass M and radius R we expect for neutrons may be $(M, R) = (1.4M_{\odot}, 10^6\text{cm})$ and those we use for normal stars are $(M, R) = (M_{\odot}, R_{\odot})$, respectively. Thus, for the neutron star model having $B_0 = 10^{16}$ G, we obtain $\bar{\omega}_A = 4.42 \times 10^{-3}$, while we obtain $\bar{\omega}_A = 7.39 \times 10^{-4}$ for the normal star having $B_0 = 10^6$ G. For $n = 1$ polytropic stellar model, we plot the functions $\alpha(a)/\bar{\omega}_A^2$ and $\beta(a)/\bar{\omega}_A^2$ for a/R in Figure 2. Further, we plot the shapes of magnetically deformed stars for $B_0 = 0$, 10^{16}, 10^{18}, 3×10^{18}, and 5×10^{18} G for $n = 1$ polytrope in Figure 3. From Figure 3, we find that the stellar shape looks oblate (crushed in the z-direction) near the stellar surface (left panel), and looks prolate (extended in the z-direction) in the interior of the star (right panel).

3.2 numerical results

In this subsection, we discuss the oscillations of uniformly rotating stars magnetized by purely toroidal fields, using polytropes with the indices $n = 1$, 1.5, and 3. Polytropes of indices $n = 1$, 1.5, and 3 can be regarded as simple models of neutron stars and normal stars. For the polytropes, we estimates the effects of magnetic deformation of the equilibrium on normal modes.

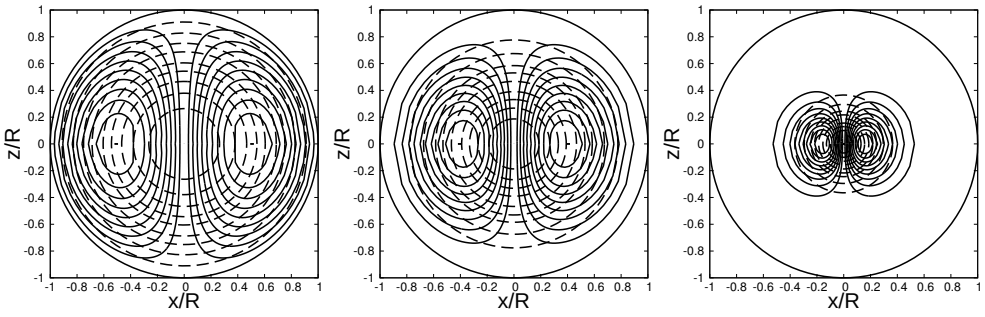

Figure 1: Equi-magnetic field strength contours (solid lines) and equi-density contours (long-dashed lines) on the meridional cross sections are plotted, from left to right panels, for the polytropes of the index n =1, 1.5, and 3, respectively. The outer-most solid circles show stellar surfaces. The solid contours correspond to $B/B_{\rm max}$ = 0.1, 0.2, 0.3, 0.4, 0.5, 0.6, 0.7, 0.8, and 0.9, and the long-dashed contours to ρ/ρ_c = 0.1, 0.2, 0.3, 0.4, 0.5, 0.6, 0.7, 0.8, and 0.9.

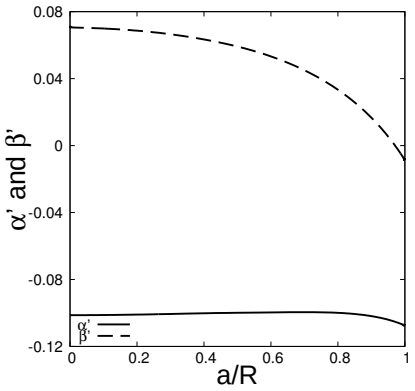

Figure 2: Functions $\alpha' \equiv \alpha/\bar{\omega}_A^2$ and $\beta' \equiv \beta/\bar{\omega}_A^2$ versus the fractional radius a/R for the $n = 1$ polytrope.

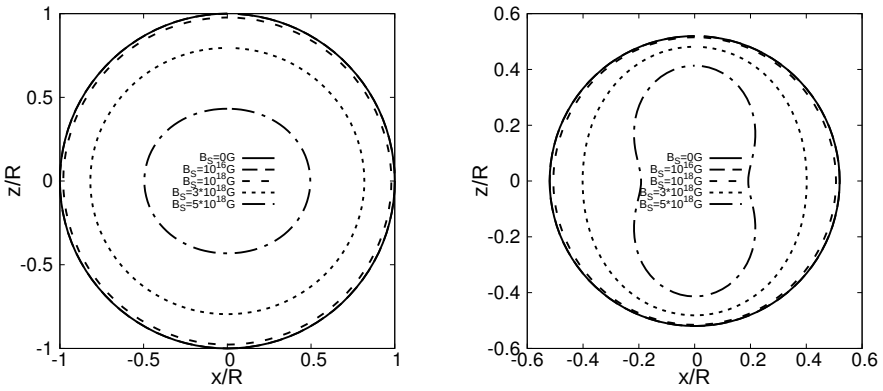

Figure 3: Stellar deformation due to purely toroidal magnetic field for surface ($x/R = z/R = 1$) of the star (left pannel) and interior ($x/R = z/R \sim 0.5$) of the star (right pannel) for the $n = 1$ polytrope.

3.2.1 g-, f-, and p-modes

We first calculate f-modes, and low radial order g- and p-modes for magnetized stars with purely toroidal magnetic field. In this calculation, we do not take account of the effects of the stellar rotation. In order to calculate non-radial oscillations for magnetized stars, we assume that the adiabatic exponent is given by

$$\frac{1}{\Gamma_1} = \frac{n}{n+1} + \gamma, \tag{3.37}$$

where γ is a constant, and we obtain the relation $aA = -\gamma(\mathrm{d}\ln p/\mathrm{d}\ln a)$. In this subsection, we assume $\gamma = -10^{-4}$ for $n = 1$ and 1.5 polytropes and $\Gamma_1 = 5/3$, that is, $\gamma = -3/20$ for $n = 3$ polytrope. Since the magnetic terms in the oscillation equations are all proportional to $\bar{\omega}_A^2$, the frequency of the oscillation modes are written as (see, Appendix A , C and Unno et al. 1989)

$$\bar{\sigma} = \bar{\sigma}_0 + \bar{E}_2\bar{\omega}_A^2 + \cdots, \tag{3.38}$$

where $\bar{\sigma}_0$ denotes the frequency of the non-magnetized stars. $\bar{E}_2$ is a proportional coefficient and estimated by calculating mode frequencies for two different values of $\bar{\omega}_A^2$, for example $\bar{\omega}_A^2 = 0$ and $\bar{\omega}_A^2 \sim 10^{-6}$. Here, the quantities $\bar{\sigma}_0$ and $\bar{E}_2$ are normalized by the Kepler frequency $\Omega_{\rm K}$ of the stars. Treating Alfvén frequency $\bar{\omega}_A^2$ as a small parameter, it is also possible to compute the coefficient $\bar{E}_2$, by using the eigenfunctions of the oscillation mode of the non-magnetized stars. We describe this method of calculation of $\bar{E}_2$ in the Appendix C.

In Tables 1-3, we tabulated the coefficients $\bar{E}_2$, $\bar{E}_2'$, and eigenfrequency $\bar{\sigma}_0$ of f-modes, and low radial order g-, and p-modes of $m = 1$, 2, and 3 for $n = 1$, 1.5, and 3 polytropes. Except for low frequency g-modes, the two coefficients $\bar{E}_2$ and $\bar{E}_2'$ show good agreement with each other, where $\bar{E}_2'$ is the coefficient $\bar{E}_2$ calculated by using the integration formula (see Appendix C). In this table, we also tabulate $\bar{E}_2^0$, which is the coefficient $\bar{E}_2$ calculated by using the integration formula that neglects deformation effects. Comparing $\bar{E}_2'$ with $\bar{E}_2^0$, we find that f- and p-modes are strongly affected by the deformation of the stars, while g-modes are hardly affected. The effects of magnetic deformation on the oscillation modes are quite similar to those of rotational deformation (see e.g., Saio 1981). We note that the frequency of f-mode obtained in this paper is consistent with that of Lander et al. (2010) so long as $\Omega/\sqrt{G\rho_c} \lesssim 0.1$ (because they consider second order of the stellar rotation).

Tables 1 and 2 are for the oscillation modes of neutron stars. The eigenfrequency $\bar{\sigma}_0$ of g-modes are quite small since $|\gamma|$ is small, which may be consistent with almost isentropic structure expected in the cold neutron star. The ratios E_2/σ_0 of g-modes are larger than those of f- and p-modes. This means that low frequency g-modes are easy to be affected by the magnetic fields. The ratios E_2/σ_0 of g-modes increase as the azimuthal wavenumber m increases, while those of f- and p-modes are insensitive to m.

Table 3 is for the oscillation modes of a normal star. The magnitudes of the ratios E_2/σ_0 are almost the same among g-, f-, and p-modes except for the g-modes of $m = 1$, for which the ratios are order of 0.1, which value is much smaller than those for $n = 1$ and 1.5 polytropes ($\gamma = -10^{-4}$).

In Figure 4, we plot the expansion coefficients S_{l_1}, H_{l_1}, and $T_{l_1'}$ of g_1-, f-, and p_1-modes of $l = m = 2$ for $B_0 = 10^{16}$ G for the polytrope of index $n = 1$. The first expansion coefficients are

Table 1: Coefficients E_2, E_2', and $\bar{E}_2^0$ for g-, f-, and p-modes of $l = m$ for the polytropic model with $n = 1$ and $\gamma = -10^{-4}$ *

mode	$\bar{\sigma}_0$	$\bar{E}_2$	$\bar{E}_2'$	$\bar{E}_2^0$
		$m = 1$		
$g_3 \cdots\cdots$	0.00570	-1.578(+0)	-1.490(+0)	-1.491(+0)
$g_2 \cdots\cdots$	0.00770	-2.051(+0)	-2.095(+0)	-2.095(+0)
$g_1 \cdots\cdots$	0.01203	-3.003(+0)	-3.063(+0)	-3.064(+0)
$p_1 \cdots\cdots$	3.26931	6.162(−1)	6.164(−1)	3.553(−1)
$p_2 \cdots\cdots$	5.09325	1.113(+0)	1.114(+0)	5.650(−1)
$p_3 \cdots\cdots$	6.85013	1.550(+0)	1.554(+0)	7.586(−1)
		$m = 2$		
$g_3 \cdots\cdots$	0.00884	3.518(+1)	3.488(+1)	3.487(+1)
$g_2 \cdots\cdots$	0.01152	2.427(+1)	2.402(+1)	2.402(+1)
$g_1 \cdots\cdots$	0.01678	1.133(+1)	1.130(+1)	1.130(+1)
$f \cdots\cdots$	1.65562	4.107(−1)	4.109(−1)	3.567(−1)
$p_1 \cdots\cdots$	3.79225	7.099(−1)	7.103(−1)	4.387(−1)
$p_2 \cdots\cdots$	5.67886	1.173(+0)	1.175(+0)	6.713(−1)
$p_3 \cdots\cdots$	7.48089	1.605(+0)	1.608(+0)	8.874(−1)
		$m = 3$		
$g_3 \cdots\cdots$	0.01136	7.583(+1)	7.498(+1)	7.498(+1)
$g_2 \cdots\cdots$	0.01443	5.352(+1)	5.319(+1)	5.319(+1)
$g_1 \cdots\cdots$	0.02008	2.732(+1)	2.732(+1)	2.731(+1)
$f \cdots\cdots$	1.97094	6.696(−1)	6.696(−1)	5.545(−1)
$p_1 \cdots\cdots$	4.22956	8.280(−1)	8.282(−1)	5.196(−1)
$p_2 \cdots\cdots$	6.18783	1.272(+0)	1.272(+0)	7.593(−1)
$p_3 \cdots\cdots$	8.04091	1.701(+0)	1.703(+0)	9.900(−1)

* We use the notation of $1.000 \times 10^N \equiv 1.000(N)$.

Table 2: Coefficients E_2, E_2', and $\bar{E}_2^0$ for g-, f-, and p-modes of $l = m$ for the polytropic model with $n = 1.5$ and $\gamma = -10^{-4}$ *

mode	$\bar{\sigma}_0$	$\bar{E}_2$	$\bar{E}_2'$	$\bar{E}_2^0$
		$m = 1$		
$g_3 \cdots\cdots$	0.00788	-8.899(−1)	-8.120(−1)	-8.123(−1)
$g_2 \cdots\cdots$	0.01057	-1.179(+0)	-1.193(+0)	-1.193(+0)
$g_1 \cdots\cdots$	0.01626	-1.797(+0)	-1.856(+0)	-1.856(+0)
$p_1 \cdots\cdots$	3.08199	5.763(−1)	5.761(−1)	9.406(−2)
$p_2 \cdots\cdots$	4.64233	9.672(−1)	9.668(−1)	1.600(−1)
$p_3 \cdots\cdots$	6.15692	1.329(+0)	1.328(+0)	2.190(−1)
		$m = 2$		
$g_3 \cdots\cdots$	0.01214	2.316(+1)	2.286(+1)	2.286(+1)
$g_2 \cdots\cdots$	0.01564	1.628(+1)	1.607(+1)	1.607(+1)
$g_1 \cdots\cdots$	0.02217	8.198(+0)	8.153(+0)	8.152(+0)
$f \cdots\cdots$	1.84930	4.027(−1)	4.027(−1)	1.621(−1)
$p_1 \cdots\cdots$	3.55537	7.093(−1)	7.093(−1)	1.205(−1)
$p_2 \cdots\cdots$	5.14850	1.073(+0)	1.073(+0)	1.808(−1)
$p_3 \cdots\cdots$	6.69114	1.429(+0)	1.428(+0)	2.454(−1)
		$m = 3$		
$g_3 \cdots\cdots$	0.01547	4.950(+1)	4.872(+1)	4.872(+1)
$g_2 \cdots\cdots$	0.01935	3.546(+1)	3.511(+1)	3.511(+1)
$g_1 \cdots\cdots$	0.02596	1.941(+1)	1.938(+1)	1.938(+1)
$f \cdots\cdots$	2.15084	5.640(−1)	5.640(−1)	2.301(−1)
$p_1 \cdots\cdots$	3.93952	8.393(−1)	8.391(−1)	1.504(−1)
$p_2 \cdots\cdots$	5.58066	1.192(+0)	1.191(+0)	2.007(−1)
$p_3 \cdots\cdots$	7.15896	1.544(+0)	1.542(+0)	2.653(−1)

* We use the notation of $1.000 \times 10^N \equiv 1.000(N)$.

Table 3: Coefficients E_2, E_2', and $\bar{E}_2^0$ for g-, f-, and p-modes of $l = m$ for the polytropic model with $n = 3$ and $\Gamma_1 = 5/3$ *

mode	$\bar{\sigma}_0$	$\bar{E}_2$	$\bar{E}_2'$	$\bar{E}_2^0$
		$m = 1$		
$g_3 \cdots\cdots$	0.88994	-1.088(−3)	-7.875(−4)	-7.747(−3)
$g_2 \cdots\cdots$	1.16154	-1.270(−3)	-1.079(−3)	-9.976(−3)
$g_1 \cdots\cdots$	1.68082	9.069(−4)	7.333(−4)	-1.306(−2)
$p_1 \cdots\cdots$	3.81006	2.906(−1)	2.905(−1)	2.689(−3)
$p_2 \cdots\cdots$	5.01208	4.335(−1)	4.331(−1)	2.803(−3)
$p_3 \cdots\cdots$	6.25522	5.541(−1)	5.538(−1)	3.836(−3)
		$m = 2$		
$g_3 \cdots\cdots$	1.35792	1.948(−1)	1.930(−1)	1.802(−1)
$g_2 \cdots\cdots$	1.70580	1.502(−1)	1.494(−1)	1.332(−1)
$g_1 \cdots\cdots$	2.29614	1.103(−1)	1.099(−1)	8.008(−2)
$f \cdots\cdots$	3.06379	2.193(−1)	2.194(−1)	1.814(−2)
$p_1 \cdots\cdots$	4.14666	3.521(−1)	3.521(−1)	1.064(−2)
$p_2 \cdots\cdots$	5.39097	4.792(−1)	4.788(−1)	7.335(−3)
$p_3 \cdots\cdots$	6.65382	5.990(−1)	5.978(−1)	6.608(−3)
		$m = 3$		
$g_3 \cdots\cdots$	1.70370	4.161(−1)	4.122(−1)	3.942(−1)
$g_2 \cdots\cdots$	2.07374	3.245(−1)	3.227(−1)	3.007(−1)
$g_1 \cdots\cdots$	2.64527	2.338(−1)	2.334(−1)	1.920(−1)
$f \cdots\cdots$	3.12498	2.567(−1)	2.566(−1)	3.173(−2)
$p_1 \cdots\cdots$	4.37567	3.947(−1)	3.946(−1)	1.118(−2)
$p_2 \cdots\cdots$	5.68481	5.193(−1)	5.189(−1)	8.675(−3)
$p_3 \cdots\cdots$	6.98164	6.392(−1)	6.383(−1)	8.076(−3)

* We use the notation of $1.000 \times 10^N \equiv 1.000(N)$.

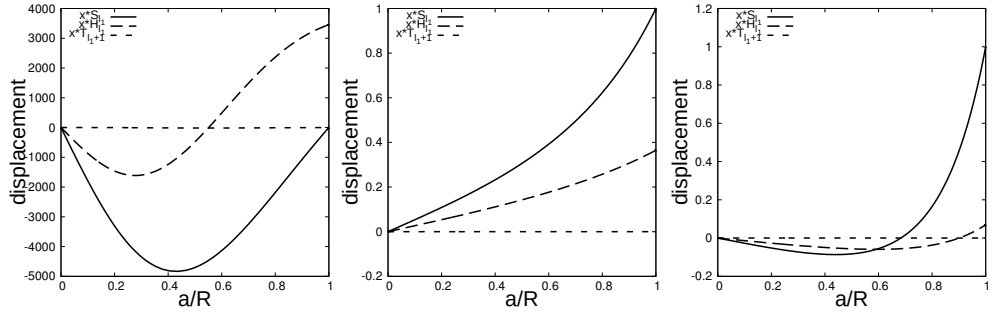

Figure 4: Eigenfunctions of $m = 2$ even modes for the polytrope with $n = 1$ and $\gamma = -10^{-4}$ for $B_0 = 10^{16}$ G, where, from left to right panels, the eigenfunctions plotted are those of the g_1, f, and p_1 modes. The solid lines, the long dashed lines and the short dashed lines are for the functions xS_{l_1}, xH_{l_1}, and xT_{l_1+1} with $x = a/R$, and the amplitude normalization is given by $S_{l_1} = 1$ at the surface, respectively

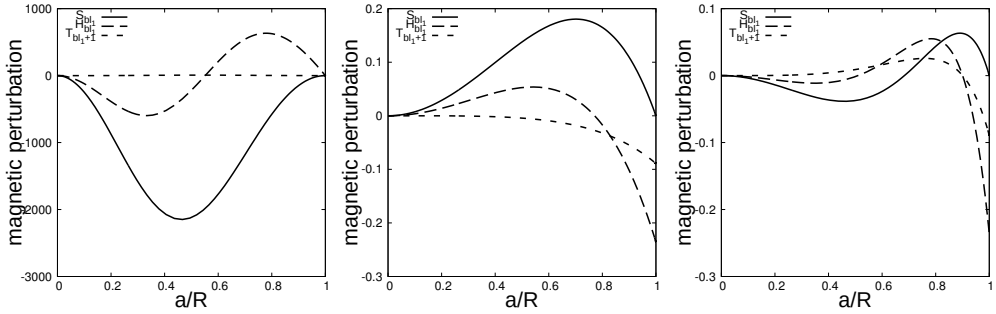

Figure 5: Same as Figure 4 but for the eigenfunctions $S_{bl_1} \equiv k\rho a h_l^S/B_0$ (solid lines), $H_{bl_1} \equiv k\rho a h_l^H/B_0$ (long dashed lines), and $T_{bl_1+1} \equiv k\rho a h_{l'}^T/B_0$ (short dashed lines).

corresponding to angular degrees l_1 and l_1', and they dominate other coefficients of higher degrees of l_j $(j > 1)$. These first expansion coefficients are almost the same as the eigenfunctions of the modes of the non-magnetized stars, for which separation of variables is possible. According to the surface boundary condition and algebraic relation in the Appendix A, since $H_{l_1} \simeq S_{l_1}/\bar{\sigma}^2$ at the stellar surface for $\bar{\Omega} = 0$ and $\bar{\omega}_A^2 \ll 1$, H_{l_1} has large amplitudes at the stellar surface under the normalization condition $S_{l_1}(R) = 1$ for low frequency $(\bar{\sigma} \ll 1)$ g-modes. We plot the magnetic perturbations S_{bl_1}, H_{bl_1}, and $T_{bl_1'}$ of g_1-, f-, and p_1-modes of $l = m = 2$ for $B_0 = 10^{16}$ G for the $n = 1$ polytrope in Figure 5, where $S_{bl_1} \equiv k\rho a h_{l_1}^S/B_0$, $H_{bl_1} \equiv k\rho a h_{l_1}^H/B_0$, and $T_{bl_1'} \equiv k\rho a h_{l_1'}^T/B_0$.

For slowly rotating stars, the frequency ω observed in an inertial frame is written as

$$\omega = \omega_0 + m(C_1 - 1)\Omega + E_2\bar{\omega}_A^2 + \cdots , \tag{3.39}$$

where C_1 is a coefficient related to correction term of the modal frequency affected by slow rotation. For $B_0 = 10^{16}$ - 10^{17} G, since $\bar{\omega}_A^2 \simeq 10^{-5}$ - 10^{-3} and $E_2 \sim 10$, rotational effects dominate magnetic ones for $\bar{\Omega} \gtrsim 10^{-1}$.

3.2.2 rotational modes

Here, we consider the effects of the magnetic field on rotational modes such as inertial mode and r-mode, for which the restoring force is the Coriolis force and the frequencies are proportional to Ω. As shown by Yoshida & Lee (2000b), stratification in the interior of the stars strongly affects the properties of rotational modes. Since we consider only magnetic effects on rotational modes, we assume isentropic stars ($\gamma = 0$). In this assumption, the adiabatic exponent for the perturbations reduces to $\Gamma_1 = 1 + 1/n$. In order to describe the effects of the magnetic field on rotational modes, it is convenient to introduce the frequency ratio $\kappa = \sigma/\Omega$, where $\sigma = \omega + m\Omega$ is the frequency observed in the co-rotating frame of the star. For small $\bar{\omega}_A^2$ ($\ll \bar{\Omega}^2$), we can write the frequency ratio as

$$\kappa = \kappa_0(\Omega)\left[1 + \eta_2 \frac{\bar{\omega}_A^2}{\bar{\Omega}^2}\right] + \cdots , \tag{3.40}$$

where the coefficient κ_0 is a quantity depending on rotation rate Ω, and η_2 reduces to a constant in the limit of $\bar{\omega}_A^2/\bar{\Omega}^2 \to 0$ (see Appendix C). For uniformly rotating isentropic stars, inertial mode and r-mode are examined by e.g., Lokitch & Friedman (1999) and Yoshida & Lee (2000a). r-modes are retrograde mode and have $l' \geq |m|$ ($m \neq 0$), and the frequency ratio κ_0 reduces to $2m/[l'(l'+1)]$ for $\Omega \to 0$. The ratio κ_0 for inertial mode can be defined in the limit of $\Omega \to 0$, and its value depends on azimuthal wavenumber m and polytropic index n (see e.g., Yoshida & Lee 2000a). We use $\kappa_0(0)$ for labeling inertial mode and r-mode.

Because strongly magnetized stars (magnetars) are known to rotate slowly, we analyze rotational modes of slowly rotating stars. In Table 4, we tabulated the coefficients η_2, η_2', and κ_0 of r-modes of $l' = |m|$ and inertial modes ($m = 2$ and $\gamma = 0$) for the polytropes of $n = 1$, 1.5, and 3. η_2' denotes the coefficient calculated with the integration formula using the perturbations of the non-magnetized stars. η_2 is calculated by adopting least square method to fitting formula $y = \eta_2 x$, where $x \equiv 1/\bar{\Omega}^2$ and $y \equiv E_2/\sigma_0$. In Table 4, $l_0 - m = 1$ is corresponding to r-mode and $l_0 - m \geq 2$ is corresponding to inertial mode (see e.g., Yoshida & Lee 2000a). The parity of $l_0 - m$ is related to even and odd parities of modes. Using κ_0, we can write the frequency of rotational modes as $\kappa = \kappa_0 + \kappa_2 \bar{\Omega}^2$. Intercept κ_0 of the fitting formula $y = \kappa_0 + \kappa_2 x$ is also obtained by using least square method. From table 4, we find that η_2 and η_2' are in good agreement with each other. It is important to note that the effects of the deformation due to the toroidal magnetic field on the rotational mode are quite small. This property is similar to that found for low frequency g-modes. We also note that the r-mode obtained in this paper is consistent with that of Lander et al. (2010).

In Figure 6, we plot the eigenfunctions of the rotational modes of $m = 2$ for $B_0 = 10^{16}$ G for the $n = 1$ polytrope, where we assume $\bar{\Omega} = 0.05$ and use the normalization condition $T_{l_1'}(R) = 1$ at the stellar surface. In Figure 7, we plot the magnetic perturbations of the rotational modes of $m = 2$ for $B_0 = 10^{16}$ G. In Figure 8 and 9, we plot the eigenfunctions and magnetic perturbations of the rotational modes of $m = 2$ for $B_0 = 10^6$ G for polytropic index $n = 3$ and $\gamma = 0$ (isentropic).

Table 4: Coefficient η_2 of $m = 2$ rotational modes for isentropic polytropes with the indices $n = 1$, 1.5, and 3 *

$l_0 - \|m\|$	κ_0	η_2	η_2'
		$n = 1$	
1	0.66666	8.324(−1)	8.326(−1)
2	-0.55660	9.105(−1)	9.171(−1)
	1.10002	2.398(−1)	2.401(−1)
3	-1.02590	3.304(−1)	3.316(−1)
	0.51734	1.784(+0)	1.785(+0)
	1.35777	1.402(−1)	1.404(−1)
4	-1.27290	2.481(−1)	2.511(−1)
	-0.27533	7.103(+0)	7.100(+0)
	0.86296	5.805(−1)	5.820(−1)
	1.51956	9.950(−2)	9.957(−2)
		$n = 1.5$	
1	0.66666	5.247(−1)	5.244(−1)
2	-0.69650	3.688(−1)	3.696(−1)
	1.06257	1.752(−1)	1.753(−1)
3	-1.12782	1.439(−1)	1.443(−1)
	0.53564	1.071(+0)	1.069(+0)
	1.31001	1.103(−1)	1.104(−1)
4	-1.34198	8.378(−2)	8.382(−2)
	-0.36425	2.999(+0)	2.993(+0)
	0.85864	3.516(−1)	3.520(−1)
	1.47217	8.210(−2)	8.237(−2)
		$n = 3$	
1	0.66667	1.329(−1)	1.328(−1)
2	-1.07669	2.505(−2)	2.520(−2)
	0.99492	3.902(−2)	3.892(−2)
3	-1.37189	1.849(−2)	1.872(−2)
	0.57976	2.620(−1)	2.622(−1)
	1.20940	2.680(−2)	2.665(−2)
4	-1.51785	6.058(−3)	6.101(−3)
	-0.66228	2.063(−1)	2.064(−1)
	0.85853	6.254(−2)	6.253(−2)
	1.36256	2.973(−2)	3.023(−2)

* We use the notation of $1.000 \times 10^N \equiv 1.000(N)$.

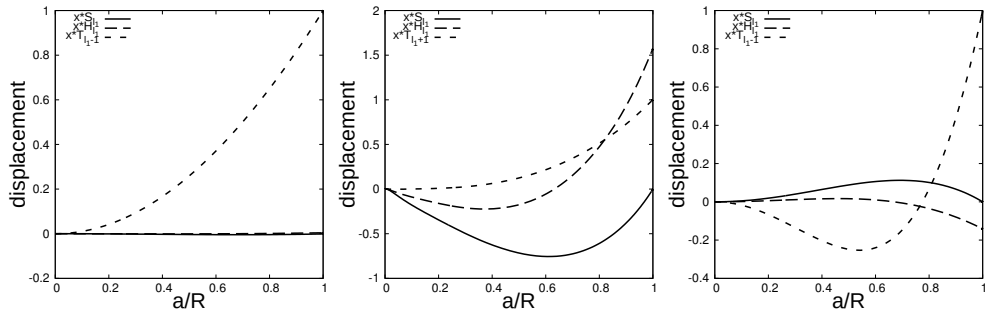

Figure 6: Eigenfunctions of $m = 2$ rotational modes for the isentropic $n = 1$ polytrope for $B_0 = 10^{16}$ G: r mode of $\kappa_0 = 0.6667$ (left), and inertial modes of $\kappa_0 = 1.1000$ (center) and $\kappa_0 = 0.5173$ (right). The solid lines, the long dashed lines, and the short dashed lines are for the functions xS_{l_1}, xH_{l_1}, and $xT_{l'_1}$ with $x = a/R$, respectively, and the amplitude normalization is given by $\max(xT_{l'_1}) = 1$.

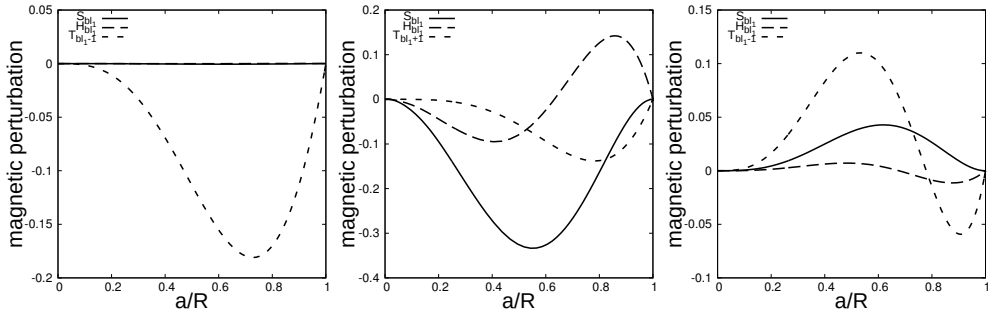

Figure 7: Same as Figure 6 but for the eigenfunctions $S_{bl_1} \equiv k\rho a h_l^S / B_0$ (solid lines), $H_{bl_1} \equiv k\rho a h_l^H / B_0$ (long dashed lines), and $T_{bl'_1} \equiv k\rho a h_{l'}^T / B_0$ (short dashed lines).

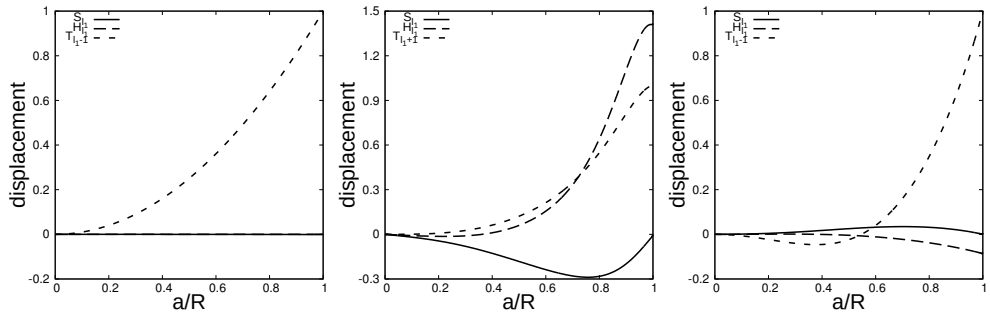

Figure 8: Eigenfunctions of $m = 2$ rotational modes for the isentropic $n = 3$ polytrope for $B_0 = 10^6$ G: r mode of $\kappa_0 = 0.6667$ (left), and inertial modes of $\kappa_0 = 0.9949$ (center) and $\kappa_0 = 0.5798$ (right). The solid lines, the long dashed lines, and the short dashed lines are for the functions xS_{l_1}, xH_{l_1}, and $xT_{l'_1}$ with $x = a/R$, respectively, and the amplitude normalization is given by $\max(xT_{l'_1}) = 1$.

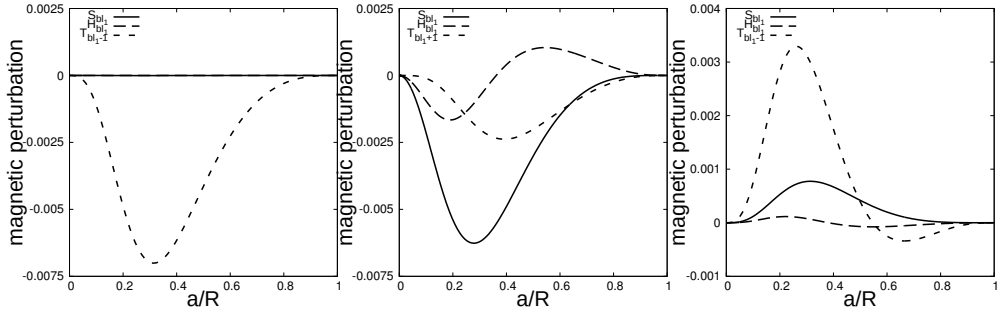

Figure 9: Same as Figure 8 but for the eigenfunctions $S_{bl_1} \equiv k\rho a h_l^S/B_0$ (solid lines), $H_{bl_1} \equiv k\rho a h_l^H/B_0$ (long dashed lines), and $T_{bl'_1} \equiv k\rho a h_{l'}^T/B_0$ (short dashed lines).

3.2.3 magnetic modes

In order to find magnetic modes (which have frequencies comparable with the characteristic Alfvén frequency of the star) having real frequencies ($\sigma^2 > 0$), we looked for low frequency modes for non-rotating stars, but we could not find any of such low frequency magnetic modes. We do obtain solutions having pure imaginary frequencies ($\sigma^2 < 0$), but we cannot regard them as correct magnetic modes because they depend on $j_{\max}$. We note that we cannot obtain g-modes either in the low frequency ranges corresponding to frequency ranges expected for magnetic modes. The function $\boldsymbol{\xi}$ of these modes in the low frequency ranges have discontinuity as a function of a. This phenomenon may suggest that modes having this discontinuity belong to continuum bands of frequency spectra (see section 7.4 of Goedbloed & Poedts 2004). The discontinuity of the function $\boldsymbol{\xi}$ may be associated with the relation $\mathbf{A}\boldsymbol{\Psi} = \mathbf{B}\boldsymbol{\Phi}$, that is, there exist regions in which the determinant of the matrix $\mathbf{A}$ vanishes, where $\boldsymbol{\Psi} = (\boldsymbol{H}, \boldsymbol{T})^T$, $\boldsymbol{\Phi} = (\boldsymbol{y}_1, \boldsymbol{y}_2)^T$, and $\mathbf{A}$ and $\mathbf{B}$ are matrices (see Appendix A). Goedbloed & Poedts (2004) discuss a system in which a second order differential equation governing magnetic waves becomes singular in a certain frequency band. Note that the situation we have in our calculation system for low-frequency range is essentially the same as the second order differential equation assuming anelastic approximation $\nabla \cdot (\rho\boldsymbol{\xi}) \approx 0$.

Our results discussed above are quite different from those obtained by Lander et al. (2010). They found polar Alfvén and axial Alfvén modes for magnetized rotating star with purely toroidal magnetic field. They suggest that pure Alfvén mode for non-rotating star or purely inertial mode for magnetized non-rotating star are replaced by hybrid magneto-inertial mode for magnetized rotating star (see also Mathis & Brye 2011, 2012). They also suggest that hybrid magneto-inertial mode reduces to purely inertial mode in the limit of $\mathcal{M}/\mathcal{T} \to 0$, where $\mathcal{M}$ and $\mathcal{T}$ are magnetic energy and kinetic energy of equilibrium model, respectively. The method of solution of Lander et al. (2010) is MHD simulation following time evolution of linear oscillation modes and differs from our method (normal mode analysis). At the moment we do not understand why we can not calculate the magnetic modes found by Lander et al (2010).

4 Normal magnetic modes of neutron stars magnetized with purely poloidal magnetic fields

In this section, we discuss low frequency magnetic modes of neutron stars magnetized with purely poloidal magnetic fields. We no not take account of the effects of rotation and equilibrium deformation due to the magnetic fields. We use polytropes of indices $n = 1$ and 1.5 as back ground models for modal analysis.

4.1 method of solution

4.1.1 equilibrium model

As back ground models for modal analysis of neutron stars, we use polytropes of indices $n = 1$ and 1.5. We assume the stars are magnetized with purely poloidal fields, and for simplicity we do not take account of the effects of equilibrium deformation due to the magnetic fields. We do not consider the effects of rotation either.

The density and pressure of the stars are given by

$$\rho = \rho_0 \Theta^n, \quad p = p_0 \Theta^{n+1}, \tag{4.1}$$

where ρ_0 and p_0 are the central density and pressure of the stars, and n and Θ denote the polytropic index and Lane-Emden function.

Purely poloidal magnetic fields are given by (see §2.4)

$$B_r = 2f(r)\cos\theta, \quad B_\theta = -\left[r\frac{\mathrm{d}f(r)}{\mathrm{d}r} + 2f(r)\right]\sin\theta, \quad B_\phi = 0. \tag{4.2}$$

This configuration automatically satisfies $\nabla \cdot \boldsymbol{B} = 0$. Here we use spherical polar coordinates (r, θ, ϕ). The function $f(r)$ satisfies the following Grad-Shafranov equation derived from the Ampere's law $\nabla \times \boldsymbol{B} = 4\pi j_\phi r \sin\theta \boldsymbol{e}_\phi$ (see §2.4):

$$\frac{\mathrm{d}^2 f}{\mathrm{d}r^2} + \frac{4}{r}\frac{\mathrm{d}f}{\mathrm{d}r} = -4\pi j_\phi, \tag{4.3}$$

where j_ϕ is related to the toroidal current and need to satisfy integrability condition (see §2.4). Therefore, we assume $j_\phi = c_0\rho$, where c_0 is a constant determined by outer boundary condition at stellar surface. The function $f(r)$ behaves near the center of the star as follows:

$$f(r) \sim \alpha_0 + \mathcal{O}(r^2), \tag{4.4}$$

where α_0 is another constant determined by the outer boundary condition at the surface of the star. We assume $j_\phi = 0$ in the outside of the star. Thus, exterior solution $f^{(\mathrm{ex})}$ is given by $f^{(\mathrm{ex})} = \mu_b/r^3$, where μ_b denotes magnetic dipole moment. The constants α_0 and c_0 are determined by imposing continuity conditions $f = f^{(\mathrm{ex})}$ and $\mathrm{d}f/\mathrm{d}r = \mathrm{d}f^{(\mathrm{ex})}/\mathrm{d}r$ at the stellar surface. In Figure 10, we plot magnetic field lines for $n = 1$ and 1.5 polytropes. From Figure 10 we find there are closed field lines in the interior of the stars.

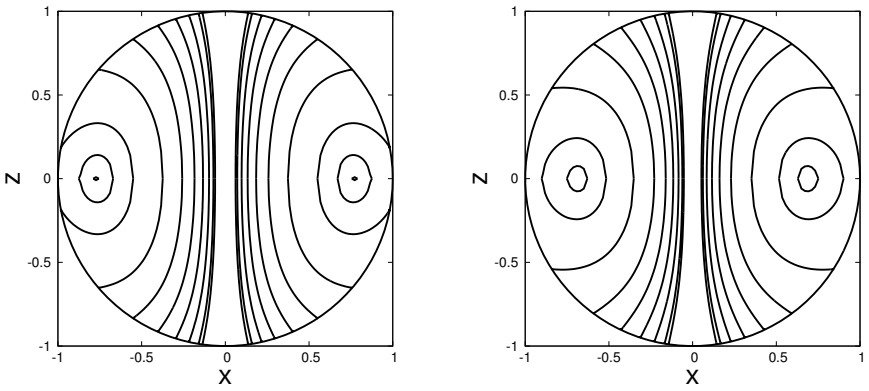

Figure 10: Magnetic field lines in the polytropic model of index $n = 1$ (left pannel) and $n = 1.5$ (right pannel).

4.1.2 perturbation equations

The basic perturbed equations we employ here are the same as those for stars magnetized with purely toroidal magnetic fields, except that we take, in equations (3.23)-(3.26), the limits $\epsilon \to 0$, $a \to r$, and $\boldsymbol{D} \to 0$. We then obtain

$$-\sigma^2 \boldsymbol{\xi} = -\nabla \delta\Phi - \frac{1}{\rho}\nabla \delta p + \frac{\delta\rho}{\rho^2}\frac{\mathrm{d}p}{\mathrm{d}r}\boldsymbol{e}_r + \frac{1}{4\pi\rho}[(\nabla \times \delta\boldsymbol{B}) \times \boldsymbol{B} + (\nabla \times \boldsymbol{B}) \times \delta\boldsymbol{B}], \tag{4.5}$$

$$\delta\rho + \nabla \cdot (\rho\boldsymbol{\xi}) = 0, \tag{4.6}$$

$$\frac{\delta\rho}{\rho} = \frac{\delta p}{\Gamma_1 p} - \frac{\xi_r}{r} rA, \tag{4.7}$$

$$\delta\boldsymbol{B} = \nabla \times (\boldsymbol{\xi} \times \boldsymbol{B}). \tag{4.8}$$

Since separation of variables between radial coordinate (r) and angular coordinates (θ, ϕ) is not possible because of the Lorentz force term, we expand perturbations in terms of spherical harmonic functions $Y_l^m(\theta, \phi)$. The displacement vector is given by equations (3.30)-(3.32) in the limit of $a \to r$, that is (see e.g., Lee 2005, 2007),

$$\xi_r = \sum_{j=1}^{j_{\max}} r S_{l_j}(r) Y_{l_j}^m(\theta, \phi), \tag{4.9}$$

$$\xi_\theta = \sum_{j=1}^{j_{\max}} \left[r H_{l_j}(r) \frac{\partial}{\partial\theta} Y_{l_j}^m(\theta, \phi) - ir T_{l'_j}(r) \frac{1}{\sin\theta} \frac{\partial}{\partial\phi} Y_{l'_j}^m(\theta, \phi) \right], \tag{4.10}$$

$$\xi_\phi = \sum_{j=1}^{j_{\max}} \left[r H_{l_j}(r) \frac{1}{\sin\theta} \frac{\partial}{\partial\phi} Y_{l_j}^m(\theta, \phi) + ir T_{l'_j}(r) \frac{\partial}{\partial\theta} Y_{l'_j}^m(\theta, \phi) \right], \tag{4.11}$$

and the magnetic perturbations (3.33) to (3.35) are

$$\delta B_r = \sum_{j=1}^{j_{\max}} r b_{l'_j}(r) Y_{l'_j}^m(\theta, \phi), \tag{4.12}$$

$$\delta B_\theta = \sum_{j=1}^{j_{\max}} \left[r b_{l'_j}^H(r) \frac{\partial}{\partial \theta} Y_{l'_j}^m(\theta,\phi) - i r b_{l_j}^T(r) \frac{1}{\sin\theta} \frac{\partial}{\partial \phi} Y_{l_j}^m(\theta,\phi) \right], \tag{4.13}$$

$$\delta B_\phi = \sum_{j=1}^{j_{\max}} \left[r b_{l'_j}^H(r) \frac{1}{\sin\theta} \frac{\partial}{\partial \phi} Y_{l'_j}^m(\theta,\phi) + i r b_{l_j}^T(r) \frac{\partial}{\partial \theta} Y_{l_j}^m(\theta,\phi) \right]. \tag{4.14}$$

The perturbed density and pressure in (3.36) reduce to in the limit of $a \to r$:

$$\delta p = \sum_{j=1}^{j_{\max}} \delta p_{l_j}(r) Y_{l_j}^m(\theta,\phi), \quad \delta\rho = \sum_{j=1}^{j_{\max}} \delta\rho_{l_j}(r) Y_{l_j}^m(\theta,\phi), \tag{4.15}$$

where $l_j = |m| + 2(j-1)$ and $l'_j = l_j + 1$ for even modes, and $l_j = |m| + 2j - 1$ and $l'_j = l_j - 1$ for odd modes ($j = 1, 2, 3, ..., j_{\max}$).

Substituting expansion forms (4.9)-(4.15) into linearized basic equations (4.5)-(4.8), we obtain a system of coupled linear ordinary differential equations for the expansion coefficients $S_{l_j}(r)$, $T_{l'_j}(r)$, $b_{l'_j}^S(r)$, $b_{l'_j}^H(r)$, $b_{l_j}^T(r)$, and $r\mathrm{d}b_{l'_j}^H(r)/\mathrm{d}r$. These equations are solved as a boundary and eigenvalue problem under the suitable boundary conditions (see Appendix D for the detail). The oscillation modes are separated into even modes and odd modes. For example, for an even mode, $(\xi_r, \xi_\phi, \delta B_\theta)$ and $(\xi_\theta, \delta B_r, \delta B_\phi)$ are even and odd functions about the equatorial plane for purely poloidal magnetic fields. Since eigenvalues σ^2 are real number for the boundary conditions, positive value of $\sigma^2 > 0$ are corresponding to stable oscillation modes with frequencies $\pm\sigma$, and negative value of $\sigma^2 < 0$ are corresponding to unstable monotonically growing modes with growth rates $\eta = \sqrt{-\sigma^2}$.

4.2 numerical results

We calculate non-axisymmetric ($m \neq 0$) magnetic modes for polytropes of indices $n = 1$ and 1.5, where the frequency of the magnetic modes is proportional to the strength of magnetic field $B_{\rm S}$ measured at the stellar surface. In contrast to the case of purely toroidal magnetic fields, we can not find g-, f-, and p-modes, and oscillation modes we can find are magnetic modes only. We obtain two kinds of magnetic modes, that is, stable oscillatory magnetic modes with $\sigma^2 > 0$ and unstable monotonically growing magnetic mode with $\sigma^2 < 0$. For unstable monotonically growing magnetic modes ($\sigma^2 < 0$), describing $\sigma = \sigma_{\rm I} i = \pm\eta i$ (η is a positive constant), time dependence of the mods is given by $\exp(\mp\eta t)$. The magnetic modes having time dependence of $\exp(\eta t)$ grow monotonically with time. Then, we can regard η as the growth rate, and the modes with $\sigma^2 < 0$ are corresponding to magnetic instability. It is well known that magnetized stars having purely poloidal magnetic fields are unstable and magnetic energies stored in the equilibrium configuration are quickly dispersed in several ten milliseconds (e.g., Marky & Tayler 1973; van Assche, Goossens & Tayler 1982; Braithwaite 2007; Laskey et al. 2011; Ciolfi & Rezzolla 2012).

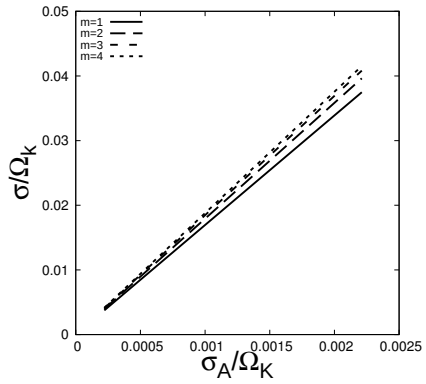

Figure 11: Eigenfrequency σ of the stable magnetic modes of odd parity for $m = 1$, 2, 3, and 4 versus the Alfvén frequency σ_A for the $n = 1$ polytrope.

4.2.1 stable magnetic modes

In Figure 11, we plot eigenfrequencies of stable magnetic modes which have no radial nodes of S_{l_1} of $m = 1$, 2, 3, and 4 versus the Alfvén frequency σ_A, where σ_A is defined by

$$\sigma_A \equiv \frac{B_{\rm S}}{\sqrt{4\pi\rho_c R^2}}, \tag{4.16}$$

where ρ_c is the central density, R is the radius, and $B_{\rm S} = \mu_b/R^3$ denotes the strength of magnetic field measured at the stellar surface. Here, σ and σ_A are normalized by $\Omega_{\rm K} = \sqrt{GM/R^3}$ where M is the mass and G is the gravitational constant. We also assume $M = 1.4M_\odot$ and $R = 10^6$ cm for the polytropes of indices $n = 1$ and 1.5, and we have $\sigma_A/\Omega_{\rm K} = 4.42 \times 10^{-4}(B_{\rm S}/10^{15}{\rm G})$. It is important to note that the eigenfrequencies of magnetic modes obtained in this subsection form a discrete frequency spectrum, and that the frequencies are proportional to the Alfvén frequency σ_A, that is, $B_{\rm S}$, and that the functions $\boldsymbol{\xi}$ have no discontinuity in the interior of the stars. We also note that stable magnetic modes are found only for odd parity.

In Table 5, we tabulated eigenfrequency $\bar{\sigma} = \sigma/\Omega_{\rm K}$ of stable magnetic modes for the $n = 1$ and 1.5 polytropes for $B_{\rm S} = 10^{15}$ G, where we have assumed $\gamma = 0$ for $1/\Gamma_1 = n/(n+1) + \gamma$. We calculate only magnetic modes that have a few radial nodes of S_{l_1} for a given azimuthal wavenumber m. It becomes more difficult to calculate magnetic modes as the number of radial nodes increases. From Table 5, the eigenfrequencies of magnetic modes for $n = 1.5$ are larger than those for $n = 1$ for a given m and a given number of radial nodes of S_{l_1}. For a given m, the frequency decreases as the number of radial nodes of S_{l_1} increases. This property of the eigenfrequencies of the magnetic modes means that the magnetic modes are anti-Strumian and behave in a similar to the axisymmetric toroidal modes calculated by Asai & Lee (2014), who analised axisymmetric toroidal modes of magnetized neutron stars with purely poloidal magnetic fields under general relativistic framework. Further, the frequencies of the magnetic modes increase as m increases.

In Figure 12, we plot the eigenfunctions of the magnetic mode of $m = 1$ for $B_0 = 10^{15}$ G for the polytrope of index $n = 1$, where the number of radial nodes of S_{l_1} is zero. We find $\boldsymbol{S}$, $\boldsymbol{H}$, and $\boldsymbol{T}$ have large amplitudes in the core, and the horizontal component $\boldsymbol{H}$ and toroidal component

Table 5: Normalized eigenfrequency $\bar{\sigma}$ of the stable magnetic modes of odd parity for $B_{\rm S} = 10^{15}$ G.

$n = 1$			
m	number of radial nodes		
	0	1	2
1	0.007523	0.007120	0.006954
2	0.007943	0.007464	0.007216
3	0.008174	0.007710	0.007439
4	0.008310	0.007887	0.007618
$n = 1.5$			
m	number of radial nodes		
	0	1	2
1	0.010304	0.009975	0.009817
2	0.010720	0.010247	0.010038
3	0.010961	0.010485	0.010229
4	0.011106	0.010663	0.010397

$\boldsymbol{T}$ show rapid spacial oscillations near the stellar surface, while the radial component $\boldsymbol{S}$ does not. For isentropic ($\gamma = 0$) cases, we can calculate stable magnetic modes even for the field strength $B_{\rm S} \sim 10^{12}$ G.

Assuming $\phi = 0$, the spacial oscillation pattern $\hat{\boldsymbol{\xi}}$ of the displacement vector $\boldsymbol{\xi}$ is defined by

$$\hat{\xi}_j(r,\theta) = \xi_j(r,\theta,\phi=0), \tag{4.17}$$

where $j = r$, θ, and ϕ. The oscillation patterns $\hat{\xi}_j(r,\theta)$ of a stable magnetic mode are shown in Figure 13, where the z-axis given by $x = 0$ is the symmetry axis and we have applied the amplitude normalization condition given by $\max(|\hat{\xi}_j(r,\theta)|) = 1$. Since stable magnetic modes have odd parity, the patterns $\hat{\xi}_r(r,\theta)$ and $\hat{\xi}_\phi(r,\theta)$ are antisymmetric to the equatorial plane ($z = 0$), while $\hat{\xi}_\theta(r,\theta)$ is symmetric. The oscillation patterns have large amplitudes along the symmetry axis. We find the ϕ-component of $\hat{\boldsymbol{\xi}}$ reflects the closed magnetic field lines near the stellar surface.

In Table 6, we tabulated the ratios $|\hat{\xi}_\theta^{\max}|/|\hat{\xi}_r^{\max}|$ and $|\hat{\xi}_\phi^{\max}|/|\hat{\xi}_r^{\max}|$ of magnetic modes that have no radial nodes of S_{l_1} for the $n = 1$ and 1.5 polytropes for $B_0 = 10^{15}$ G and $\gamma = 0$, where $|\hat{\xi}_j^{\max}| = \max(|\hat{\xi}_j(r,\theta)|)$. From Table 6, we find that the ratios $|\hat{\xi}_\theta^{\max}|/|\hat{\xi}_r^{\max}|$ and $|\hat{\xi}_\phi^{\max}|/|\hat{\xi}_r^{\max}|$ do not strongly depend on the azimuthal wavenumber m, and that $\hat{\xi}_r$ and $\hat{\xi}_\theta$ dominate $\hat{\xi}_\phi$. The pressure perturbation $\delta U \equiv \delta p(r,\theta,\phi=0)/(\rho g r)$ is negligible compared with the displacement vector. We find the oscillation patterns for the $n = 1$ polytrope are almost the same as those for the $n = 1.5$ polytrope. The ratios $|\hat{\xi}_\phi^{\max}|/|\hat{\xi}_r^{\max}|$ for the polytrope of index $n = 1$ are slightly larger than those for the polytrope of index $n = 1.5$. As the azimuthal index $|m|$ increases, the amplitudes of oscillation patterns are pushed from the symmetry axis to the envelope region.

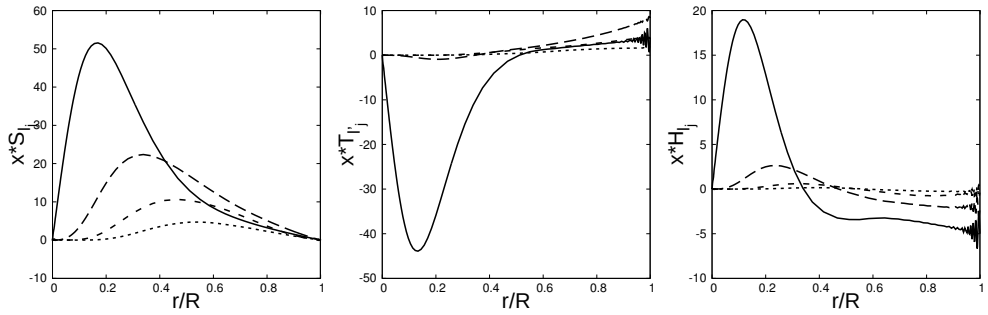

Figure 12: Expansion coefficients xS_l, $xT_{l'}$, and xH_l as a function of $x = r/R$ for an $m = 1$ stable magnetic mode of odd parity for the polytrope with $n = 1$ for $B_{\rm S} = 10^{15}$ G, where the solid lines, the long dashed lines, the short dashed lines, and the dotted lines are for the expansion coefficients associated with l_j (or l'_j) from $j = 1$ to 4. The amplitude normalization is given by $T_{l'_{l_1}} = 1$ at the surface. Here, the frequency $\bar{\sigma} \equiv \sigma/\Omega_{\rm K}$ of the mode is 0.007523.

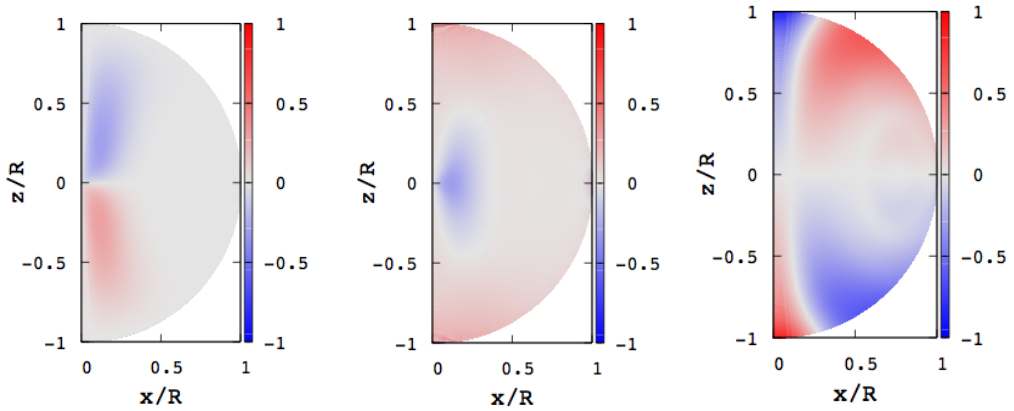

Figure 13: Spatial oscillation patterns $\hat{\xi}_r(r,\theta)$ (left), $\hat{\xi}_\theta(r,\theta)$ (middle), and $\hat{\xi}_\phi(r,\theta)$ (right) of the $m = 1$ stable magnetic mode of Figure 12, where the amplitudes are normalized such that $\max(|\hat{\xi}_j(r,\theta)|) = 1$.

Table 6: Amplitude ratios between the components of the displacement vector of stable magnetic modes of odd parity for $B_{\rm S} = 10^{15}$ G

$n = 1$			
m	$\lvert\hat{\xi}_\theta^{\max}\rvert/\lvert\hat{\xi}_r^{\max}\rvert$	$\lvert\hat{\xi}_\phi^{\max}\rvert/\lvert\hat{\xi}_r^{\max}\rvert$	$\lvert\delta U^{\max}\rvert/\lvert\hat{\xi}_r^{\max}\rvert$
1	1.109	0.322	9.833×10^{-6}
2	0.787	0.304	1.236×10^{-5}
3	1.234	0.366	1.408×10^{-5}
4	1.121	0.396	1.595×10^{-5}
$n = 1.5$			
1	2.552	0.111	6.954×10^{-6}
2	0.897	0.047	3.358×10^{-6}
3	1.124	0.051	5.376×10^{-6}
4	1.365	0.103	7.191×10^{-6}

Table 7: Growth rate $\bar{\eta} \equiv \eta/\Omega_{\rm K}$ of the monotonically growing magnetic modes of even and odd parities for $B_{\rm S} = 10^{15}$ G

$n = 1$							
	even parity				odd parity		
m	number of radial nodes			m	number of radial nodes		
	1	2	3		1	2	3
1	0.000961	0.000580	0.000405	1			
2	0.001557	0.000977	0.000709	2	0.003562		
3	0.001964	0.001273	0.000949	3	0.004435	0.002038	
4	0.002260	0.001505	0.001144	4	0.004879	0.003088	
5	0.002488	0.001695	0.001452	5	0.005147	0.003685	0.002008
6	0.002676	0.001859	0.001452	6	0.005326	0.004086	0.002728
7	0.002852	0.002110	0.001889	7	0.005454	0.004377	0.003209
8	0.003096	0.002616	0.002069	8	0.005548	0.004598	0.003566
$n = 1.5$							
	even parity				odd parity		
m	number of radial nodes			m	number of radial nodes		
	1	2	3		1	2	3
1	0.000898	0.000430		1			
2	0.001601	0.000804		2			
3	0.002114	0.001121		3			
4	0.002482	0.001386		4	0.006170	0.003683	
5	0.002769	0.001618		5	0.006510	0.004506	0.002007
6	0.003328	0.002611		6	0.006734	0.005047	0.003147
7	0.004089	0.002895		7	0.006892	0.005435	0.003849
8	0.004659	0.003053		8	0.007009	0.005727	0.004354

4.2.2 unstable magnetic modes

Unstable magnetic modes are found for both even and odd parities. If we define the growth rate $\eta > 0$ as $\sigma = \pm\eta i$, η is exactly proportional to the strength of magnetic field $B_{\rm S}$ for $\gamma = 0$. In Table 7, we tabulated normalized growth rate $\bar{\eta} = \eta/\Omega_{\rm K}$ of unstable magnetic modes for $\gamma = 0$ and $B_{\rm S} = 10^{15}$ G for the polytropes of indices $n = 1$ and 1.5. We note that there exists unstable magnetic modes even for weak magnetic field as $B_{\rm S} \sim 10^{12}$ G. In Table 7, we find the growth rates $\bar{\eta}$ of unstable magnetic modes of $n = 1$ and 1.5 polytropes are quite similar to each other. It becomes difficult to calculate unstable magnetic modes as the number of radial nodes of S_{l_1} increases, especially for the polytrope of index $n = 1.5$. Unstable magnetic modes of odd parity are found only for $m \geq 2$ for the $n = 1$ polytrope, and only for $m \geq 4$ for the $n = 1.5$ polytrope. For a given m, the growth rate $\bar{\eta}$ decreases as the number of radial nodes of S_{l_1} increases. On the other hand, the growth rate of unstable modes become larger as the azimuthal index m increases. Using the normalized growth rate $\bar{\eta}$, the growth timescale $\tau_g = 1/\eta$ is given by

$$\tau_g = 7.33 \times 10^{-5}/\bar{\eta} \text{ s}, \tag{4.18}$$

where we assume $M = 1.4M_\odot$ and $R = 10^6$ cm. Using a characteristic value of $\bar{\eta} \sim 10^{-3}$, we obtain the growth timescale as $\tau_g \sim 5 \times 10^{-2}$ s. This estimate is consistent with the results obtained by e.g., Laskey et al. (2011) and Ciolfi & Rezzolla (2012).

In Figure 14, we plot the eigenfunctions of an unstable magnetic mode of even parity of $m = 1$

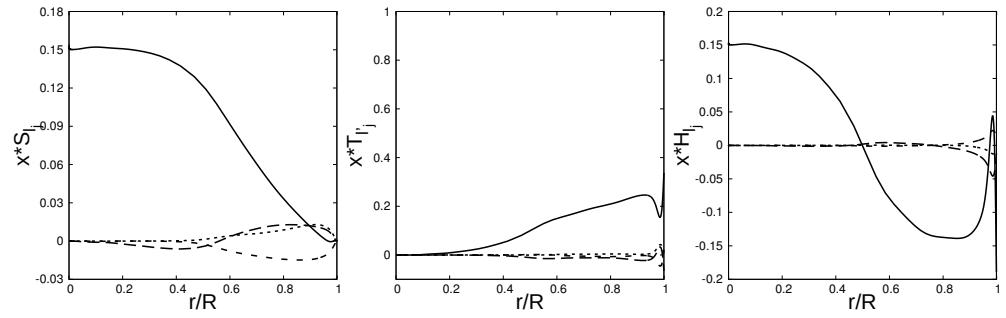

Figure 14: Same as Figure 12 but for an $m = 1$ unstable magnetic mode of even parity with the growth rate $\bar{\eta} = 0.00096$.

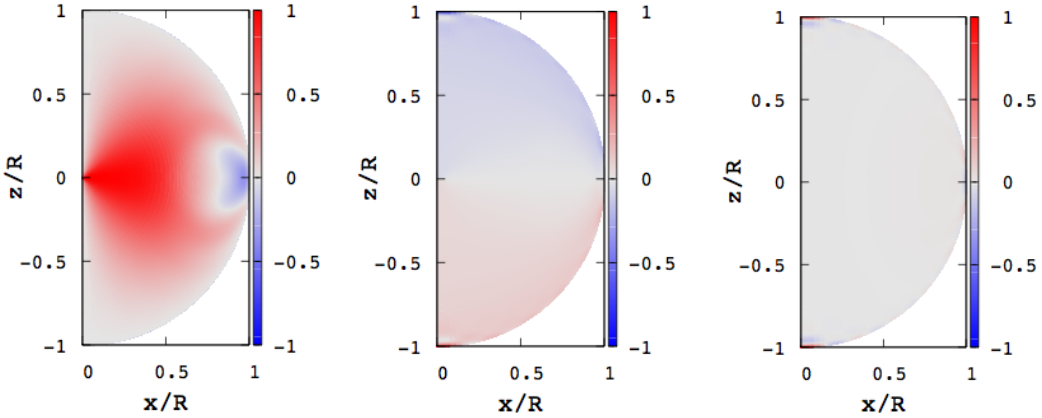

Figure 15: Same as Figure 13 but for the $m = 1$ unstable magnetic mode of Figure 14.

that has one radial node of S_{l_1} for $B_{\rm S} = 10^{15}$ G for the polytrope of index $n = 1$, where we normalize the amplitudes as $T_{l_1'}(R) = 1$. We find that S_{l_1} has large amplitudes in the core, while $T_{l_1'}$ in the envelope. H_{l_1} has large amplitudes both in the core and in the envelope. We note that first components of $\boldsymbol{S}$, $\boldsymbol{H}$, and $\boldsymbol{T}$ dominate the other components of higher l_j or l_j'.

The oscillation patterns $\hat{\xi}_r(r,\theta)$, $\hat{\xi}_\theta(r,\theta)$, and $\hat{\xi}_\phi(r,\theta)$ of the unstable magnetic mode of $m = 1$ are shown in Figure 15. Since this unstable mode has even parity, $\hat{\xi}_r(r,\theta)$ and $\hat{\xi}_\phi(r,\theta)$ are symmetric about the equatorial surface, and $\hat{\xi}_\theta(r,\theta)$ is antisymmetric. The pattern $\hat{\xi}_r(r,\theta)$ has large amplitudes along the equatorial surface, while the θ and ϕ components of $\hat{\boldsymbol{\xi}}$ have in the polar regions. We find that the closed magnetic field lines affects the r component of $\hat{\boldsymbol{\xi}}$.

In Table 8, we tabulated relative amplitudes $|\hat{\xi}_\theta^{\rm max}|/|\hat{\xi}_r^{\rm max}|$ and $|\hat{\xi}_\phi^{\rm max}|/|\hat{\xi}_r^{\rm max}|$ of unstable magnetic modes for $B_0 = 10^{15}$ G for the polytropes of indices $n = 1$ and 1.5. From Table 8, we find that the ratios $|\hat{\xi}_\theta^{\rm max}|/|\hat{\xi}_r^{\rm max}|$ and $|\hat{\xi}_\phi^{\rm max}|/|\hat{\xi}_r^{\rm max}|$ decrease as the azimuthal wavenumber m increases, and $\hat{\xi}_\phi(r,\theta)$ dominate the other components of $\hat{\boldsymbol{\xi}}$. The pressure perturbation is negligible compared with the displacement vector, as in the case of stable magnetic modes. We note that oscillation patterns of the modes for $n = 1$ and 1.5 polytropes are almost the same with each other.

In Figures 16 and 17, we plot the eigenfunctions and spacial oscillation patterns of an unstable

Table 8: Amplitude ratios between the components of the displacement vector of the unstable magnetic modes of even parity for $B_{\rm S} = 10^{15}$ G

m	$\lvert\hat{\xi}_\theta^{\max}\rvert/\lvert\hat{\xi}_r^{\max}\rvert$	$\lvert\hat{\xi}_\phi^{\max}\rvert/\lvert\hat{\xi}_r^{\max}\rvert$	$\lvert\delta U^{\max}\rvert/\lvert\hat{\xi}_r^{\max}\rvert$
	$n = 1$		
1	17.05	319.1	3.462×10^{-4}
2	10.95	120.5	3.706×10^{-4}
3	9.183	72.64	3.137×10^{-4}
4	7.996	49.24	2.538×10^{-4}
	$n = 1.5$		
1	31.98	685.1	1.471×10^{-4}
2	14.39	159.9	1.166×10^{-4}
3	7.662	63.72	7.266×10^{-5}
4	10.66	69.91	1.082×10^{-4}

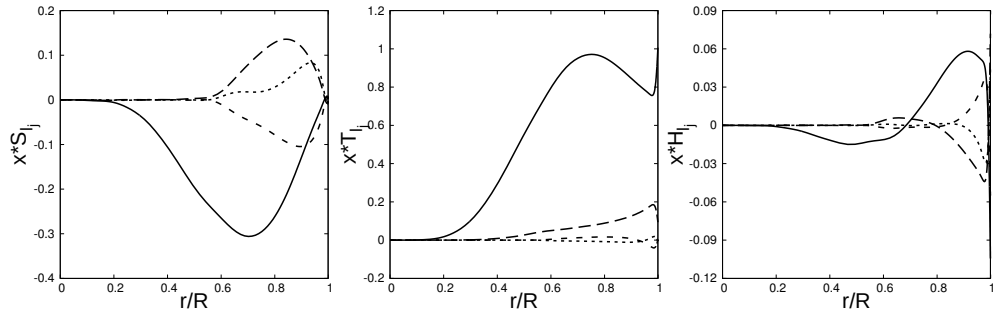

Figure 16: Same as Figure 14 but for an $m = 5$ oscillatory magnetic modes of odd parity with the growth rate $\bar{\eta} = 0.005147$.

mode of odd parity of $m = 5$ that has one radial node of S_{l_1} for $B_0 = 10^{15}$ G for the polytrope of index $n = 1$. The toroidal components $T_{l'_j}$ of the displacement vector $\boldsymbol{\xi}$ are similar to those of even parity of $m = 1$, however the amplitudes of the components S_{l_j} and H_{l_j} are confined to the envelope region in contrast to those of even parity of $m = 1$. From Figure 17, we find the amplitudes of the unstable modes of $m = 5$ are large in envelope region.

4.2.3 discussion

In Figure 18, we plot the frequency σ/σ_A of a stable magnetic mode of $m = 2$ and the growth rate η/σ_A of an unstable magnetic mode of even parity of $m = 2$ having no radial nodes of S_{l_1} for $B_0 = 10^{15}$ G for the polytrope of index $n = 1$ as a function of $\sqrt{|\gamma|}$. As $|\gamma|$ increases, the frequency σ/σ_A gradually increases (decreases) for $\gamma < 0$ ($\gamma > 0$), where we cannot calculate magnetic modes for $\sqrt{|\gamma|}/\sigma_A \gtrsim 10$. On the other hand, the growth rate η/σ_A decreases (increases) for $\gamma < 0$ ($\gamma > 0$) as $|\gamma|$ increases, where we cannot calculate for $\sqrt{|\gamma|}/\sigma_A \gtrsim 4$. For radiative star ($\gamma < 0$), the buoyant force contributes to stabilizing magnetic instability as $|\gamma|$ increases. We note the relations between σ/σ_A and $|\gamma|^{1/2}/\sigma_A$ and between η/σ_A and $|\gamma|^{1/2}/\sigma_A$ are insensitive

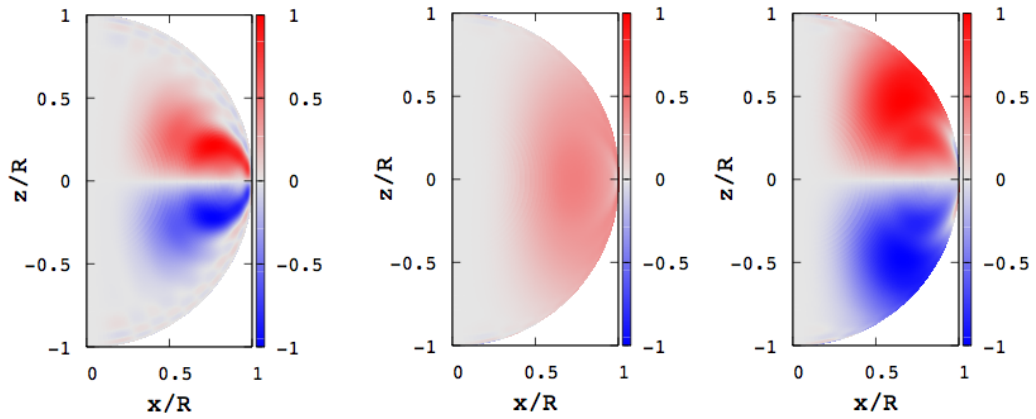

Figure 17: Same as Figure 15 but for the $m = 5$ unstable magnetic mode of Figure 16.

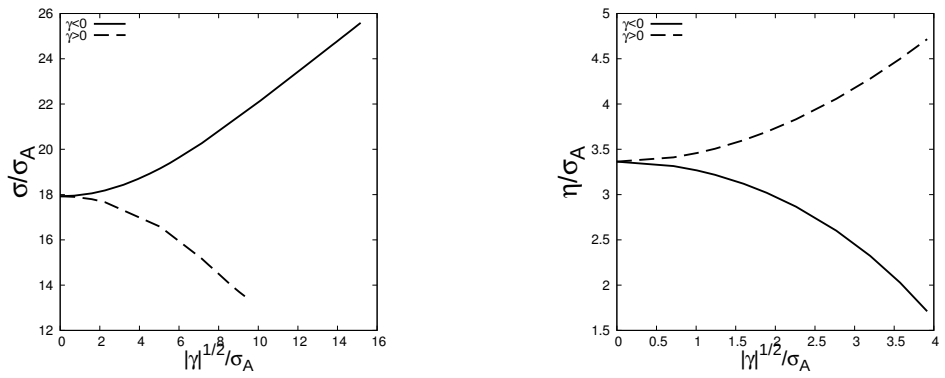

Figure 18: Eigenfrequency σ/σ_A (left) and the growth rate η/σ_A (right) of the $m = 2$ magnetic modes versus the $|\gamma|^{1/2}/\sigma_A$ for the $n = 1$ polytrope.

to the strength of the magnetic field where the Brunt-Väisälä frequency $N \propto \sqrt{|\gamma|}$.

Using a dispersion relation given by Lee (2010) for waves in a magnetized star, we try to explain the rapid spacial oscillations of eigenfunctions $\boldsymbol{H}$ and $\boldsymbol{T}$ in the stellar surface layer (see Figure 12). For a non-rotating isentropic star, the dispersion relation is given by

$$\begin{aligned} &-pq^2\cos^4\alpha(Rk)^6 + q^2\cos^2\alpha\left(2\frac{p}{q}+1\right)\bar{\sigma}^2(Rk)^4 \\ &+q\left[\bar{\beta}^2\cos^2\alpha - \left(\frac{p}{q}+1+\cos^2\alpha\right)\bar{\sigma}^2\right](Rk)^2 \\ &+\bar{\sigma}^2\left[\bar{\sigma}^4 - \bar{\sigma}^2\bar{\beta}^2 + q(Rk_H)^2\bar{\beta}^2\sin^2\psi\right] = 0, \end{aligned} \tag{4.19}$$

where

$$p = \frac{a^2}{(R\Omega_{\rm K})^2}, \quad q = \frac{B^2/(4\pi\rho)}{(R\Omega_{\rm K})^2}, \quad \bar{\beta} = \frac{g^2/a^2}{\Omega_{\rm K}^2}, \quad a = \Gamma_1\frac{p}{\rho},$$

$$g = \frac{GM_r}{r^2}, \quad \cos\alpha = \frac{\boldsymbol{k}\cdot\boldsymbol{B}}{kB}, \quad \sin\psi = \frac{(\boldsymbol{k}\times\boldsymbol{B})_z}{k_H B_H}, \tag{4.20}$$

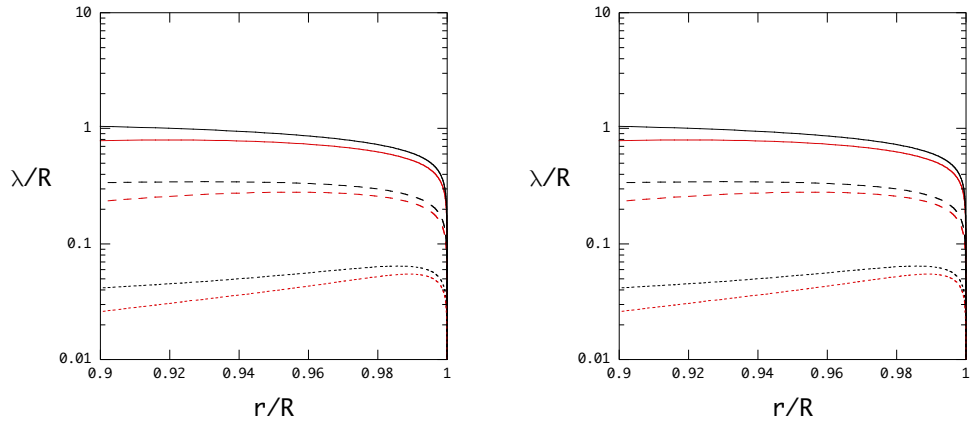

Figure 19: Local wavelengths $\lambda/R = 2\pi/(Rk_z)$ derived using the dispersion relation (4.19) for the $n = 1$ polytrpoe of $M = 1.4M_\odot$ and $R = 10^6$cm and for $B_S = 10^{15}$G, where the black lines and red lines are for $\cos\theta = 0.5$ and 0, respectively, and the solid lines, dashed lines, and dotted lines are for $\cos\alpha = 0.5$, 0.1, and 0.01, respectively. Here, we assume $\bar{\sigma}^2 = 10^{-5}$ (left) and $\bar{\sigma}^2 = 10^{-4}$ (right).

and $k = |\boldsymbol{K}|$ and $B = |\boldsymbol{B}|$. Using local Cartesian coordinates (x, y, z) and assuming z, x, and y directions are along r, θ, and ϕ directions, respectively, we obtain $B_z = 2f\cos\theta$, $B_y = -(2f + r\mathrm{d}f/\mathrm{d}r)\sin\theta$, $k_H = \sqrt{k_x^2 + k_y^2}$, $B_H = |B_x|$, and $\sin\psi = -k_y B_x/(k_H|B_x|)$. Assuming $M = 1.4M_\odot$, $R = 10^6$ cm, and $B_{\rm S} = 10^{15}$ G for an $n = 1$ polytrope, we can calculate the parameters p, q, $\bar{\beta}^2$, and a^2 as functions of r. For simplicity, we assume $k_x R = k_y R = 1$ near the surface layer for $|m| \sim l \sim 1$. Then solving equation (4.19), we obtain the value of $(Rk_z)^2$ for given $\bar{\sigma}^2$, $\cos\theta$, and $\cos\alpha$. In Figure 19, we plot local wavelength $\lambda/R = 2\pi/(Rk_z)$ for given parameters $\bar{\sigma}^2$, $\cos\theta$, and $\cos\alpha$. From Figure 19, we find the waves propagating across the field lines near the stellar surface tend to have short wavelengths. The rapid spacial oscillations of the eigenfunctions $\boldsymbol{H}$ and $\boldsymbol{T}$ near the stellar surface layer may correspond to the case of $\cos\alpha \sim 0.01$. Since we have $\boldsymbol{k}\cdot\boldsymbol{\xi} \sim 0$ for low frequency modes, we have $|\xi_z|/|\xi_H| \ll 1$ for $|k_z|/k_H \gg 1$, and hence rapid spacial oscillations of the eigenfunction $\boldsymbol{S}$ are not revealed because of small amplitudes of ξ_z.

We fail to calculate g-, f-, and p-modes of stars magnetized with purely poloidal magnetic fields, in contrast to the case of the oscillations of stars with purely toroidal magnetic fields. Assuming the limit of $|\boldsymbol{B}| \to 0$, the eigensolutions for magnetized stars (for simplicity, we take $\gamma = 0$) are given by

$$\sigma = \sigma_0 + \mathcal{O}(\bar{\sigma}_A^2), \quad \boldsymbol{\xi} = \boldsymbol{\xi}_0 + \mathcal{O}(\bar{\sigma}_A^2), \quad \delta p = \delta p_0 + \mathcal{O}(\bar{\sigma}_A^2), \quad \delta\rho = \delta\rho_0 + \mathcal{O}(\bar{\sigma}_A^2), \tag{4.21}$$

where $\bar{\sigma}_0$, $\boldsymbol{\xi}_0$, δp_0, and $\delta\rho_0$ are eigenfrequency and eigenfunctions of non-magnetized stars, respectively. It is clear that equations (4.21) are solutions to equations (4.5)-(4.7), and these solutions satisfy the outer boundary conditions $\Delta p(R) = 0$ in the weak field limit $|\boldsymbol{B}| \to 0$. From equation (4.8), we obtain

$$\frac{\delta\boldsymbol{B}}{B_{\rm S}} = \nabla \times \left(\boldsymbol{\xi}_0 \times \frac{\boldsymbol{B}}{B_{\rm S}}\right) + \mathcal{O}(\bar{\sigma}_A^2). \tag{4.22}$$

However, in general $\delta\boldsymbol{B}/B_{\rm S}$ cannot satisfy the boundary condition that guarantes $\delta\boldsymbol{B}/B_{\rm S} \to 0$ for $r \to \infty$. Therefore, equations (4.21) and (4.22) cannot be regarded as eigensolutions for

magnetized stars in the limit of $|\boldsymbol{B}| \to 0$. In other word, oscillation modes that exist for non-magnetized stars do not necessarily exist for magnetized stars even if magnetic fields are very weak. In physical point of view, however, it is reasonable to expect that f- and p-modes exist even for magnetized stars. This contradiction might be resolved if we admit that in normal mode analyses the Lorentz force term in equation (4.5) must not vanish even when we take weak field limit of $|\boldsymbol{B}| \to 0$. This occurs when $\nabla \times (\delta\boldsymbol{B}/B_{\rm S}) \propto \bar{\sigma}_A^{-1}$ is satisfied somewhere in the interior of the stars in the limit of $|\boldsymbol{B}| \to 0$. In this case, $\delta\boldsymbol{B}$ shows rapid spatial oscillations in the interior of the star to keep the Lorentz force term finite in the limit of $|\boldsymbol{B}| \to 0$, and hence eigenfrequencies and eigenfunctions of f- and p-modes of magnetized stars may be slightly different from those of non-magnetized stars. Usually, it is difficult to properly treat such very rapid spacial oscillations caused by the term $\nabla \times (\delta\boldsymbol{B}/B_{\rm S}) \propto \bar{\sigma}_A^{-1}$ with our numerical code used in this paper. Interestingly, we can obtain f- and p-like modes if we largely reduce the number of radial mesh points in the interior of the stars. This reduction of the number of radial mesh points of the stars are corresponding to averaging rapid spatial oscillations of $\delta\boldsymbol{B}$ over length scales much longer than wavelength of the spatial oscillations. In this case, we can avoid numerical difficulty related to the rapid spatial oscillations of $\delta\boldsymbol{B}$, however we cannot regard these f- and p-like modes calculated as correct normal modes.

5 Conclusion

In this paper, we calculated non-axisymmetric ($m \neq 0$) oscillation modes for magnetized and uniformly rotating stars with purely toroidal magnetic fields and for magnetized stars with purely poloidal magnetic fields. As background models for the modal analyses, we use polytropes and ignore the solid crust region for simplicity.

For magnetized and uniformly rotating stars having purely toroidal magnetic field, we use three polytopes of the indices $n = 1$, 1.5, and 3, and consider the effects of stellar deformation due to the magnetic field. Assuming no rotation, we calculate non-radial g-, f-, and p-modes, and we find that the frequency changes caused by the magnetic fields scale with the square of the characteristic Alfvén frequency $\bar{\omega}_A^2 = B_0^2/(4\pi\rho_0 R^2)$. Assuming uniform rotation, we calculate rotational modes such as inertial mode and r-mode, and find that the frequency changes of the rotational modes by the magnetic field scale with the square of the characteristic Alfvén frequency $\bar{\omega}_A^2$. We find that high-frequency modes such as f- and p-modes are strongly affected by the deformation of the stars due to the magnetic field, although low-frequency modes such as g- and rotational modes are hardly affected by the stellar deformation. It is important to note that we fail to obtain $j_{\rm max}$-independent magnetic modes for purely toroidal magnetic fields. The low-frequency modes we obtained in the frequency range of magnetic modes have discontinuity in the eigenfunctions as a function of r, which may suggest that the frequencies of the modes we found are in a continuum frequency band.

For magnetized stars having purely poloidal magnetic field, we use two polytropes with polytropic indices $n = 1$ and 1.5. We ignore the stellar rotation and the equilibrium deformation due to the magnetic fields. We find stable (oscillatory) magnetic modes ($\sigma^2 > 0$) of odd parity and unstable (monotonically growing) magnetic modes ($\sigma^2 < 0$) of both even and odd parities. The

frequency σ of stable magnetic mode and the growth rate η of unstable magnetic mode are proportional to the strength of the magnetic field $B_{\rm S}$ measured at the stellar surface (for assuming $\gamma = 0$). The eigenvalue spectra of the stable magnetic modes and unstable magnetic modes are anti-Strumian and the frequency and the growth rate decrease as the number of radial nodes of the eigenfunctions increases for a given m. We find non-axisymmetric magnetic modes are affected by stratification in the interior of the stars. For radiative stars ($\gamma < 0$), the frequency of stable magnetic modes increases as $|\gamma|$ increases, while for convective stars ($\gamma > 0$), the frequency decreases as $|\gamma|$ increases. On the other hand, for unstable magnetic modes, the growth rate η decreases as $|\gamma|$ increases for $\gamma < 0$, and it increases as $|\gamma|$ increases for $\gamma > 0$, which means that the buoyant force reduces the magnetic instability, but convective instability intensifies the magnetic instability. The frequency σ of stable magnetic mode and the growth rate η of unstable magnetic mode increase as the azimuthal wavenumber $|m|$ increases. We note that Lasky et al. (2011) obtain strong instability of magnetized star with purely poloidal magnetic field especially for $m = 4$. It is shown that purely poloidal magnetic fields having closed field lines in the interior of the star become unstable in the limit of $m \to \infty$ (see e.g., Markey & Tayler 1973; van Assche et al. 1982).

For given m and $B_{\rm S}$, we find only one mode sequence of (stable) magnetic modes, where we have classified the magnetic modes using the number of radial nodes of the eigenfunctions. This result is different from that found for axisymmetric ($m = 0$) toroidal modes of magnetized neutron stars with purely poloidal magnetic field discussed by Lee (2008) and Asai & Lee (2014), who obtained several discrete sequences of magnetically modified toroidal modes, whose surface oscillation patterns are different from each other.

The frequencies of magnetar QPOs observationally identified are order of several ten Hz to several hundred Hz. These QPO frequencies may be explained by using magnetic modes of strongly magnetized neutron stars. For example, the eigenfrequencies of magnetic modes are order of several hundred Hz for $B_{\rm S} \sim 10^{15}$ G. For detailed comparisons between the observations and theoretical predictions, however, we need to take account of various effects such as a solid crust, magnetic field configurations, superfluidity, and general relativity on the magnetic modes, which is among future works.

Present analyses are a part of series of our researches on the oscillations of magnetized stars. It is well known that purely toroidal or poloidal magnetic fields are unstable and magnetic energy are dissipated quickly. Therefore, it is difficult to observe long-lived magnetic modes as QPOs. We note that considering stellar rotations, instability of purely poloidal and toroidal magnetic fields may be weaken (e.g., Lander & Jones 2011a, b). It is thought that mixed poloidal and toroidal magnetic field such as twisted-torus magnetic field may be stable (e.g., Braithwaite & Spruit 2004; Yoshida & Eriguchi 2006; Yoshida, Yoshida & Eriguchi 2006; Ciolfi et al. 2009), that is, such magnetic field configuration may continue to exist for a long time. Thus, it is interesting to carry out the analysis of stability and examine frequency spectra for magnetized stars having such magnetic field configurations. For magnetic fields having both poloidal and toroidal field components, spheroidal and toroidal modes are coupled with each other even for assuming axisymmetric perturbations, and equatorial-symmetry is lost, which makes it difficult to analyze the oscillation modes.

We need to consider the effects of the solid crust, superfluidity of neutrons, and superconduc-

tivity of protons on the oscillation modes as the important properties of cold neutron stars (e.g., Andersson, Glampedakis & Samuelsson 2009; Glampedakis, Andersson & Samuelsson 2011). It is thought that neutrons become superfluid in the inner crust and fluid core, and protons become superconductor in the fluid core. For example, if the fluid core contains type I superconductor, magnetic fields are expelled from the core due to Meissner effect, and confined to the solid crust (e.g., Colaiuda et al. 2008; Sotani et al. 2008b). In this case, it may be reasonable to calculate magnetically modified toroidal modes confined in the solid crust so long as axisymmetric toroidal modes are concerned, while for spheroidal modes or coupled spheroidal and toroidal modes, we need to consider both non-magnetic core and magnetic crust. However, recent analyses of spectra of timing noise for SGR 1806-20 and SGR 1900+14 suggest the fluid core is type II superconductor (Arras, Cumming & Thompson 2004). In this case, the fluid core as well as the solid crust is threaded by magnetic field lines, and frequency spectra of oscillation modes are affected by superconductivity of the core (e.g., Colaiuda et al. 2008; Sotani et al. 2008b). Examining oscillation modes of magnetized stars using normal mode analysis taking account of the effects of superfluidity and superconductivity is our future studies (see e.g., Glampedakis, Andersson & Samuelsson 2011; Gabler et al. 2013b; Passamonti & Lander 2013, 2014).

Acknowledgments

I am deeply grateful to Tohoku University Astronomical Institute. I am particularly grateful for the guidance and persistent help given by Umin Lee and Shijun Yoshida.

REFFERENCES

[1] Andersson N., Glampedakis K., Samuelsson L., 2009, MNRAS, 396, 894

[2] Arras P., Cumming A., Thompson C., 2004, ApJ, 608, L49

[3] Asai H., Lee U., 2014, ApJ, 790, 66

[4] Braithwaite J., 2007, A&A, 469, 275

[5] Braithwaite J., Spruit H. C., 2004, Nature, 431, 819

[6] Cerdá-Durán P., Stergioulas N., Font J. A., 2009, MNRAS, 397, 1607

[7] Ciolfi R., Ferrari V., Gualtieri L., Pons J. A., 2009, MNRAS,

[8] Ciolfi R., Rezzolla L., 2012, ApJ, 760, 1 397, 913

[9] Colaiuda A., Ferrari V., Gualtieri L., Pons J. A., 2008, MNRAS, 385, 2080

[10] Colaiuda A., Kokkotas K. D., 2011, MNRAS, 414, 3014

[11] Colaiuda A., Kokkotas K. D., 2012, MNRAS, 423, 811

[12] Duncan R. C., Thompson C., 1992, ApJ, 392, L9

[13] Duncan R. C., 1998, ApJ, 498, L45

[14] Frieben J., Rezzolla L., 2012, MNRAS, 427, 3406

[15] Gabler M., Cerdá-Durán P., Font J. A., Müller E., Stergioulas N., 2011, MNRAS, 410, L37

[16] Gabler M., Cerdá-Durán P., Stergioulas N., Font J. A., Müller E., 2012, MNRAS, 421, 2054

[17] Gabler M., Cerdá-Durán P., Font J. A., Müller E., Stergioulas N., 2013a, MNRAS, 430, 1811

[18] Gabler M., Cerdán-Durán P., Stergioulas N., Font J. A., Müller E., 2013b, Phys. Rev. Lett., 111

[19] Glampedakis K., Samuelsson L., Andersson N., 2006, MNRAS, 371, L74

[20] Glampedakis K., Andersson N., Samuelsson L., 2011 MNRAS, 410, 805

[21] Goedbloed H., Poedts S., 2004, Principles of Magnetohydrodynamics with Applications to Laboratory and Astrophysical Plasma. Cambridge Univ. Press, Cambridge

[22] Hambaryan V., Neuhäuser R., Kokkotas K. D., 2011, A&A, 528, A45

[23] Huppenkothen D. et al., 2014, ApJ, 787, 128

[24] Israel G. et al., 2005, ApJ, 628, L53

[25] Kiuchi K., Yoshida S., 2008, Phys. Rev., 78, 044045

[26] Kotake K., Sato K., Takahashi K., 2006, Rep. Prog. Phys., 69, 971

[27] Lander S. K., Jones D. L., Passamonti A., 2010 MNRAS, 405, 318

[28] Lander S. K., Jones D. L., 2011a, MNRAS, 412, 1394

[29] Lander S. K., Jones D. L., 2011b, MNRAS, 412, 1730

[30] Lasky P. D., Zink B., Kokkotas K. D., Glampedakis K., 2011, ApJ, 735, L20

[31] Lee U., 1993, ApJ, 405, 359

[32] Lee U., 2005, MNRAS, 357, 97

[33] Lee U., 2007, MNRAS, 374, 1015

[34] Lee U., 2008, MNRAS, 385, 2069

[35] Lee U., 2010, MNRAS, 405, 1444

[36] Lee U., Strohmayer T. E., 1996, A&A, 311, 155

[37] Levin Y., 2006, MNRAS, 368, L35

[38] Levin Y., 2007, MNRAS, 377, 159

[39] Lockitch K. H., Friedman J. L., 1999, ApJ, 521, 764

[40] Markey P., Tayler R. J., 1973, MNRAS, 163, 77

[41] Mathis S., Brye N., 2011, A&A, 526, A65

[42] Mathis S., Brye N., 2012, A&A, 540, A37

[43] McDermott P. N., van Horn H. M., Hansen C. J., 1988, ApJ, 325, 725

[44] Mereghetti S., 2008, A&AR, 15, 225

[45] Miketinac M. J., 1973, Ap&SS, 22, 413

[46] Morsink S. M., Rezania V., 2002, ApJ, 574, 908

[47] Passamonti A., Lander S. K., 2013, MNRAS, 429, 767

[48] Passamonti A., Lander S. K., 2014, MNRAS, 438, 156

[49] Piro A. L., 2005, ApJ, 634, L153

[50] Saio H., 1981, ApJ, 244, 299

[51] Saio H., 1998, psrd, conf, 151S

[52] Sotani H., Kokkotas K. D., Stergioulas N., 2007, MNRAS, 375, 261

[53] Sotani H., Kokkotas K. D., Stergioulas N., 2008a, MNRAS, 385, L5

[54] Sotani H., Colaiuda A., Kokkotas K. D., 2008b, MNRAS, 385, 2161

[55] Sotani H., Kokkotas K. D., 2009, MNRAS, 395, 1163

[56] Strohmayer T. E., Watts A. L., 2005, ApJ, 632, L111

[57] Strohmayer T. E., Watts A. L., 2006, ApJ, 653, 593

[58] Thompson C., Duncan R. C., 1993, ApJ, 408, 194

[59] Thompson C., Duncan R. C., 1996, ApJ, 473, 322

[60] Thompson C., Lyuitikov M., Kulkarni S. R., 2002, ApJ, 574, 332

[61] Unno W., Osaki Y., Ando H., Saio H., Shibahashi H., 1989, Nonradial Oscillations of Stars, 2nd edn. Univ. of Tokyo Press, Tokyo

[62] van Assche W., Coossens M., Tayler R. J., 1982, A&A, 109, 166

[63] van Hoven M. B., Levin Y., 2011, MNRAS, 410, 1036

[64] van Hoven M. B., Levin Y., 2012, MNRAS, 420, 3035

[65] Watts A. L., 2011, preprint (arXiv:1111.0514v1)

[66] Watts A. L., Strohmayer T. E., 2006, ApJ, 637, L117

[67] Yoshida S., Eriguchi Y., 2006, ApJS, 164, 156

[68] Yoshida S., Lee U., 2000a, ApJ, 529, 997

[69] Yoshida S., Lee U., 2000b, ApJS, 120, 353

[70] Yoshida S., Yoshida S., Eriguchi Y., 2006, ApJ, 651, 462

[71] Zavlin V. E., Pavlov G. G., 2002, nsps, conf, 263

APPENDIX: A Oscillation equations for slowly rotating stars magnetized with purely toroidal magnetic fields

In order to describe the master equations of magnetized uniformly rotating stars with purely toroidal magnetic field, we introduce following column vectors for expansion coefficients of the perturbations:

$$(\boldsymbol{S})_j = S_{l_j}, \quad (\boldsymbol{H})_j = H_{l_j}, \quad (\boldsymbol{T})_j = T_{l'_j}, \quad (\boldsymbol{h}^S)_j = h^S_{l_j}, \quad (\boldsymbol{h}^H) = h^H_{l_j}, \\ (\boldsymbol{h}^T)_j = h^T_{l'_j}, \quad (\boldsymbol{y}_2)_j = \frac{\delta p_{l_j}}{\rho a g}, \tag{A.1}$$

where $(\boldsymbol{X})_j$ denotes j-th components of the column vector $\boldsymbol{X}$, and $g = GM(a)/a^2$ is a gravitational acceleration. Perturbed continuity equation (3.24) and a-, θ-, and ϕ-components of perturbed Euler equation (3.23) reduce to

$$\begin{aligned} a\frac{\mathrm{d}\boldsymbol{S}}{\mathrm{d}a} &= \left\{ \left[V_G - 3 - a\frac{\mathrm{d}\vartheta(\alpha)}{\mathrm{d}a} \right] \mathsf{I} - a\frac{\mathrm{d}\vartheta(\beta)}{\mathrm{d}a}\boldsymbol{\mathcal{A}}_0 \right\} \boldsymbol{S} - V_G \boldsymbol{y}_2 + [\boldsymbol{\Lambda}_0 + 3\vartheta(\beta)\boldsymbol{\mathcal{B}}_0]\, \boldsymbol{H} \\ &\quad + 3m\vartheta(\beta)\mathsf{Q}_0 \boldsymbol{T}\,, \end{aligned} \tag{A.2}$$

$$\begin{aligned} a\frac{\mathrm{d}\boldsymbol{y}_2}{\mathrm{d}a} &= \left[c_1\bar{\sigma}^2 \left\{ [1+2\eta(\alpha)]\,\mathsf{I} + 2\eta(\beta)\boldsymbol{\mathcal{A}}_0 \right\} + aA\mathsf{I} \right] \boldsymbol{S} \\ &\quad - \frac{aA}{3}\left(2 + \frac{\mathrm{d}\ln\rho}{\mathrm{d}\ln a} \right) \hat{\rho} c_1 \bar{\omega}_A^2 \left(\mathsf{I} - \boldsymbol{\mathcal{A}}_0 \right) \boldsymbol{S} + (1 - aA - U)\boldsymbol{y}_2 \\ &\quad + \frac{V_G}{3}\left(2 + \frac{\mathrm{d}\ln\rho}{\mathrm{d}\ln a} \right) \hat{\rho} c_1 \bar{\omega}_A^2 \left(\mathsf{I} - \boldsymbol{\mathcal{A}}_0 \right) \boldsymbol{y}_2 \\ &\quad - \{ 2mc_1\bar{\sigma}\bar{\Omega}[1 + \alpha + \eta(\alpha)]\mathsf{I} + 2mc_1\bar{\sigma}\bar{\Omega}[\beta + \eta(\beta)]\boldsymbol{\mathcal{A}}_0 + 3c_1\bar{\sigma}^2\beta\boldsymbol{\mathcal{B}}_0 \} \boldsymbol{H} \\ &\quad - \{ 2c_1\bar{\sigma}\bar{\Omega}[1 + \alpha + \eta(\alpha)]\mathsf{C}_0 + 2c_1\bar{\sigma}\bar{\Omega}[\beta + \eta(\beta)]\boldsymbol{\mathcal{A}}_0\mathsf{C}_0 + 3mc_1\bar{\sigma}^2\beta\mathsf{Q}_0 \} \boldsymbol{T} \\ &\quad + \frac{1}{2}\hat{\rho} c_1 \bar{\omega}_A^2 \left\{ m\left[a\frac{\mathrm{d}\boldsymbol{h}^H}{\mathrm{d}a} - \boldsymbol{h}^S + 2\left(2 + \frac{\mathrm{d}\ln\rho}{\mathrm{d}\ln a} \right) \boldsymbol{h}^H \right] \right. \\ &\quad \left. - \mathsf{C}_0 \left[a\frac{\mathrm{d}\boldsymbol{h}^T}{\mathrm{d}a} + 2\left(2 + \frac{\mathrm{d}\ln\rho}{\mathrm{d}\ln a} \right) \boldsymbol{h}^T \right] \right\}, \end{aligned} \tag{A.3}$$

$$
\begin{aligned}
&-\{m\nu\left[1+\alpha+\eta(\alpha)\right]\mathsf{I}+m\nu\left[\beta+\eta(\beta)\right]\boldsymbol{\mathcal{A}}_0-3\beta\left(2\boldsymbol{\mathcal{A}}_0+\boldsymbol{\mathcal{B}}_0\right)\}\boldsymbol{S}\\
&+aA\hat{\rho}\frac{\bar{\omega}_A^2}{\bar{\sigma}^2}\left(2\boldsymbol{\mathcal{A}}_0+\boldsymbol{\mathcal{B}}_0\right)\boldsymbol{S}-\frac{1}{c_1\bar{\sigma}^2}\boldsymbol{\Lambda}_0\boldsymbol{y}_2-\hat{\rho}\frac{\bar{\omega}_A^2}{\bar{\sigma}^2}V_G\left(2\boldsymbol{\mathcal{A}}_0+\boldsymbol{\mathcal{B}}_0\right)\boldsymbol{y}_2\\
&+\left[(1+2\alpha)\boldsymbol{\Lambda}_0\mathsf{L}_0+2\beta\left(\boldsymbol{\mathcal{A}}_0\boldsymbol{\Lambda}_0+3\boldsymbol{\mathcal{B}}_0\right)-2m\nu\beta\left(\mathsf{I}+6\boldsymbol{\mathcal{A}}_0\right)\right]\boldsymbol{H}\\
&+\left[-\nu\left(1+2\alpha-2\beta\right)\boldsymbol{\Lambda}_0\mathsf{M}_1-4\nu\beta\left(\boldsymbol{\mathcal{A}}_0\boldsymbol{\Lambda}_0\mathsf{M}_1+3\mathsf{Q}_0\boldsymbol{\mathcal{B}}_1\right)+6m\beta\mathsf{Q}_0\right]\boldsymbol{T}\\
&+\frac{1}{2}m\hat{\rho}\frac{\bar{\omega}_A^2}{\bar{\sigma}^2}\left(2+\frac{\mathrm{d}\ln\rho}{\mathrm{d}\ln a}\right)\boldsymbol{h}^S+m\hat{\rho}\frac{\bar{\omega}_A^2}{\bar{\sigma}^2}\boldsymbol{h}^H-\frac{1}{2}\hat{\rho}\frac{\bar{\omega}_A^2}{\bar{\sigma}^2}\boldsymbol{\Lambda}_0\mathsf{R}\boldsymbol{h}^T=0\,,
\end{aligned}
\tag{A.4}
$$

$$
\begin{aligned}
&\{\nu\left[1+\alpha+\eta(\alpha)\right]\boldsymbol{\Lambda}_1\mathsf{K}+\nu\left[\beta+\eta(\beta)\right]\left[\boldsymbol{\mathcal{A}}_1\boldsymbol{\Lambda}_1\mathsf{K}-2\mathsf{Q}_1(\mathsf{I}-\boldsymbol{\mathcal{A}}_0)\right]\\
&-3m\beta\mathsf{Q}_1\}\boldsymbol{S}-maA\hat{\rho}\frac{\bar{\omega}_A^2}{\bar{\sigma}^2}\mathsf{Q}_1\boldsymbol{S}+m\hat{\rho}\frac{\bar{\omega}_A^2}{\bar{\sigma}^2}V_G\mathsf{Q}_1\boldsymbol{y}_2\\
&+\left[-\nu(1+2\alpha-2\beta)\boldsymbol{\Lambda}_1\mathsf{M}_0-4\nu\beta\left(\boldsymbol{\mathcal{A}}_1\boldsymbol{\Lambda}_1\mathsf{M}_0+3\mathsf{Q}_1\boldsymbol{\mathcal{B}}_0\right)+6m\beta\mathsf{Q}_1\right]\boldsymbol{H}\\
&+\left[(1+2\alpha)\boldsymbol{\Lambda}_1\mathsf{L}_1+2\beta\left(\boldsymbol{\mathcal{A}}_1\boldsymbol{\Lambda}_1+3\boldsymbol{\mathcal{B}}_1\right)-2m\nu\beta\left(\mathsf{I}+6\boldsymbol{\mathcal{A}}_1\right)\right]\boldsymbol{T}\\
&-\frac{1}{2}\hat{\rho}\frac{\bar{\omega}_A^2}{\bar{\sigma}^2}\left(2+\frac{\mathrm{d}\ln\rho}{\mathrm{d}\ln a}\right)\boldsymbol{\Lambda}_1\mathsf{K}\boldsymbol{h}^S+\hat{\rho}\frac{\bar{\omega}_A^2}{\bar{\sigma}^2}\boldsymbol{\Lambda}_1\mathsf{M}_0\boldsymbol{h}^H+\frac{1}{2}m\hat{\rho}\frac{\bar{\omega}_A^2}{\bar{\sigma}^2}\left(\boldsymbol{\Lambda}_1-2\mathsf{I}\right)\boldsymbol{h}^T=0\,.
\end{aligned}
\tag{A.5}
$$

a-, θ-, and ϕ-components of perturbed induction equation (3.26) reduce to

$$
\boldsymbol{h}^S=m\boldsymbol{S},
\tag{A.6}
$$

$$
\boldsymbol{h}^H=maA\boldsymbol{\Lambda}_0^{-1}\boldsymbol{S}-mV_G\boldsymbol{\Lambda}_0^{-1}\boldsymbol{y}_2+m\boldsymbol{H},
\tag{A.7}
$$

$$
\boldsymbol{h}^T=aA\mathsf{K}\boldsymbol{S}-V_G\mathsf{K}\boldsymbol{y}_2-m\boldsymbol{T},
\tag{A.8}
$$

where

$$
U=\frac{\mathrm{d}\ln M(a)}{\mathrm{d}\ln a},\quad V_G=-\frac{1}{\Gamma_1}\frac{\mathrm{d}\ln p}{\mathrm{d}\ln a},\quad \vartheta(\alpha)=3\alpha+a\frac{\mathrm{d}\alpha}{\mathrm{d}a},\quad \eta(\alpha)=\alpha+a\frac{\mathrm{d}\alpha}{\mathrm{d}a}\,,
\tag{A.9}
$$

$\bar{\omega}_A^2\equiv\omega_A(GM/R^3)^{1/2}$ and $\bar{\sigma}\equiv\sigma(GM/R^3)^{1/2}$ are normalized frequency, $\omega_A=\sqrt{B_0^2/(4\pi\rho_0R^2)}$ is characteristic Alfvén frequency of the star, and $\nu\equiv2\Omega/\sigma$. The quantities Q_0, Q_1, C_0, C_1, K, M_0, M_1, $\boldsymbol{\Lambda}_0$, $\boldsymbol{\Lambda}_1$, R, L_0, L_1, $\boldsymbol{\mathcal{A}}_0$, $\boldsymbol{\mathcal{A}}_1$, $\boldsymbol{\mathcal{B}}_0$, and $\boldsymbol{\mathcal{B}}_1$ are matrices defined as follows: for even modes,

$$
(\mathsf{Q}_0)_{jj}=J^m_{l_j+1},\quad (\mathsf{Q}_0)_{j+1,j}=J^m_{l_j+2},\quad (\mathsf{Q}_1)_{jj}=J^m_{l_j+1},\quad (\mathsf{Q}_1)_{j,j+1}=J^m_{l_j+2},
$$

$$
(\mathsf{C}_0)_{jj}=-(l_j+2)J^m_{l_j+1},\quad (\mathsf{C}_0)_{j+1,j}=(l_j+1)J^m_{l_j+2},
$$

$$
(\mathsf{C}_1)_{jj}=l_jJ^m_{l_j+1},\quad (\mathsf{C}_1)_{j,j+1}=-(l_j+3)J^m_{l_j+2},
$$

$$
(\mathsf{K})_{jj}=\frac{J^m_{l_j+1}}{l_j+1},\quad (\mathsf{K})_{j,j+1}=-\frac{J^m_{l_j+2}}{l_j+2},
$$

$$
(\mathsf{M}_0)_{jj}=\frac{l_j}{l_j+1}J^m_{l_j+1},\quad (\mathsf{M}_0)_{j,j+1}=\frac{l_j+3}{l_j+2}J^m_{l_j+2},
$$

$$
(\mathsf{M}_1)_{jj}=\frac{l_j+2}{l_j+1}J^m_{l_j+1},\quad (\mathsf{M}_1)_{j+1,j}=\frac{l_j+1}{l_j+2}J^m_{l_j+2},
$$

$$
(\boldsymbol{\Lambda}_0)_{jj}=l_j(l_j+1),\quad (\boldsymbol{\Lambda}_1)_{jj}=(l_j+1)(l_j+2),
$$

$$(\mathbf{R})_{jj} = -\frac{(l_j+2)(l_j-1)}{l_j+1} J^m_{l_j+1}, \quad (\mathbf{R})_{j+1,j} = \frac{(l_j+1)(l_j+4)}{l_j+2} J^m_{l_j+2},$$

$$\mathbf{L}_0 = \mathbf{I} - m\nu\boldsymbol{\Lambda}_0^{-1}, \quad \mathbf{L}_1 = \mathbf{I} - m\nu\boldsymbol{\Lambda}_1^{-1}, \quad \boldsymbol{\mathcal{A}}_0 = \frac{1}{2}(3\mathbf{Q}_0\mathbf{Q}_1 - \mathbf{I}),$$
$$\boldsymbol{\mathcal{A}}_1 = \frac{1}{2}(3\mathbf{Q}_1\mathbf{Q}_0 - \mathbf{I}), \quad \boldsymbol{\mathcal{B}}_0 = \mathbf{Q}_0\mathbf{C}_1, \quad \boldsymbol{\mathcal{B}}_1 = \mathbf{Q}_1\mathbf{C}_0, \tag{A.10}$$

where $l_j = |m| + 2j - 2$ for $j = 1, 2, 3, ..., j_{\max}$, and

$$J^m_{l_j} = \left[\frac{(l_j+m)(l_j-m)}{(2l_j-1)(2l_j+1)}\right]^{1/2}, \tag{A.11}$$

and for odd modes,

$$(\mathbf{Q}_0)_{jj} = J^m_{l_j+1}, \quad (\mathbf{Q}_0)_{j,j+1} = J^m_{l_j+2}, \quad (\mathbf{Q}_1)_{jj} = J^m_{l_j+1}, \quad (\mathbf{Q}_1)_{j+1,j} = J^m_{l_j+2},$$

$$(\mathbf{C}_0)_{jj} = l_j J^m_{l_j+1}, \quad (\mathbf{C}_0)_{j,j+1} = -(l_j+3) J^m_{l_j+2},$$

$$(\mathbf{C}_1)_{jj} = -(l_j+2) J^m_{l_j+1}, \quad (\mathbf{C}_1)_{j+1,j} = (l_j+1) J^m_{l_j+2},$$

$$(\mathbf{K})_{jj} = -\frac{J^m_{l_j+1}}{l_j+1}, \quad (\mathbf{K})_{j+1,j} = \frac{J^m_{l_j+2}}{l_j+2},$$

$$(\mathbf{M}_0)_{jj} = \frac{l_j+2}{l_j+1} J^m_{l_j+1}, \quad (\mathbf{M}_0)_{j+1,j} = \frac{l_j+1}{l_j+2} J^m_{l_j+2},$$

$$(\mathbf{M}_1)_{jj} = \frac{l_j}{l_j+1} J^m_{l_j+1}, \quad (\mathbf{M}_1)_{j,j+1} = \frac{l_j+3}{l_j+2} J^m_{l_j+2},$$

$$(\boldsymbol{\Lambda}_0)_{jj} = (l_j+1)(l_j+2), \quad (\boldsymbol{\Lambda}_1)_{jj} = l_j(l_j+1),$$

$$(\mathbf{R})_{jj} = \frac{l_j(l_j+3)}{l_j+1} J^m_{l_j+1}, \quad (\mathbf{R})_{j,j+1} = -\frac{l_j(l_j+3)}{l_j+2} J^m_{l_j+2},$$

$$\mathbf{L}_0 = \mathbf{I} - m\nu\boldsymbol{\Lambda}_0^{-1}, \quad \mathbf{L}_1 = \mathbf{I} - m\nu\boldsymbol{\Lambda}_1^{-1}, \quad \boldsymbol{\mathcal{A}}_0 = \frac{1}{2}(3\mathbf{Q}_0\mathbf{Q}_1 - \mathbf{I}),$$
$$\boldsymbol{\mathcal{A}}_1 = \frac{1}{2}(3\mathbf{Q}_1\mathbf{Q}_0 - \mathbf{I}), \quad \boldsymbol{\mathcal{B}}_0 = \mathbf{Q}_0\mathbf{C}_1, \quad \boldsymbol{\mathcal{B}}_1 = \mathbf{Q}_1\mathbf{C}_0, \tag{A.12}$$

where $l_j = |m| + 2j - 1$ for $j = 1, 2, 3, ..., j_{\max}$.

Eliminating $\boldsymbol{h}^S$, $\boldsymbol{h}^H$, and $\boldsymbol{h}^T$ in equations (A.3)-(A.5) using equations (A.6)-(A.8), and eliminating $\boldsymbol{H}$ and $\boldsymbol{T}$ using equations (A.4)-(A.5), we obtain coupled first order linear ordinary differential equations for $\boldsymbol{y}_1 = \boldsymbol{S}$ and $\boldsymbol{y}_2$ as follows:

$$a\frac{\mathrm{d}}{\mathrm{d}a}\begin{pmatrix} \boldsymbol{y}_1 \\ \boldsymbol{y}_2 \end{pmatrix} = \boldsymbol{\mathcal{F}}\begin{pmatrix} \boldsymbol{y}_1 \\ \boldsymbol{y}_2 \end{pmatrix}, \tag{A.13}$$

where $\boldsymbol{\mathcal{F}}$ is coefficient matrix. Outer boundary condition is given by

$$-\boldsymbol{y}_1 + \boldsymbol{y}_2 + \hat{\rho}c_1\bar{\omega}_A^2\left[\frac{1}{3}\left(1 + \frac{\mathrm{d}\ln\rho}{\mathrm{d}\ln a}\right)(\mathbf{I} - \boldsymbol{\mathcal{A}}_0)\,\boldsymbol{S} + \frac{1}{2}\boldsymbol{\mathcal{B}}_0\,\boldsymbol{H}\right.$$
$$\left. + \frac{1}{2}m\mathbf{Q}_0\boldsymbol{T} - \frac{1}{2}m\boldsymbol{h}^H + \frac{1}{2}\mathbf{C}_0\,\boldsymbol{h}^T\right] = 0, \tag{A.14}$$

which means that $\Delta[p + |\boldsymbol{B}|^2/(8\pi)] = 0$ at stellar surface, where ΔQ denotes Lagrangian perturbation of quantity Q. Inner boundary conditions imposed at the center of the star are regularity conditions for eigenfunctions $\boldsymbol{y}_1$ and $\boldsymbol{y}_2$ (see Appendix F).

APPENDIX: B Surface boundary condition for the function ψ_2

In order to determine the function $\psi_2(x)$ satisfying the ordinary differential equation (3.13), we need to impose outer boundary condition on $\psi_2(x)$. Assuming difference between stellar suface $r = R_s(R, \theta)$ for the magnetized star and $r = R$ for non-magnetized star is small, we can write

$$R_s(R, \theta) = R[1 + \delta\zeta(\theta)]. \tag{B.1}$$

Since we assume $\rho(R_s, \theta) = 0$ and $\rho_0(R) = 0$, we obtain following relation from equation (3.10):

$$\delta\zeta = 2R^2\omega_A^2 \frac{\mathrm{d}x}{\mathrm{d}\Psi_0}[\psi_0(1) + \psi_2(1)P_2(\cos\theta)]. \tag{B.2}$$

Using equation (3.7), gravitational potential $\Phi(r, \theta)$ and its partial differentiation $\partial\Phi(r, \theta)/\partial x$ are given by

$$\begin{aligned}\Phi(r, \theta) = \Psi_0(r) + c_0 - 2R^2\omega_A^2 \left[c_{1,0} + \psi_0(x) + \psi_2(x)P_2(\cos\theta)\right] \\ -\frac{1}{3}\omega_A^2 r^2 \hat{\rho}\left[1 - P_2(\cos\theta)\right],\end{aligned} \tag{B.3}$$

$$\begin{aligned}\frac{\partial\Phi(r, \theta)}{\partial x} = \frac{\partial\Psi_0(r)}{\partial x} - 2R^2\omega_A^2 \left[\frac{d\psi_0}{dx}(x) + \frac{d\psi_2}{dx}(x)P_2(\cos\theta)\right] \\ -\frac{1}{3}\omega_A^2 \left(r^2\frac{d\hat{\rho}}{dx} + 2Rr\hat{\rho}\right)\left[1 - P_2(\cos\theta)\right],\end{aligned} \tag{B.4}$$

where we assume constant C in equation (3.7) as $C = c_0 - 2R^2\omega_A^2 c_{1,0}$. Since $\hat{\rho}(R_s, \theta) = 0$, $\Psi_0(R_s) \approx \Psi_0(R) + (\mathrm{d}\Psi_0/\mathrm{d}r)_{r=R}R\delta\zeta$, and $(\partial\Psi_0(r)/\partial r)_{r=R_s} = GM/R_s^2 \approx (GM/R^2)(1 - 2\delta\zeta)$ for deformed stellar surface, gravitational potential $\Phi(R_s, \theta)$ and its partial differentiation $\partial\Phi(R_s, \theta)/\partial x$ reduce to

$$\Phi(R_s, \theta) = \Psi_0(R) + c_0 - 2R^2\omega_A^2 c_{1,0}, \tag{B.5}$$

$$\begin{aligned}\frac{\partial\Phi}{\partial x}(R_s, \theta) = \frac{\partial\Psi_0(R)}{\partial x} - 2R^2\omega_A^2 \left[\frac{\mathrm{d}\psi_0}{\mathrm{d}x}(1) + \frac{\mathrm{d}\psi_2}{\mathrm{d}x}(1)P_2(\cos\theta)\right] \\ -\frac{1}{3}\omega_A^2 R^2 \frac{\mathrm{d}\hat{\rho}}{\mathrm{d}x}\left[1 - P_2(\cos\theta)\right] - 4R^2\omega_A^2 \left[\psi_0(1) + \psi_2(1)P_2(\cos\theta)\right],\end{aligned} \tag{B.6}$$

where we use $\mathrm{d}\Psi_0/\mathrm{d}x = GM/R^2$ for stellar surface. On the other hand, gravitational potential and its partial differentiation in the exterior of the star are given by

$$\Phi = -\frac{\kappa_0}{x} - 2R^2\omega_A^2 \left[\frac{\kappa_{1,0}}{x} + \frac{\kappa_{1,2}}{x^3}P_2(\cos\theta)\right], \tag{B.7}$$

$$\frac{\partial\Phi}{\partial x} = \frac{\kappa_0}{x^2} + 2R^2\omega_A^2 \left[\frac{\kappa_{1,0}}{x^2} + 3\frac{\kappa_{1,2}}{x^4}P_2(\cos\theta)\right], \tag{B.8}$$

and for the stellar surface $x = x_s \equiv 1 + \delta\zeta$, they reduce to

$$\Phi = -\kappa_0 - 2R^2\omega_A^2 \left[\kappa_{1,0} + \kappa_{1,2}P_2(\cos\theta)\right] + \kappa_0\delta\zeta, \tag{B.9}$$

$$\frac{\partial\Phi}{\partial x} = \kappa_0 + 2R^2\omega_A^2 \left[\kappa_{1,0} + 3\kappa_{1,2}P_2(\cos\theta)\right] - 2\kappa_0\delta\zeta, \tag{B.10}$$

where κ_0, $\kappa_{1,0}$, and $\kappa_{1,2}$ are arbitrary constants. Assuming both Φ and $\partial\Phi/\partial x$ of the interior and the exterior of the star connect at the surface of the star, we obtain following relations for non-perturbed terms:

$$\Psi_0(R) + c_0 = -\kappa_0, \quad \kappa_0 = \frac{\partial \Psi_0(R)}{\partial x}. \tag{B.11}$$

Therefore, we obtain

$$\Psi_0(R) = -\kappa_0 = -\frac{\partial \Psi_0(R)}{\partial x}, \quad c_0 = 0. \tag{B.12}$$

For perturbed terms, we obtain following relations:

$$-c_{1,0} = -\kappa_{1,0} + \psi_0(1), \quad \kappa_{1,2} = \psi_2(1), \tag{B.13}$$

$$\kappa_{1,0} = -\frac{d\psi_0}{dx}(1) - \frac{1}{6}\frac{d\hat{\rho}}{dx}(1), \quad 3\kappa_{1,2} = -\frac{d\psi_2}{dx}(1) + \frac{1}{6}\frac{d\hat{\rho}}{dx}(1). \tag{B.14}$$

From these relations, unknown constants $c_{1,0}$ and $\kappa_{1,0}$ for ψ_0 are determined uniquely by integrating equation (3.12) from center to surface of the star:

$$\kappa_{1,0} = -\frac{d\psi_0}{dx}(1) - \frac{1}{6}\frac{d\hat{\rho}}{dx}(1), \quad c_{1,0} = -\frac{d\psi_0}{dx}(1) - \psi_0(1) - \frac{1}{6}\frac{d\hat{\rho}}{dx}(1). \tag{B.15}$$

On the other hand for ψ_2, eliminating constant $\kappa_{1,2}$, we obtain

$$3\psi_2(1) + \frac{d\psi_2}{dx}(1) = \frac{1}{6}\frac{d\hat{\rho}}{dx}(1), \tag{B.16}$$

and this equation gives outer boundary condition for ψ_2.

APPENDIX: C Frequency changes due to the purely toroidal magnetic field

Using continuity equation (3.24) and adiabatic relation (3.25), we can write Euler equation (3.23) as follows:

$$\begin{aligned} -\sigma^2[(1+2\epsilon)\,\boldsymbol{\xi} + a\xi^a\nabla_0\epsilon + a(\boldsymbol{\xi}\cdot\nabla_0\epsilon)\boldsymbol{e}_a] &= -\nabla_0\chi + \boldsymbol{e}_a\frac{\Gamma_1 p}{\rho}A\left[\nabla_0\cdot\boldsymbol{\xi} + \boldsymbol{\xi}\cdot\nabla_0\left(3\epsilon + a\frac{\partial\epsilon}{\partial a}\right)\right] \\ &+ i\sigma\boldsymbol{D} + \frac{(\boldsymbol{\xi}\cdot\nabla_0\ln\rho + \nabla_0\cdot\boldsymbol{\xi})}{4\pi\rho}(\nabla_0\times\boldsymbol{B})\times\boldsymbol{B} + \frac{1}{4\pi\rho}\left[(\nabla_0\times\boldsymbol{B})\times\delta\boldsymbol{B} + (\nabla_0\times\delta\boldsymbol{B})\times\boldsymbol{B}\right], \end{aligned} \tag{C.1}$$

where $\chi \equiv \delta p/\rho$. we describe eigenfunctions and eigenfrequency as follows (see e.g., Saio 1981):

$$\boldsymbol{\xi} = \boldsymbol{\xi}_0 + \boldsymbol{\xi}_2, \tag{C.2}$$

$$\chi = \chi_0 + \chi_2, \tag{C.3}$$

$$\sigma = \sigma_0 + \sigma_2, \tag{C.4}$$

where subscripts 0 or 2 mean the quantities of order of ω_A^0 or ω_A^2, respectively. Then, Coriolis force term $\boldsymbol{D}$ is written as

$$\boldsymbol{D} = \boldsymbol{D}^{(0)}[\boldsymbol{\xi}_0] + \boldsymbol{D}^{(0)}[\boldsymbol{\xi}_2] + \boldsymbol{D}^{(2)}[\boldsymbol{\xi}_0], \tag{C.5}$$

where

$$
\begin{aligned}
&D_a^{(0)}[\boldsymbol{\xi}] = 2\Omega \sin\theta \xi^\phi, \quad D_\theta^{(0)}[\boldsymbol{\xi}] = 2\Omega\cos\theta\xi^\phi, \quad D_\phi^{(0)}[\boldsymbol{\xi}] = -2\Omega\left(\sin\theta\xi^a + \cos\theta\xi^\theta\right), \\
&D_a^{(2)}[\boldsymbol{\xi}] = 2\Omega\left(2\epsilon + a\frac{\partial\epsilon}{\partial a}\right)\sin\theta\xi^\phi, \quad D_\theta^{(2)}[\boldsymbol{\xi}] = 2\Omega\left(2\epsilon + \frac{\sin\theta}{\cos\theta}\frac{\partial\epsilon}{\partial\theta}\right)\cos\theta\xi^\phi, \\
&D_\phi^{(2)}[\boldsymbol{\xi}] = -2\Omega\left[\left(2\epsilon + a\frac{\partial\epsilon}{\partial a}\right)\sin\theta\xi^a + \left(2\epsilon + \frac{\sin\theta}{\cos\theta}\frac{\partial\epsilon}{\partial\theta}\right)\cos\theta\xi^\theta\right].
\end{aligned}
$$

Substituting equations (C.2)-(C.5) into equation (C.1) and summarizing the same order of ω_A, we obtain following equation for order of ω_A^0:

$$
-\sigma_0^2\boldsymbol{\xi}_0 = -\nabla_0\chi_0 + \boldsymbol{e}_a\frac{\Gamma_1 p}{\rho}A\nabla_0\cdot\boldsymbol{\xi}_0 + i\sigma_0\boldsymbol{D}^{(0)}[\boldsymbol{\xi}_0]. \tag{C.6}
$$

For order of ω_A^2, we obtain

$$
\begin{aligned}
&-\sigma_0^2\boldsymbol{\xi}_2 - 2\sigma_0^2\epsilon\boldsymbol{\xi}_0 - \sigma_0^2 a\xi_0^a\nabla_0\epsilon - \sigma_0^2(\boldsymbol{\xi}_0\cdot\nabla_0\epsilon)\boldsymbol{e}_a - 2\sigma_0\sigma_2\boldsymbol{\xi}_0 \\
&= -\nabla_0\chi_2 + \boldsymbol{e}_a\frac{\Gamma_1 p}{\rho}A\left[\nabla_0\cdot\boldsymbol{\xi}_2 + \boldsymbol{\xi}_0\cdot\nabla_0\left(3\epsilon + a\frac{\partial\epsilon}{\partial a}\right)\right] + i\sigma_0\boldsymbol{D}^{(0)}[\boldsymbol{\xi}_2] + i\sigma_2\boldsymbol{D}^{(0)}[\boldsymbol{\xi}_0] \\
&+ i\sigma_0\boldsymbol{D}^{(2)}[\boldsymbol{\xi}_0] + \frac{(\boldsymbol{\xi}_0\cdot\nabla_0\ln\rho + \nabla_0\cdot\boldsymbol{\xi}_0)}{4\pi\rho}(\nabla_0\times\boldsymbol{B})\times\boldsymbol{B} \\
&+ \frac{1}{4\pi\rho}\left[(\nabla_0\times\delta\boldsymbol{B})\times\boldsymbol{B} + (\nabla_0\times\boldsymbol{B})\times\delta\boldsymbol{B}\right],
\end{aligned} \tag{C.7}
$$

where equation (C.6) means the oscillations for the non-magnetized slowly rotating star. Using $\boldsymbol{\xi}_0$ and $\boldsymbol{\xi}_2$, functions χ_0, χ_2, and $\delta\boldsymbol{B}$ are given by

$$
\begin{aligned}
\chi_0 &= -\frac{p\Gamma_1}{\rho}\left(\nabla_0\cdot\boldsymbol{\xi}_0 + \boldsymbol{\xi}_0\cdot\nabla_0\ln\rho - \boldsymbol{\xi}_0\cdot\boldsymbol{e}_a A\right), \\
\chi_2 &= -\frac{p\Gamma_1}{\rho}\left\{\nabla_0\cdot\boldsymbol{\xi}_2 + \boldsymbol{\xi}_0\cdot\nabla_0\left(3\epsilon + a\frac{\partial\epsilon}{\partial a}\right) + \boldsymbol{\xi}_2\cdot\nabla_0\ln\rho - \boldsymbol{\xi}_2\cdot\boldsymbol{e}_a A\right\},
\end{aligned}
$$

$$
(\delta B)^i = \frac{1}{a^2\sin\theta}\epsilon^{ijk}\frac{\partial}{\partial x^j}\left(a^2\sin\theta\,\epsilon_{lmk}\xi_0^l B^m\right). \tag{C.8}
$$

Multiplying complex conjugate of displacement vector $\boldsymbol{\xi}^*$ to equation (C.7) and integrating over stellar mass, we obtain following integral relation:

$$
\begin{aligned}
&-2\sigma_0^2\int_0^M \epsilon\left|\boldsymbol{\xi}_0\right|^2 \mathrm{d}M_a - \sigma_0^2\int_0^M (a\xi_0^a\nabla_0\epsilon)\cdot\boldsymbol{\xi}_0^*\mathrm{d}M_a - \sigma_0^2\int_0^M [(\boldsymbol{\xi}_0\cdot\nabla_0\epsilon)\boldsymbol{e}_a]\cdot\boldsymbol{\xi}_0^*\mathrm{d}M_a \\
&-2\sigma_0\sigma_2\int_0^M \left|\boldsymbol{\xi}_0\right|^2\mathrm{d}M_a = \int_0^M \chi_0^*\,\boldsymbol{\xi}_0\cdot\nabla_0\left(3\epsilon + a\frac{\partial\epsilon}{\partial a}\right)\mathrm{d}M_a + i\sigma_0\int_0^M \boldsymbol{D}^{(2)}[\boldsymbol{\xi}_0]\cdot\boldsymbol{\xi}_0^*\mathrm{d}M_a \\
&+ i\sigma_2\int_0^M \boldsymbol{D}^{(0)}[\boldsymbol{\xi}_0]\cdot\boldsymbol{\xi}_0^*\mathrm{d}M_a + \frac{1}{4\pi}\int_0^M \frac{1}{\rho}\left(-\frac{\rho}{p\Gamma_1}\chi_0 + \boldsymbol{\xi}_0\cdot\boldsymbol{e}_a A\right)[(\nabla_0\times\boldsymbol{B})\times\boldsymbol{B}]\cdot\boldsymbol{\xi}_0^*\mathrm{d}M_a \\
&+ \frac{1}{4\pi}\int_0^M \frac{1}{\rho}[(\nabla_0\times\delta\boldsymbol{B})\times\boldsymbol{B} + (\nabla_0\times\boldsymbol{B})\times\delta\boldsymbol{B}]\cdot\boldsymbol{\xi}_0^*\mathrm{d}M_a,
\end{aligned} \tag{C.9}
$$

where $\mathrm{d}M_a = \rho(a)a^2\sin\theta\mathrm{d}a\mathrm{d}\theta\mathrm{d}\phi$. Substituting eigenfunctions of expansion forms (3.30)-(3.36) into equation (C.9) and assuming $\sigma_2 = E_2'\bar{\omega}_A^2$, we can derive following relation for E_2'.

$$
\begin{aligned}
E_2' &= -\left[\frac{\Omega_{\mathrm{K}}^2}{4\sigma_0}\int_0^R f_1(a)\hat{\rho}\rho a^4\mathrm{d}a + \sigma_0\int_0^R f_2(a)\rho a^4\mathrm{d}a\right. \\
&\quad \left. + \frac{\Omega_{\mathrm{K}}^2}{2\sigma_0}\int_0^R \frac{1}{c_1}f_3(a)\rho a^4\mathrm{d}a + \Omega\int_0^R f_4(a)\rho a^4\mathrm{d}a\right] \Big/ W_I,
\end{aligned} \tag{C.10}
$$

where

$$
\begin{aligned}
W_I &= \int_0^R \left[|\boldsymbol{S}|^2 + \boldsymbol{H}^\dagger \boldsymbol{\Lambda}_0 \, \boldsymbol{H} + \boldsymbol{T}^\dagger \boldsymbol{\Lambda}_1 \, \boldsymbol{T} \right] \rho \, a^4 \mathrm{d}a \\
&\quad - \frac{\Omega}{\sigma_0} \int_0^R \left[m \left(\boldsymbol{S}^\dagger \boldsymbol{H} + \boldsymbol{H}^\dagger \boldsymbol{S} + |\boldsymbol{H}|^2 + |\boldsymbol{T}|^2 \right) + \boldsymbol{S}^\dagger \mathsf{C}_0 \, \boldsymbol{T} - \boldsymbol{T}^\dagger \boldsymbol{\Lambda}_1 \mathsf{K} \, \boldsymbol{S} \right. \\
&\quad \left. + \boldsymbol{H}^\dagger \boldsymbol{\Lambda}_0 \mathsf{M}_1 \, \boldsymbol{T} + \boldsymbol{T}^\dagger \boldsymbol{\Lambda}_1 \mathsf{M}_0 \, \boldsymbol{H} \right] \rho \, a^4 \mathrm{d}a \, ,
\end{aligned} \tag{C.11}
$$

$$
\begin{aligned}
f_1(a) &= \boldsymbol{S}^\dagger \left\{ ma \frac{\mathrm{d}\boldsymbol{h}^H}{\mathrm{d}a} - m\boldsymbol{h}^S + 2m \left(2 + \frac{\mathrm{d}\ln\rho}{\mathrm{d}\ln a} \right) \boldsymbol{h}^H - \mathsf{C}_0 \left[a \frac{\mathrm{d}\boldsymbol{h}^T}{\mathrm{d}a} + 2 \left(2 + \frac{\mathrm{d}\ln\rho}{\mathrm{d}\ln a} \right) \boldsymbol{h}^T \right] \right\} \\
&\quad + \boldsymbol{H}^\dagger \left[m \left(2 + \frac{\mathrm{d}\ln\rho}{\mathrm{d}\ln a} \right) \boldsymbol{h}^S + 2m\boldsymbol{h}^H - \boldsymbol{\Lambda}_0 \mathsf{R} \, \boldsymbol{h}^T \right] \\
&\quad + \boldsymbol{T}^\dagger \left[- \left(2 + \frac{\mathrm{d}\ln\rho}{\mathrm{d}\ln a} \right) \boldsymbol{\Lambda}_1 \mathsf{K} \, \boldsymbol{h}^S + 2\boldsymbol{\Lambda}_1 \mathsf{M}_0 \, \boldsymbol{h}^H + m(\boldsymbol{\Lambda}_1 - 2\mathsf{I}) \boldsymbol{h}^T \right] \\
&\quad - \frac{2aA}{3} \left(2 + \frac{\mathrm{d}\ln\rho}{\mathrm{d}\ln a} \right) \boldsymbol{S}^\dagger \left(\mathsf{I} - \boldsymbol{\mathcal{A}}_0 \right) \boldsymbol{S} + \frac{2V_G}{3} \left(2 + \frac{\mathrm{d}\ln\rho}{\mathrm{d}\ln a} \right) \boldsymbol{S}^\dagger \left(\mathsf{I} - \boldsymbol{\mathcal{A}}_0 \right) \boldsymbol{y}_2 \\
&\quad + 2aA \boldsymbol{H}^\dagger \left(2\boldsymbol{\mathcal{A}}_0 + \boldsymbol{\mathcal{B}}_0 \right) \boldsymbol{S} - 2V_G \boldsymbol{H}^\dagger \left(2\boldsymbol{\mathcal{A}}_0 + \boldsymbol{\mathcal{B}}_0 \right) \boldsymbol{y}_2 - 2maA \boldsymbol{T}^\dagger \mathsf{Q}_1 \boldsymbol{S} + 2mV_G \boldsymbol{T}^\dagger \mathsf{Q}_1 \boldsymbol{y}_2 \, ,
\end{aligned}
$$

$$
\begin{aligned}
f_2(a) &= \boldsymbol{S}^\dagger \left[\eta(\bar{\alpha}) \mathsf{I} + \eta(\bar{\beta}) \boldsymbol{\mathcal{A}}_0 \right] \boldsymbol{S} + \bar{\alpha} \left(\boldsymbol{H}^\dagger \boldsymbol{\Lambda}_0 \, \boldsymbol{H} + \boldsymbol{T}^\dagger \boldsymbol{\Lambda}_1 \, \boldsymbol{T} \right) + \bar{\beta} \, \boldsymbol{H}^\dagger \left(\boldsymbol{\mathcal{A}}_0 \boldsymbol{\Lambda}_0 + 3\boldsymbol{\mathcal{B}}_0 \right) \boldsymbol{H} \\
&\quad + \bar{\beta} \, \boldsymbol{T}^\dagger (\boldsymbol{\mathcal{A}}_1 \boldsymbol{\Lambda}_1 + 3\boldsymbol{\mathcal{B}}_1) \, \boldsymbol{T} - \frac{3}{2} \bar{\beta} \boldsymbol{S}^\dagger \boldsymbol{\mathcal{B}}_0 \, \boldsymbol{H} + \frac{3}{2} \bar{\beta} \boldsymbol{H}^\dagger \left(2\boldsymbol{\mathcal{A}}_0 + \boldsymbol{\mathcal{B}}_0 \right) \boldsymbol{S} \\
&\quad + 3m\bar{\beta} \left(\boldsymbol{H}^\dagger \mathsf{Q}_0 \, \boldsymbol{T} + \boldsymbol{T}^\dagger \mathsf{Q}_1 \, \boldsymbol{H} \right) - \frac{3}{2} m\bar{\beta} \left(\boldsymbol{S}^\dagger \mathsf{Q}_0 \, \boldsymbol{T} + \boldsymbol{T}^\dagger \mathsf{Q}_1 \, \boldsymbol{S} \right) ,
\end{aligned}
$$

$$
f_3(a) = \boldsymbol{y_2}^\dagger \left[a \frac{\mathrm{d}\vartheta(\bar{\alpha})}{\mathrm{d}a} \mathsf{I} + a \frac{\mathrm{d}\vartheta(\bar{\beta})}{\mathrm{d}a} \boldsymbol{\mathcal{A}}_0 \right] \boldsymbol{S} - 3\vartheta(\bar{\beta}) \boldsymbol{y_2}^\dagger \boldsymbol{\mathcal{B}}_0 \, \boldsymbol{H} - 3m\vartheta(\bar{\beta}) \boldsymbol{y_2}^\dagger \mathsf{Q}_0 \, \boldsymbol{T} \, ,
$$

$$
\begin{aligned}
f_4(a) &= -m\boldsymbol{S}^\dagger \left\{ [\bar{\alpha} + \eta(\bar{\alpha})] \, \mathsf{I} + [\bar{\beta} + \eta(\bar{\beta})] \boldsymbol{\mathcal{A}}_0 \right\} \boldsymbol{H} - m\boldsymbol{H}^\dagger \left\{ [\bar{\alpha} + \eta(\bar{\alpha})] \, \mathsf{I} + [\bar{\beta} + \eta(\bar{\beta})] \boldsymbol{\mathcal{A}}_0 \right\} \boldsymbol{S} \\
&\quad - 2m\bar{\alpha} \left(|\boldsymbol{H}|^2 + |\boldsymbol{T}|^2 \right) - 4\bar{\beta} \, \boldsymbol{T}^\dagger \left(\boldsymbol{\mathcal{A}}_1 \boldsymbol{\Lambda}_1 \mathsf{M}_0 + 3\mathsf{Q}_1 \boldsymbol{\mathcal{B}}_0 \right) \boldsymbol{H} \\
&\quad - \boldsymbol{S}^\dagger \left\{ [\bar{\alpha} + \eta(\bar{\alpha})] \mathsf{C}_0 + [\bar{\beta} + \eta(\bar{\beta})] \boldsymbol{\mathcal{A}}_0 \mathsf{C}_0 \right\} \boldsymbol{T} - 2(\bar{\alpha} - \bar{\beta}) \, \boldsymbol{H}^\dagger \boldsymbol{\Lambda}_0 \mathsf{M}_1 \, \boldsymbol{T} \\
&\quad - 2(\bar{\alpha} - \bar{\beta}) \, \boldsymbol{T}^\dagger \boldsymbol{\Lambda}_1 \mathsf{M}_0 \, \boldsymbol{H} - 2m\bar{\beta} \, \boldsymbol{H}^\dagger \left(\mathsf{I} + 6\boldsymbol{\mathcal{A}}_0 \right) \boldsymbol{H} - 4\bar{\beta} \, \boldsymbol{H}^\dagger \left(\boldsymbol{\mathcal{A}}_0 \boldsymbol{\Lambda}_0 \mathsf{M}_1 + 3\mathsf{Q}_0 \boldsymbol{\mathcal{B}}_1 \right) \boldsymbol{T} \\
&\quad - 2m\bar{\beta} \, \boldsymbol{T}^\dagger \left(\mathsf{I} + 6\boldsymbol{\mathcal{A}}_1 \right) \boldsymbol{T} + [\bar{\alpha} + \eta(\bar{\alpha})] \, \boldsymbol{T}^\dagger \boldsymbol{\Lambda}_1 \mathsf{K} \, \boldsymbol{S} \\
&\quad + [\beta + \eta(\beta)] \, \boldsymbol{T}^\dagger \left[\boldsymbol{\mathcal{A}}_1 \boldsymbol{\Lambda}_1 \mathsf{K} - 2\mathsf{Q}_1 (\mathsf{I} - \boldsymbol{\mathcal{A}}_0) \right] \boldsymbol{S} \, .
\end{aligned} \tag{C.12}
$$

$\bar{\alpha} \equiv \alpha/\bar{\omega}_A^2$, $\bar{\beta} \equiv \beta/\bar{\omega}_A^2$, and $\Omega_{\mathrm{K}} \equiv (GM/R^3)^{1/2}$. $\boldsymbol{X}^\dagger$ denotes Hermitian conjugate of complex vector $\boldsymbol{X}$. Magnetic perturbations $\boldsymbol{h}^S$, $\boldsymbol{h}^H$, and $\boldsymbol{h}^T$ are given by

$$
\boldsymbol{h}^S = m\boldsymbol{S} \, , \tag{C.13}
$$

$$
\boldsymbol{h}^H = maA \, \boldsymbol{\Lambda}_0^{-1} \boldsymbol{S} - mV_G \boldsymbol{\Lambda}_0^{-1} \boldsymbol{y_2} + m\boldsymbol{H} \, , \tag{C.14}
$$

$$
\boldsymbol{h}^T = aA \, \mathsf{K} \boldsymbol{S} - V_G \mathsf{K} \, \boldsymbol{y_2} - m\boldsymbol{T} \, . \tag{C.15}
$$

For above expression of E_2', expansion coefficients $\boldsymbol{S}$, $\boldsymbol{H}$, $\boldsymbol{T}$, and $\boldsymbol{y}_2$ denote eigenfunctions of non-magnetized star even if subscript 0 vanishes.

Considering inertial modes for eigensolutions of order of ω_A^0, we find following relation from equation (C.10) in the limit of $\lim_{\Omega\to 0}(\sigma_0/\Omega)=\kappa_0$.

$$\frac{\sigma_2}{\sigma_0}\to\frac{\eta_2'}{\bar{\Omega}^2}\bar{\omega}_A^2 \quad \text{as } \bar{\Omega}\to 0, \tag{C.16}$$

where η_2' is a constant. This constant is given by

$$\eta_2'=-\lim_{\Omega\to 0}\frac{1}{4\kappa_0^2 W_I}\left[\int_0^R f_1(a)\hat{\rho}\rho a^4\mathrm{d}a+2\int_0^R\frac{1}{c_1}f_3(a)\rho a^4\mathrm{d}a\right]. \tag{C.17}$$

Equation (C.16) suggests that our expression of σ_2 of inertial mode is not appropriate for $\bar{\Omega}^2\lesssim\bar{\omega}_A^2$. Therefore, for inertial mode, the condition of $\bar{\omega}_A^2\lesssim\bar{\Omega}^2\lesssim 1$ is requried in order to assure the validity of expression of σ_2. For general magnetic field configurations, the expression likely to equation (C.16) is derived by Morsink & Rezania (2002).

APPENDIX: D Oscillation equations for stars magnetized with purely poloidal magnetic fields

In order to describe the master equations of oscillations of magnetized stars with purely poloidal magnetic field, we introduce following column vectors for expansion coefficients of the perturbations:

$$(\boldsymbol{S})_j=S_{l_j},\quad (\boldsymbol{H})_j=H_{l_j},\quad (\boldsymbol{T})_j=T_{l'_j},\quad (\boldsymbol{b}^S)_j=b^S_{l'_j},\quad (\boldsymbol{b}^H)_j=b^H_{l'_j},\quad (\boldsymbol{b}^T)_j=b^T_{l_j},$$
$$(\delta\boldsymbol{U})_j=\frac{\delta p_{l_j}}{\rho g r}, \tag{D.1}$$

where $(\boldsymbol{X})_j$ denotes j-th component of column vector $\boldsymbol{X}$, and $g=GM(r)/r^2$ is a gravitational acceleration. Perturbed continuity equation (4.6) and perturbed Euler equation (4.5) reduce to

$$r\frac{\mathrm{d}\boldsymbol{S}}{\mathrm{d}r}=\left(\frac{V}{\Gamma_1}-3\right)\boldsymbol{S}-\frac{V}{\Gamma_1}\delta\boldsymbol{U}+\boldsymbol{\Lambda}_0\boldsymbol{H}, \tag{D.2}$$

$$\begin{aligned}&-\frac{4\pi p}{rf}Vr\frac{\mathrm{d}\delta\boldsymbol{U}}{\mathrm{d}r}+\frac{4\pi p}{rf}V(c_1\bar{\sigma}^2+rA)\boldsymbol{S}+\frac{4\pi p}{rf}V(1-rA-U)\delta\boldsymbol{U}\\&+\mathbf{C}_0\left[(\mathrm{d}f+2)r\frac{\mathrm{d}\boldsymbol{b}^H}{\mathrm{d}r}-(\mathrm{d}f+2)\boldsymbol{b}^S+(\mathrm{d}^2f+6\mathrm{d}f+4)\boldsymbol{b}^H\right]\\&+m\left[(\mathrm{d}f+2)r\frac{\mathrm{d}\boldsymbol{b}^T}{\mathrm{d}r}+(\mathrm{d}^2f+6\mathrm{d}f+4)\boldsymbol{b}^T\right]=0,\end{aligned} \tag{D.3}$$

$$\begin{aligned}\frac{V}{\Gamma_1}\delta\boldsymbol{U}&=\frac{V}{\Gamma_1}c_1\bar{\sigma}^2(\mathrm{d}f+2)\mathbf{A}_1^{-1}\mathbf{B}_1\boldsymbol{S}-\frac{V}{\Gamma_1}mc_1\bar{\sigma}^2(\mathbf{A}_1^{-1}+\boldsymbol{\Lambda}_0^{-1}\mathbf{A}_1^{-1}\boldsymbol{\Lambda}_1)\boldsymbol{T}+\left\{\frac{V}{\Gamma_1}c_1\bar{\sigma}^2\frac{r}{2f}\mathbf{A}_1^{-1}\right.\\&\left.+\frac{rf}{2\pi\Gamma_1 p}\left[(\mathrm{d}^2f+4\mathrm{d}f)\boldsymbol{\Lambda}_0^{-1}\mathbf{B}_0-\boldsymbol{\Lambda}_0^{-1}\mathbf{A}_0+\frac{1}{2}m^2(\mathrm{d}^2f+4\mathrm{d}f+2)\boldsymbol{\Lambda}_0^{-1}\mathbf{A}_1^{-1}\right]\right\}\boldsymbol{b}^S\\&+\frac{rf}{\pi\Gamma_1 p}(\boldsymbol{\Lambda}_0^{-1}\mathbf{A}_0-m^2\boldsymbol{\Lambda}_0^{-1}\mathbf{A}_1^{-1})\boldsymbol{b}^H+\frac{rf}{2\pi\Gamma_1 p}m\left[\frac{1}{2}(\mathrm{d}f+2)\mathbf{I}+2\boldsymbol{\Lambda}_0^{-1}\right.\\&\left.\mathrm{d}f\boldsymbol{\Lambda}_0^{-1}\mathbf{A}_1^{-1}\mathbf{B}_1\boldsymbol{\Lambda}_0+\boldsymbol{\Lambda}_0^{-1}\mathbf{A}_1^{-1}\tilde{\mathbf{C}}_1\right]\boldsymbol{b}^T+\frac{rf}{2\pi\Gamma_1 p}\boldsymbol{\Lambda}_0^{-1}\mathbf{A}_0\mathbf{L}_0 r\frac{\mathrm{d}\boldsymbol{b}^H}{\mathrm{d}r},\end{aligned} \tag{D.4}$$

$$\mathbf{A}_1 r\frac{\mathrm{d}\boldsymbol{b}^T}{\mathrm{d}r} = -\frac{2\pi p}{rf}Vc_1\bar{\sigma}^2\boldsymbol{\Lambda}_1\boldsymbol{T} + \frac{1}{2}m(\mathrm{d}^2f+4\mathrm{d}f+2)\boldsymbol{b}^S - 2m\boldsymbol{b}^H + \left(\mathrm{d}f\mathbf{B}_1\boldsymbol{\Lambda}_0 + \tilde{\mathbf{C}}_1\right)\boldsymbol{b}^T - mr\frac{\mathrm{d}\boldsymbol{b}^H}{\mathrm{d}r}. \tag{D.5}$$

Substituting $\delta\boldsymbol{U}$ given by equation (D.4) into equation (D.3), we obtain

$$\begin{aligned}
\mathbf{L}_0 r\frac{\mathrm{d}}{\mathrm{d}r}\left(r\frac{\mathrm{d}\boldsymbol{b}^H}{\mathrm{d}r}\right) = {} & \frac{2\pi p}{rf}V\left(c_1\bar{\sigma}^2+rA\right)\mathbf{A}_0^{-1}\boldsymbol{\Lambda}_0\boldsymbol{S} + \frac{4\pi p}{rf}mVc_1\bar{\sigma}^2\mathbf{A}_0^{-1}\mathbf{A}_1^{-1}\boldsymbol{\Lambda}_1\boldsymbol{T} \\
& + \Big\{ -\frac{1}{2}\left(\mathrm{d}f+2\right)\mathbf{A}_0^{-1}\tilde{\mathbf{C}}_0 - \left(\mathrm{d}\rho - rA + 4\right)\mathbf{I} \\
& + \left[-\mathrm{d}^3f + \mathrm{d}^2f\left(\mathrm{d}\rho - rA - 4\right) + 4\mathrm{d}f\left(\mathrm{d}\rho - rA + 1\right)\right]\mathbf{A}_0^{-1}\mathbf{B}_0 \\
& - \frac{1}{2}\left[\mathrm{d}^3f - \mathrm{d}^2f(\mathrm{d}\rho - 4) - 2\mathrm{d}f(2\mathrm{d}\rho+1) - 2(\mathrm{d}\rho+2)\right]m^2\mathbf{A}_0^{-1}\mathbf{A}_1^{-1}\Big\}\boldsymbol{b}^S \\
& + \Big[\left(\mathrm{d}f+1\right)\mathbf{A}_0^{-1}\tilde{\mathbf{C}}_0 + \boldsymbol{\Lambda}_1 + 2\mathbf{A}_0^{-1}\mathbf{B}_0\boldsymbol{\Lambda}_1 + 2(\mathrm{d}\rho - rA)\mathbf{I} \\
& - \frac{1}{2}(\mathrm{d}^2f + 4\mathrm{d}f + 2)m^2\mathbf{A}_0^{-1}\mathbf{A}_1^{-1}\tilde{\boldsymbol{\Lambda}}_1 - (\mathrm{d}^2f + 2\mathrm{d}f + 2\mathrm{d}\rho)m^2\mathbf{A}_0^{-1}\mathbf{A}_1^{-1}\Big]\boldsymbol{b}^H \\
& + \Big\{ -m\Big\{2(\mathrm{d}f - \mathrm{d}\rho + rA + 1)\mathbf{A}_0^{-1} \\
& + \frac{1}{2}[-\mathrm{d}f(\mathrm{d}\rho+2) + (\mathrm{d}f+2)rA - 2(\mathrm{d}\rho+1)]\mathbf{A}_0^{-1}\boldsymbol{\Lambda}_0\Big\} \\
& - m\left[(\mathrm{d}^2f - \mathrm{d}\rho\mathrm{d}f + 2\mathrm{d}f)\mathbf{A}_0^{-1}\mathbf{A}_1^{-1}\mathbf{B}_1\boldsymbol{\Lambda}_0 + (\mathrm{d}f - \mathrm{d}\rho + 1)\mathbf{A}_0^{-1}\mathbf{A}_1^{-1}\tilde{\mathbf{C}}_1\right]\Big\}\boldsymbol{b}^T \\
& + \left[\frac{1}{2}(\mathrm{d}f+2)\mathbf{A}_0^{-1}\tilde{\mathbf{C}}_0 + (\mathrm{d}\rho - rA - 1)\mathbf{I} + m^2(\mathrm{d}f - \mathrm{d}\rho + 3)\mathbf{A}_0^{-1}\mathbf{A}_1^{-1}\right]r\frac{\mathrm{d}\boldsymbol{b}^H}{\mathrm{d}r} \\
& - \frac{2\pi p}{rf}(2+rA)Vc_1\bar{\sigma}^2\mathbf{A}_0^{-1}\boldsymbol{\Lambda}_0\boldsymbol{H} \\
& - \frac{2\pi p}{rf}Vc_1\bar{\sigma}^2\mathbf{A}_0^{-1}\boldsymbol{\Lambda}_0 r\frac{\mathrm{d}\boldsymbol{H}}{\mathrm{d}r} + \frac{2\pi p}{rf}mVc_1\bar{\sigma}^2\mathbf{A}_0^{-1}\mathbf{A}_1^{-1}\boldsymbol{\Lambda}_1 r\frac{\mathrm{d}\boldsymbol{T}}{\mathrm{d}r} \\
& - m\left[\frac{1}{2}(\mathrm{d}f+2)\mathbf{A}_0^{-1}\mathbf{A}_1^{-1}\tilde{\mathbf{C}}_1 + (\mathrm{d}f + rA + 2)\mathbf{A}_0^{-1}\right]r\frac{\mathrm{d}\boldsymbol{b}^T}{\mathrm{d}r}.
\end{aligned} \tag{D.6}$$

Perturbed induction equation (4.8) and perturbed magnetic Gauss's law reduce to

$$\boldsymbol{H} = (\mathrm{d}f+2)\mathbf{A}_1^{-1}\mathbf{B}_1\boldsymbol{S} - m\mathbf{A}_1^{-1}\boldsymbol{T} + \frac{r}{2f}\mathbf{A}_1^{-1}\boldsymbol{b}^S, \tag{D.7}$$

$$\begin{aligned}
\mathbf{L}_0 r\frac{\mathrm{d}\boldsymbol{T}}{\mathrm{d}r} = {} & -m\left[\mathrm{d}^2f + \left(2+\frac{V}{\Gamma_1}\right)\mathrm{d}f - 2\left(1-\frac{V}{\Gamma_1}\right)\right]\left(\mathbf{A}_0^{-1}\mathbf{A}_1^{-1}\mathbf{B}_1 + \frac{1}{2}\mathbf{A}_0^{-1}\right)\boldsymbol{S} \\
& + \left(\mathrm{d}f+2\right)\left(m^2\mathbf{A}_0^{-1}\mathbf{A}_1^{-1} + \frac{1}{2}\mathbf{A}_0^{-1}\tilde{\mathbf{C}}_0\right)\boldsymbol{T} - \frac{r}{2f}m\mathbf{A}_0^{-1}\mathbf{A}_1^{-1}\boldsymbol{\Lambda}_1\boldsymbol{b}^H \\
& + \frac{r}{2f}\mathbf{A}_0^{-1}\boldsymbol{\Lambda}_0\boldsymbol{b}^T - m\left(\mathrm{d}f+2\right)\left(\mathbf{A}_0^{-1} + \frac{1}{2}\mathbf{A}_0^{-1}\mathbf{A}_1^{-1}\tilde{\mathbf{C}}_1\right)\boldsymbol{H} \\
& + m\left(\mathrm{d}f+2\right)\left(\mathbf{A}_0^{-1}\mathbf{A}_1^{-1}\mathbf{B}_1 + \frac{1}{2}\mathbf{A}_0^{-1}\right)\frac{V}{\Gamma_1}\delta\boldsymbol{U},
\end{aligned} \tag{D.8}$$

$$
\begin{aligned}
\mathbf{L}_1 r\frac{\mathrm{d}\boldsymbol{H}}{\mathrm{d}r} &= \left[\mathrm{d}^2 f+\left(2+\frac{V}{\Gamma_1}\right)\mathrm{d}f-2\left(1-\frac{V}{\Gamma_1}\right)\right]\left(\mathbf{A}_1^{-1}\mathbf{B}_1+\frac{1}{2}m^2\mathbf{A}_1^{-1}\mathbf{A}_0^{-1}\right)\boldsymbol{S}\\
&\quad -m\left(\mathrm{d}f+2\right)\left(\mathbf{A}_1^{-1}+\frac{1}{2}\mathbf{A}_1^{-1}\mathbf{A}_0^{-1}\tilde{\mathbf{C}}_0\right)\boldsymbol{T}+\frac{r}{2f}\mathbf{A}_1^{-1}\boldsymbol{\Lambda}_1\boldsymbol{b}^H\\
&\quad -\frac{r}{2f}m\mathbf{A}_1^{-1}\mathbf{A}_0^{-1}\boldsymbol{\Lambda}_0\boldsymbol{b}^T+\left(\mathrm{d}f+2\right)\left(m^2\mathbf{A}_1^{-1}\mathbf{A}_0^{-1}+\frac{1}{2}\mathbf{A}_1^{-1}\tilde{\mathbf{C}}_1\right)\boldsymbol{H}\\
&\quad -\left(\mathrm{d}f+2\right)\left(\mathbf{A}_1^{-1}\mathbf{B}_1+\frac{1}{2}m^2\mathbf{A}_1^{-1}\mathbf{A}_0^{-1}\right)\frac{V}{\Gamma_1}\delta\boldsymbol{U},
\end{aligned}
\tag{D.9}
$$

$$
r\frac{\mathrm{d}\boldsymbol{b}^S}{\mathrm{d}r}=-3\boldsymbol{b}^S+\boldsymbol{\Lambda}_1\boldsymbol{b}^H,
\tag{D.10}
$$

where

$$
V=-\frac{\mathrm{d}\ln p}{\mathrm{d}\ln r},\quad c_1=\frac{M}{M(r)}\left(\frac{r}{R}\right)^3,\quad \mathrm{d}\rho=\frac{\mathrm{d}\ln\rho}{\mathrm{d}\ln r},\quad \mathrm{d}f=\frac{\mathrm{d}\ln f}{\mathrm{d}\ln r},\quad \mathrm{d}^2f=\frac{r^2}{f}\frac{\mathrm{d}^2f}{\mathrm{d}r^2},\quad \mathrm{d}^3f=\frac{r^3}{f}\frac{\mathrm{d}^3f}{\mathrm{d}r^3},
\tag{D.11}
$$

and $\bar{\sigma}\equiv\sigma/(GM/R^3)^{1/2}$. The quantities $\mathbf{A}_0$, $\mathbf{A}_1$, $\mathbf{B}_0$, $\mathbf{B}_1$, $\tilde{\mathbf{C}}_0$, $\tilde{\mathbf{C}}_1$, $\tilde{\boldsymbol{\Lambda}}_0$, $\tilde{\boldsymbol{\Lambda}}_1$, $\mathbf{L}_0$, and $\mathbf{L}_1$ are matrices defined by

$$
\mathbf{A}_0=\mathbf{C}_0+\mathbf{Q}_0\boldsymbol{\Lambda}_1,\quad \mathbf{A}_1=\mathbf{C}_1+\mathbf{Q}_1\boldsymbol{\Lambda}_0,\quad \mathbf{B}_0=\mathbf{Q}_0+\frac{1}{2}\mathbf{C}_0,\quad \mathbf{B}_1=\mathbf{Q}_1+\frac{1}{2}\mathbf{C}_1,
$$

$$
\tilde{\mathbf{C}}_0=\mathbf{C}_0(\boldsymbol{\Lambda}_1-2\mathbf{I}),\quad \tilde{\mathbf{C}}_1=\mathbf{C}_1(\boldsymbol{\Lambda}_0-2\mathbf{I}),\quad \tilde{\boldsymbol{\Lambda}}_0=\boldsymbol{\Lambda}_0-2\mathbf{I},\quad \tilde{\boldsymbol{\Lambda}}_1=\boldsymbol{\Lambda}_1-2\mathbf{I},
$$

$$
\mathbf{L}_0=\mathbf{I}-m^2\mathbf{A}_0^{-1}\mathbf{A}_1^{-1},\quad \mathbf{L}_1=\mathbf{I}-m^2\mathbf{A}_1^{-1}\mathbf{A}_0^{-1}.
\tag{D.12}
$$

Matrices $\mathbf{Q}_0$, $\mathbf{Q}_1$, $\mathbf{C}_0$, $\mathbf{C}_1$, $\boldsymbol{\Lambda}_0$, and $\boldsymbol{\Lambda}_1$ are defined as follows: for even modes,

$$
(\mathbf{Q}_0)_{jj}=J^m_{l_j+1},\quad (\mathbf{Q}_0)_{j+1,j}=J^m_{l_j+2},\quad (\mathbf{Q}_1)_{jj}=J^m_{l_j+1},\quad (\mathbf{Q}_1)_{j,j+1}=J^m_{l_j+2},
$$

$$
(\mathbf{C}_0)_{jj}=-(l_j+2)J^m_{l_j+1},\quad (\mathbf{C}_0)_{j+1,j}=(l_j+1)J^m_{l_j+2},
$$

$$
(\mathbf{C}_1)_{jj}=l_jJ^m_{l_j+1},\quad (\mathbf{C}_1)_{j,j+1}=-(l_j+3)J^m_{l_j+2},
$$

$$
(\boldsymbol{\Lambda}_0)_{jj}=l_j(l_j+1),\quad (\boldsymbol{\Lambda}_1)_{jj}=(l_j+1)(l_j+2),
\tag{D.13}
$$

where $l_j=|m|+2j-2$ for $j=1,2,3,....,j_{\max}$, and

$$
J^m_{l_j}=\left[\frac{(l_j+m)(l_j-m)}{(2l_j-1)(2l_j+1)}\right]^{1/2},
\tag{D.14}
$$

and for odd modes,

$$
(\mathbf{Q}_0)_{jj}=J^m_{l_j+1},\quad (\mathbf{Q}_0)_{j,j+1}=J^m_{l_j+2},\quad (\mathbf{Q}_1)_{jj}=J^m_{l_j+1},\quad (\mathbf{Q}_1)_{j+1,j}=J^m_{l_j+2},
$$

$$
(\mathbf{C}_0)_{jj}=l_jJ^m_{l_j+1},\quad (\mathbf{C}_0)_{j,j+1}=-(l_j+3)J^m_{l_j+2},
$$

$$
(\mathbf{C}_1)_{jj}=-(l_j+2)J^m_{l_j+1},\quad (\mathbf{C}_1)_{j+1,j}=(l_j+1)J^m_{l_j+2},
$$

$$(\boldsymbol{\Lambda}_0)_{jj} = (l_j+1)(l_j+2), \quad (\boldsymbol{\Lambda}_1)_{jj} = l_j(l_j+1), \tag{D.15}$$

where $l_j = |m| + 2j - 1$ for $j = 1, 2, 3, ..., j_{\max}$.

From above equations, we find non-axisymmetric oscillations of magnetized star having purely poloidal magnetic field reduce to the system of $6j_{\max}$ coupled linear ordinary differential equations. Here, we choose column vectors $\boldsymbol{S}$, $\boldsymbol{T}$, $\boldsymbol{b}^S$, $\boldsymbol{b}^H$, $\boldsymbol{b}^T$, and $r\mathrm{d}\boldsymbol{b}^H/\mathrm{d}r$ as dependent variables. If we define dimensionless vector variables as follows:

$$\boldsymbol{y}_1 = \boldsymbol{S}, \quad \boldsymbol{y}_2 = \boldsymbol{T}, \quad \boldsymbol{y}_3 = \boldsymbol{h}^S, \quad \boldsymbol{y}_4 = \boldsymbol{h}^H, \quad \boldsymbol{y}_5 = \boldsymbol{h}^T, \quad \boldsymbol{y}_6 = r\frac{\mathrm{d}}{\mathrm{d}r}\boldsymbol{h}^H, \tag{D.16}$$

where $\boldsymbol{h}^i \equiv [R/f(0)]\boldsymbol{b}^i$ $(i = S, H, T)$, the master equations are formaly written by

$$\begin{aligned} r\frac{\mathrm{d}\boldsymbol{y}_1}{\mathrm{d}r} &= \boldsymbol{\mathcal{F}}_{11}\boldsymbol{y}_1 + \boldsymbol{\Lambda}_0\boldsymbol{H} - \frac{V}{\Gamma_1}\delta\boldsymbol{U} \\ &= (\boldsymbol{\mathcal{F}}_{11} - \boldsymbol{\mathcal{E}}_{11} + \boldsymbol{\Lambda}_0\boldsymbol{\mathcal{E}}_{21})\boldsymbol{y}_1 + (-\boldsymbol{\mathcal{E}}_{12} + \boldsymbol{\Lambda}_0\boldsymbol{\mathcal{E}}_{22})\boldsymbol{y}_2 + (-\boldsymbol{\mathcal{E}}_{13} + \boldsymbol{\Lambda}_0\boldsymbol{\mathcal{E}}_{23})\boldsymbol{y}_3 \\ &\quad -\boldsymbol{\mathcal{E}}_{14}\boldsymbol{y}_4 - \boldsymbol{\mathcal{E}}_{15}\boldsymbol{y}_5 - \boldsymbol{\mathcal{E}}_{16}\boldsymbol{y}_6, \end{aligned} \tag{D.17}$$

$$\begin{aligned} r\frac{\mathrm{d}\boldsymbol{y}_2}{\mathrm{d}r} &= \boldsymbol{\mathcal{F}}_{21}\boldsymbol{y}_1 + \boldsymbol{\mathcal{F}}_{22}\boldsymbol{y}_2 + \boldsymbol{\mathcal{F}}_{24}\boldsymbol{y}_4 + \boldsymbol{\mathcal{F}}_{25}\boldsymbol{y}_5 + \boldsymbol{\mathcal{G}}_{21}\frac{V}{\Gamma_1}\delta\boldsymbol{U} + \boldsymbol{\mathcal{G}}_{22}\boldsymbol{H} \\ &= (\boldsymbol{\mathcal{F}}_{21} + \boldsymbol{\mathcal{G}}_{21}\boldsymbol{\mathcal{E}}_{11} + \boldsymbol{\mathcal{G}}_{22}\boldsymbol{\mathcal{E}}_{21})\boldsymbol{y}_1 + (\boldsymbol{\mathcal{F}}_{22} + \boldsymbol{\mathcal{G}}_{21}\boldsymbol{\mathcal{E}}_{12} + \boldsymbol{\mathcal{G}}_{22}\boldsymbol{\mathcal{E}}_{22})\boldsymbol{y}_2 \\ &\quad +(\boldsymbol{\mathcal{G}}_{21}\boldsymbol{\mathcal{E}}_{13} + \boldsymbol{\mathcal{G}}_{22}\boldsymbol{\mathcal{E}}_{23})\boldsymbol{y}_3 + (\boldsymbol{\mathcal{F}}_{24} + \boldsymbol{\mathcal{G}}_{21}\boldsymbol{\mathcal{E}}_{14})\boldsymbol{y}_4 + (\boldsymbol{\mathcal{F}}_{25} + \boldsymbol{\mathcal{G}}_{21}\boldsymbol{\mathcal{E}}_{15})\boldsymbol{y}_5 \\ &\quad +\boldsymbol{\mathcal{G}}_{21}\boldsymbol{\mathcal{E}}_{16}\boldsymbol{y}_6, \end{aligned} \tag{D.18}$$

$$r\frac{\mathrm{d}\boldsymbol{y}_3}{\mathrm{d}r} = -3\boldsymbol{y}_3 + \boldsymbol{\Lambda}_1\boldsymbol{y}_4, \tag{D.19}$$

$$r\frac{\mathrm{d}\boldsymbol{y}_4}{\mathrm{d}r} = \boldsymbol{y}_6, \tag{D.20}$$

$$r\frac{\mathrm{d}\boldsymbol{y}_5}{\mathrm{d}r} = \boldsymbol{\mathcal{F}}_{52}\boldsymbol{y}_2 + \boldsymbol{\mathcal{F}}_{53}\boldsymbol{y}_3 + \boldsymbol{\mathcal{F}}_{54}\boldsymbol{y}_4 + \boldsymbol{\mathcal{F}}_{55}\boldsymbol{y}_5 + \boldsymbol{\mathcal{F}}_{56}\boldsymbol{y}_6, \tag{D.21}$$

$$\begin{aligned} r\frac{\mathrm{d}\boldsymbol{y}_6}{\mathrm{d}r} &= \boldsymbol{\mathcal{F}}_{61}\boldsymbol{y}_1 + \boldsymbol{\mathcal{F}}_{62}\boldsymbol{y}_2 + \boldsymbol{\mathcal{F}}_{63}\boldsymbol{y}_3 + \boldsymbol{\mathcal{F}}_{64}\boldsymbol{y}_4 + \boldsymbol{\mathcal{F}}_{65}\boldsymbol{y}_5 + \boldsymbol{\mathcal{F}}_{66}\boldsymbol{y}_6 \\ &\quad +\boldsymbol{\mathcal{G}}_{62}\boldsymbol{H} + \boldsymbol{\mathcal{G}}_{63}r\frac{\mathrm{d}\boldsymbol{H}}{\mathrm{d}r} + \boldsymbol{\mathcal{G}}_{64}r\frac{\mathrm{d}\boldsymbol{y}_2}{\mathrm{d}r} + \boldsymbol{\mathcal{G}}_{65}r\frac{\mathrm{d}\boldsymbol{y}_5}{\mathrm{d}r} \\ &= [\boldsymbol{\mathcal{F}}_{61} + \boldsymbol{\mathcal{G}}_{62}\boldsymbol{\mathcal{E}}_{21} + \boldsymbol{\mathcal{G}}_{63}(\boldsymbol{\mathcal{E}}_{31} + \boldsymbol{\mathcal{E}}_{37}\boldsymbol{\mathcal{E}}_{21} + \boldsymbol{\mathcal{E}}_{38}\boldsymbol{\mathcal{E}}_{11}) + \boldsymbol{\mathcal{G}}_{64}(\boldsymbol{\mathcal{F}}_{21} + \boldsymbol{\mathcal{G}}_{21}\boldsymbol{\mathcal{E}}_{11} + \boldsymbol{\mathcal{G}}_{22}\boldsymbol{\mathcal{E}}_{21})]\,\boldsymbol{y}_1 \\ &\quad + [\boldsymbol{\mathcal{F}}_{62} + \boldsymbol{\mathcal{G}}_{62}\boldsymbol{\mathcal{E}}_{22} + \boldsymbol{\mathcal{G}}_{63}(\boldsymbol{\mathcal{E}}_{32} + \boldsymbol{\mathcal{E}}_{37}\boldsymbol{\mathcal{E}}_{22} + \boldsymbol{\mathcal{E}}_{38}\boldsymbol{\mathcal{E}}_{12}) + \boldsymbol{\mathcal{G}}_{64}(\boldsymbol{\mathcal{F}}_{22} + \boldsymbol{\mathcal{G}}_{21}\boldsymbol{\mathcal{E}}_{12} + \boldsymbol{\mathcal{G}}_{22}\boldsymbol{\mathcal{E}}_{22}) + \boldsymbol{\mathcal{G}}_{65}\boldsymbol{\mathcal{F}}_{52}]\,\boldsymbol{y}_2 \\ &\quad + [\boldsymbol{\mathcal{F}}_{63} + \boldsymbol{\mathcal{G}}_{62}\boldsymbol{\mathcal{E}}_{23} + \boldsymbol{\mathcal{G}}_{63}(\boldsymbol{\mathcal{E}}_{37}\boldsymbol{\mathcal{E}}_{23} + \boldsymbol{\mathcal{E}}_{38}\boldsymbol{\mathcal{E}}_{13}) + \boldsymbol{\mathcal{G}}_{64}(\boldsymbol{\mathcal{G}}_{21}\boldsymbol{\mathcal{E}}_{13} + \boldsymbol{\mathcal{G}}_{22}\boldsymbol{\mathcal{E}}_{23}) + \boldsymbol{\mathcal{G}}_{65}\boldsymbol{\mathcal{F}}_{53}]\,\boldsymbol{y}_3 \\ &\quad + [\boldsymbol{\mathcal{F}}_{64} + \boldsymbol{\mathcal{G}}_{63}(\boldsymbol{\mathcal{E}}_{34} + \boldsymbol{\mathcal{E}}_{38}\boldsymbol{\mathcal{E}}_{14}) + \boldsymbol{\mathcal{G}}_{64}(\boldsymbol{\mathcal{F}}_{24} + \boldsymbol{\mathcal{G}}_{21}\boldsymbol{\mathcal{E}}_{14}) + \boldsymbol{\mathcal{G}}_{65}\boldsymbol{\mathcal{F}}_{54}]\,\boldsymbol{y}_4 \\ &\quad + [\boldsymbol{\mathcal{F}}_{65} + \boldsymbol{\mathcal{G}}_{63}(\boldsymbol{\mathcal{E}}_{35} + \boldsymbol{\mathcal{E}}_{38}\boldsymbol{\mathcal{E}}_{15}) + \boldsymbol{\mathcal{G}}_{64}(\boldsymbol{\mathcal{F}}_{25} + \boldsymbol{\mathcal{G}}_{21}\boldsymbol{\mathcal{E}}_{15}) + \boldsymbol{\mathcal{G}}_{65}\boldsymbol{\mathcal{F}}_{55}]\,\boldsymbol{y}_5 \\ &\quad + (\boldsymbol{\mathcal{F}}_{66} + \boldsymbol{\mathcal{G}}_{63}\boldsymbol{\mathcal{E}}_{38}\boldsymbol{\mathcal{E}}_{16} + \boldsymbol{\mathcal{G}}_{64}\boldsymbol{\mathcal{G}}_{21}\boldsymbol{\mathcal{E}}_{16} + \boldsymbol{\mathcal{G}}_{65}\boldsymbol{\mathcal{F}}_{56})\,\boldsymbol{y}_6, \end{aligned} \tag{D.22}$$

and algebraic relations are given by

$$\frac{V}{\Gamma_1}\delta\boldsymbol{U} = \boldsymbol{\mathcal{E}}_{11}\boldsymbol{y}_1 + \boldsymbol{\mathcal{E}}_{12}\boldsymbol{y}_2 + \boldsymbol{\mathcal{E}}_{13}\boldsymbol{y}_3 + \boldsymbol{\mathcal{E}}_{14}\boldsymbol{y}_4 + \boldsymbol{\mathcal{E}}_{15}\boldsymbol{y}_5 + \boldsymbol{\mathcal{E}}_{16}\boldsymbol{y}_6, \tag{D.23}$$

$$\boldsymbol{H} = \boldsymbol{\mathcal{E}}_{21}\boldsymbol{y}_1 + \boldsymbol{\mathcal{E}}_{22}\boldsymbol{y}_2 + \boldsymbol{\mathcal{E}}_{23}\boldsymbol{y}_3, \tag{D.24}$$

$$\begin{aligned} r\frac{\mathrm{d}\boldsymbol{H}}{\mathrm{d}r} &= \boldsymbol{\mathcal{E}}_{31}\boldsymbol{y}_1 + \boldsymbol{\mathcal{E}}_{32}\boldsymbol{y}_2 + \boldsymbol{\mathcal{E}}_{34}\boldsymbol{y}_4 + \boldsymbol{\mathcal{E}}_{35}\boldsymbol{y}_5 + \boldsymbol{\mathcal{E}}_{37}\boldsymbol{H} + \boldsymbol{\mathcal{E}}_{38}\frac{V}{\Gamma_1}\delta\boldsymbol{U} \\ &= (\boldsymbol{\mathcal{E}}_{31} + \boldsymbol{\mathcal{E}}_{37}\boldsymbol{\mathcal{E}}_{21} + \boldsymbol{\mathcal{E}}_{38}\boldsymbol{\mathcal{E}}_{11})\boldsymbol{y}_1 + (\boldsymbol{\mathcal{E}}_{32} + \boldsymbol{\mathcal{E}}_{37}\boldsymbol{\mathcal{E}}_{22} + \boldsymbol{\mathcal{E}}_{38}\boldsymbol{\mathcal{E}}_{12})\boldsymbol{y}_2 \\ &\quad +(\boldsymbol{\mathcal{E}}_{37}\boldsymbol{\mathcal{E}}_{23} + \boldsymbol{\mathcal{E}}_{38}\boldsymbol{\mathcal{E}}_{13})\boldsymbol{y}_3 + (\boldsymbol{\mathcal{E}}_{34} + \boldsymbol{\mathcal{E}}_{38}\boldsymbol{\mathcal{E}}_{14})\boldsymbol{y}_4 \\ &\quad +(\boldsymbol{\mathcal{E}}_{35} + \boldsymbol{\mathcal{E}}_{38}\boldsymbol{\mathcal{E}}_{15})\boldsymbol{y}_5 + \boldsymbol{\mathcal{E}}_{38}\boldsymbol{\mathcal{E}}_{16}\boldsymbol{y}_6. \end{aligned} \tag{D.25}$$

The coefficient matrices used in equations (D.17)-(D.25) are defined by

$$\boldsymbol{\mathcal{E}}_{11} = V_G c_1 \bar{\sigma}^2 \left(\mathrm{d}f + 2\right) \boldsymbol{\mathsf{A}}_1^{-1}\boldsymbol{\mathsf{B}}_1, \quad \boldsymbol{\mathcal{E}}_{12} = -mV_G c_1 \bar{\sigma}^2 \left(\boldsymbol{\mathsf{A}}_1^{-1} + \boldsymbol{\mathsf{\Lambda}}_0^{-1}\boldsymbol{\mathsf{A}}_1^{-1}\boldsymbol{\mathsf{\Lambda}}_1\right),$$

$$\boldsymbol{\mathcal{E}}_{13} = \frac{x}{2\hat{f}} V_G c_1 \bar{\sigma}^2 \boldsymbol{\mathsf{A}}_1^{-1} + \frac{\hat{f}}{2\hat{\rho}x} V_G c_1 \bar{\omega}_A^2 \Big[\left(\mathrm{d}^2 f + 4\mathrm{d}f\right) \boldsymbol{\mathsf{\Lambda}}_0^{-1}\boldsymbol{\mathsf{B}}_0 - \boldsymbol{\mathsf{\Lambda}}_0^{-1}\boldsymbol{\mathsf{A}}_0 + \frac{1}{2}m^2 \left(\mathrm{d}^2 f + 4\mathrm{d}f + 2\right) \boldsymbol{\mathsf{\Lambda}}_0^{-1}\boldsymbol{\mathsf{A}}_1^{-1} \Big],$$

$$\boldsymbol{\mathcal{E}}_{14} = \frac{\hat{f}}{\hat{\rho}x} V_G c_1 \bar{\omega}_A^2 \left(\boldsymbol{\mathsf{\Lambda}}_0^{-1}\boldsymbol{\mathsf{A}}_0 - m^2 \boldsymbol{\mathsf{\Lambda}}_0^{-1}\boldsymbol{\mathsf{A}}_1^{-1}\right),$$

$$\boldsymbol{\mathcal{E}}_{15} = \frac{\hat{f}}{2\hat{\rho}x} V_G c_1 \bar{\omega}_A^2 m \left[\frac{1}{2}\left(\mathrm{d}f + 2\right)\boldsymbol{\mathsf{I}} + 2\boldsymbol{\mathsf{\Lambda}}_0^{-1} + \mathrm{d}f\boldsymbol{\mathsf{\Lambda}}_0^{-1}\boldsymbol{\mathsf{A}}_1^{-1}\boldsymbol{\mathsf{B}}_1\boldsymbol{\mathsf{\Lambda}}_0 + \boldsymbol{\mathsf{\Lambda}}_0^{-1}\boldsymbol{\mathsf{A}}_1^{-1}\tilde{\boldsymbol{\mathsf{C}}}_1\right],$$

$$\boldsymbol{\mathcal{E}}_{16} = \frac{\hat{f}}{2\hat{\rho}x} V_G c_1 \bar{\omega}_A^2 \boldsymbol{\mathsf{\Lambda}}_0^{-1}\boldsymbol{\mathsf{A}}_0\boldsymbol{\mathsf{L}}_0,$$

$$\boldsymbol{\mathcal{E}}_{21} = \left(\mathrm{d}f + 2\right)\boldsymbol{\mathsf{A}}_1^{-1}\boldsymbol{\mathsf{B}}_1, \quad \boldsymbol{\mathcal{E}}_{22} = -m\boldsymbol{\mathsf{A}}_1^{-1}, \quad \boldsymbol{\mathcal{E}}_{23} = \frac{x}{2\hat{f}}\boldsymbol{\mathsf{A}}_1^{-1},$$

$$\boldsymbol{\mathcal{E}}_{31} = \left[\mathrm{d}^2 f + \left(2 + V_G\right)\mathrm{d}f - 2\left(1 - V_G\right)\right] \boldsymbol{\mathsf{L}}_1^{-1} \left(\boldsymbol{\mathsf{A}}_1^{-1}\boldsymbol{\mathsf{B}}_1 + \frac{1}{2}m^2 \boldsymbol{\mathsf{A}}_1^{-1}\boldsymbol{\mathsf{A}}_0^{-1}\right),$$

$$\boldsymbol{\mathcal{E}}_{32} = -m\left(\mathrm{d}f + 2\right)\boldsymbol{\mathsf{L}}_1^{-1} \left(\boldsymbol{\mathsf{A}}_1^{-1} + \frac{1}{2}\boldsymbol{\mathsf{A}}_1^{-1}\boldsymbol{\mathsf{A}}_0^{-1}\tilde{\boldsymbol{\mathsf{C}}}_0\right), \quad \boldsymbol{\mathcal{E}}_{34} = \frac{x}{2\hat{f}}\boldsymbol{\mathsf{L}}_1^{-1}\boldsymbol{\mathsf{A}}_1^{-1}\boldsymbol{\mathsf{\Lambda}}_1,$$

$$\boldsymbol{\mathcal{E}}_{35} = -\frac{x}{2\hat{f}} m \boldsymbol{\mathsf{L}}_1^{-1}\boldsymbol{\mathsf{A}}_1^{-1}\boldsymbol{\mathsf{A}}_0^{-1}\boldsymbol{\mathsf{\Lambda}}_0, \quad \boldsymbol{\mathcal{E}}_{37} = \left(\mathrm{d}f + 2\right)\boldsymbol{\mathsf{L}}_1^{-1} \left(m^2 \boldsymbol{\mathsf{A}}_1^{-1}\boldsymbol{\mathsf{A}}_0^{-1} + \frac{1}{2}\boldsymbol{\mathsf{A}}_1^{-1}\tilde{\boldsymbol{\mathsf{C}}}_1\right),$$

$$\boldsymbol{\mathcal{E}}_{38} = -\left(\mathrm{d}f + 2\right)\boldsymbol{\mathsf{L}}_1^{-1} \left(\boldsymbol{\mathsf{A}}_1^{-1}\boldsymbol{\mathsf{B}}_1 + \frac{1}{2}m^2 \boldsymbol{\mathsf{A}}_1^{-1}\boldsymbol{\mathsf{A}}_0^{-1}\right), \tag{D.26}$$

$$\boldsymbol{\mathcal{F}}_{11} = \left(V_G - 3\right)\boldsymbol{\mathsf{I}},$$

$$\boldsymbol{\mathcal{F}}_{21} = -m\left[\mathrm{d}^2 f + \left(2 + V_G\right)\mathrm{d}f - 2\left(1 - V_G\right)\right] \boldsymbol{\mathsf{L}}_0^{-1} \left(\boldsymbol{\mathsf{A}}_0^{-1}\boldsymbol{\mathsf{A}}_1^{-1}\boldsymbol{\mathsf{B}}_1 + \frac{1}{2}\boldsymbol{\mathsf{A}}_0^{-1}\right),$$

$$\boldsymbol{\mathcal{F}}_{22} = \left(\mathrm{d}f + 2\right)\boldsymbol{\mathsf{L}}_0^{-1} \left(m^2 \boldsymbol{\mathsf{A}}_0^{-1}\boldsymbol{\mathsf{A}}_1^{-1} + \frac{1}{2}\boldsymbol{\mathsf{A}}_0^{-1}\tilde{\boldsymbol{\mathsf{C}}}_0\right), \quad \boldsymbol{\mathcal{F}}_{24} = -\frac{x}{2\hat{f}} m \boldsymbol{\mathsf{L}}_0^{-1}\boldsymbol{\mathsf{A}}_0^{-1}\boldsymbol{\mathsf{A}}_1^{-1}\boldsymbol{\mathsf{\Lambda}}_1,$$

$$\boldsymbol{\mathcal{F}}_{25}=\frac{x}{2\hat{f}}\mathbf{L}_0^{-1}\mathbf{A}_0^{-1}\boldsymbol{\Lambda}_0,\quad \boldsymbol{\mathcal{F}}_{52}=-2\frac{\hat{\rho}x}{\hat{f}}\frac{\bar{\sigma}^2}{\bar{\omega}_A^2}\mathbf{A}_1^{-1}\boldsymbol{\Lambda}_1,\quad \boldsymbol{\mathcal{F}}_{53}=\frac{1}{2}\left(\mathrm{d}^2f+4\mathrm{d}f+2\right)m\mathbf{A}_1^{-1},$$

$$\boldsymbol{\mathcal{F}}_{54}=-2m\mathbf{A}_1^{-1},\quad \boldsymbol{\mathcal{F}}_{55}=\mathbf{A}_1^{-1}\left(\mathrm{d}f\mathbf{B}_1\boldsymbol{\Lambda}_0+\tilde{\mathbf{C}}_1\right),\quad \boldsymbol{\mathcal{F}}_{56}=-m\mathbf{A}_1^{-1},$$

$$\boldsymbol{\mathcal{F}}_{61}=2\frac{\hat{\rho}x}{\hat{f}}\frac{1}{c_1\bar{\omega}_A^2}\left(c_1\bar{\sigma}^2+rA\right)\mathbf{L}_0^{-1}\mathbf{A}_0^{-1}\boldsymbol{\Lambda}_0,\quad \boldsymbol{\mathcal{F}}_{62}=4\frac{\hat{\rho}x}{\hat{f}}\frac{\bar{\sigma}^2}{\bar{\omega}_A^2}m\mathbf{L}_0^{-1}\mathbf{A}_0^{-1}\mathbf{A}_1^{-1}\boldsymbol{\Lambda}_1,$$

$$\begin{aligned}\boldsymbol{\mathcal{F}}_{63} &= \mathbf{L}_0^{-1}\Big\{-\frac{1}{2}\left(\mathrm{d}f+2\right)\mathbf{A}_0^{-1}\tilde{\mathbf{C}}_0-\left(\mathrm{d}\rho+4-rA\right)\mathbf{I}\\ &\quad+\left[-\mathrm{d}^3f+\mathrm{d}^2f\left(\mathrm{d}\rho-4-rA\right)+4\mathrm{d}f\left(\mathrm{d}\rho+1-rA\right)\right]\mathbf{A}_0^{-1}\mathbf{B}_0\\ &\quad-\frac{1}{2}\left[\mathrm{d}^3f-\mathrm{d}^2f\left(\mathrm{d}\rho-4\right)-2\mathrm{d}f\left(1+2\mathrm{d}\rho\right)-2\left(2+\mathrm{d}\rho\right)\right]m^2\mathbf{A}_0^{-1}\mathbf{A}_1^{-1}\Big\},\end{aligned}$$

$$\begin{aligned}\boldsymbol{\mathcal{F}}_{64} &= \mathbf{L}_0^{-1}\Big[\left(\mathrm{d}f+1\right)\mathbf{A}_0^{-1}\tilde{\mathbf{C}}_0+\boldsymbol{\Lambda}_1+2\mathbf{A}_0^{-1}\mathbf{B}_0\boldsymbol{\Lambda}_1+2\left(\mathrm{d}\rho-rA\right)\mathbf{I}\\ &\quad-\frac{1}{2}\left(\mathrm{d}^2f+4\mathrm{d}f+2\right)m^2\mathbf{A}_0^{-1}\mathbf{A}_1^{-1}\tilde{\boldsymbol{\Lambda}}_1-\left(\mathrm{d}^2f+2\mathrm{d}f+2\mathrm{d}\rho\right)m^2\mathbf{A}_0^{-1}\mathbf{A}_1^{-1}\Big],\end{aligned}$$

$$\begin{aligned}\boldsymbol{\mathcal{F}}_{65} &= \mathbf{L}_0^{-1}\Big\{-m\Big\{2\left(\mathrm{d}f-\mathrm{d}\rho+1+rA\right)\mathbf{A}_0^{-1}\\ &\quad+\frac{1}{2}\left[-\mathrm{d}f\left(\mathrm{d}\rho+2\right)+\left(\mathrm{d}f+2\right)rA-2\left(\mathrm{d}\rho+1\right)\right]\mathbf{A}_0^{-1}\boldsymbol{\Lambda}_0\Big\}\\ &\quad-m\left[\left(\mathrm{d}^2f-\mathrm{d}\rho\mathrm{d}f+2\mathrm{d}f\right)\mathbf{A}_0^{-1}\mathbf{A}_1^{-1}\mathbf{B}_1\boldsymbol{\Lambda}_0+\left(\mathrm{d}f-\mathrm{d}\rho+1\right)\mathbf{A}_0^{-1}\mathbf{A}_1^{-1}\tilde{\mathbf{C}}_1\right]\Big\},\end{aligned}$$

$$\boldsymbol{\mathcal{F}}_{66}=\mathbf{L}_0^{-1}\left[\frac{1}{2}\left(\mathrm{d}f+2\right)\mathbf{A}_0^{-1}\tilde{\mathbf{C}}_0+\left(\mathrm{d}\rho-1-rA\right)\mathbf{I}+\left(\mathrm{d}f-\mathrm{d}\rho+3\right)m^2\mathbf{A}_0^{-1}\mathbf{A}_1^{-1}\right],\tag{D.27}$$

$$\boldsymbol{\mathcal{G}}_{21}=m\left(\mathrm{d}f+2\right)\mathbf{L}_0^{-1}\left(\mathbf{A}_0^{-1}\mathbf{A}_1^{-1}\mathbf{B}_1+\frac{1}{2}\mathbf{A}_0^{-1}\right),$$

$$\boldsymbol{\mathcal{G}}_{22}=-m\left(\mathrm{d}f+2\right)\mathbf{L}_0^{-1}\left(\mathbf{A}_0^{-1}+\frac{1}{2}\mathbf{A}_0^{-1}\mathbf{A}_1^{-1}\tilde{\mathbf{C}}_1\right),$$

$$\boldsymbol{\mathcal{G}}_{62}=-2\frac{\hat{\rho}x}{\hat{f}}\frac{\bar{\sigma}^2}{\bar{\omega}_A^2}\left(2+rA\right)\mathbf{L}_0^{-1}\mathbf{A}_0^{-1}\boldsymbol{\Lambda}_0,\quad \boldsymbol{\mathcal{G}}_{63}=-2\frac{\hat{\rho}x}{\hat{f}}\frac{\bar{\sigma}^2}{\bar{\omega}_A^2}\mathbf{L}_0^{-1}\mathbf{A}_0^{-1}\boldsymbol{\Lambda}_0,$$

$$\boldsymbol{\mathcal{G}}_{64}=2\frac{\hat{\rho}x}{\hat{f}}\frac{\bar{\sigma}^2}{\bar{\omega}_A^2}m\mathbf{L}_0^{-1}\mathbf{A}_0^{-1}\mathbf{A}_1^{-1}\boldsymbol{\Lambda}_1,$$

$$\boldsymbol{\mathcal{G}}_{65}=-m\mathbf{L}_0^{-1}\left[\frac{1}{2}\left(\mathrm{d}f+2\right)\mathbf{A}_0^{-1}\mathbf{A}_1^{-1}\tilde{\mathbf{C}}_1+\left(\mathrm{d}f+2+rA\right)\mathbf{A}_0^{-1}\right],\tag{D.28}$$

where

$$V_G=\frac{V}{\Gamma_1},\quad x=\frac{r}{R},\quad \hat{f}=\frac{f(r)}{f(0)},\quad \hat{\rho}=\frac{\rho(r)}{\rho(0)},\quad \omega_A^2=\frac{f^2(0)}{\pi\rho(0)R^2},\quad \beta=\frac{f^2(0)}{4\pi p}.\tag{D.29}$$

Using equations (D.17)-(D.25), we can formaly summarize the master equations as follows:

$$r\frac{\mathrm{d}}{\mathrm{d}r}\begin{pmatrix}\boldsymbol{y}_1\\ \boldsymbol{y}_2\\ \boldsymbol{y}_3\\ \boldsymbol{y}_4\\ \boldsymbol{y}_5\\ \boldsymbol{y}_6\end{pmatrix} = \boldsymbol{\mathcal{M}}\begin{pmatrix}\boldsymbol{y}_1\\ \boldsymbol{y}_2\\ \boldsymbol{y}_3\\ \boldsymbol{y}_4\\ \boldsymbol{y}_5\\ \boldsymbol{y}_6\end{pmatrix}, \tag{D.30}$$

where $\boldsymbol{\mathcal{M}}$ is a coefficient matrix. We assume that there is no electric current, that is vacuum at outside of the star. Then, we can treat magnetic perturbations of exterior of the star as potential fields, which become regular at $r \to \infty$, and we can write

$$\delta\boldsymbol{B}^{\mathrm{ex}} = \nabla\left(\sum_{l=|m|}^{\infty} A_l r^{-l-1} Y_l^m\right), \tag{D.31}$$

where subscript 'ex' denotes the quantity of the exterior of the star. Assuming no surface current at the stellar surface, we find $[[\Delta\boldsymbol{B}]] = [[\delta\boldsymbol{B}]] = 0$, and from equation (D.31) we can derive

$$\boldsymbol{h}^S + \mathsf{L}^+\boldsymbol{h}^H = 0, \quad \boldsymbol{h}^T = 0, \quad \text{for } r = R \tag{D.32}$$

in assumption of $[[\boldsymbol{B}]] = 0$ at the stellar surface, where $(\mathsf{L}^+)_{ij} = (l'_j + 1)\delta_{ij}$ and $[[Q]] \equiv \lim_{\epsilon\to 0}[Q(R-\epsilon) - Q(R+\epsilon)]$ $(\epsilon > 0)$. ΔQ and δQ denote Langrangian and Eulerian perturbatoins of the quantity Q, respectively. In addition to above conditions, we generaly use outer boundary condition of $[[\Delta\{p + |\boldsymbol{B}|^2/(8\pi)\}]] = 0$ at the surface of the star. Then, using $[[\Delta\boldsymbol{B}]] = [[\delta\boldsymbol{B}]] = 0$ and $[[\boldsymbol{B}]] = 0$ at the surface of the star, above condition $[[\Delta\{p + |\boldsymbol{B}|^2/(8\pi)\}]] = 0$ reduces to $\Delta p = 0$. Using vector variables, this condition is rewritten by

$$\delta\boldsymbol{U} - \boldsymbol{y}_1 = 0. \tag{D.33}$$

The inner boundary conditions imposed at the center of the star are regularity conditions for the eigenfunctions $\boldsymbol{y}_1$ - $\boldsymbol{y}_6$ (see Appendix F). We use normalization condition as $T_{l'_1}(R) = 1$ at the stellar surface.

APPENDIX: E Relaxation method

For normal mode analyses, we need to solve oscillation equations expressed by coupled linear ordinary differential equations by boundary and eigen values problem for eigenfrequency σ. In order to solve this problem numerically, we usually carry out relaxation method. In this Appendix, we briefly explain algorithm of relaxaion method.

First of all, we define n-th order ordinary differential equation as follows:

$$\frac{\mathrm{d}^n f(x)}{\mathrm{d}x^n} = \Lambda f(x), \tag{E.1}$$

where Λ is a constant. This ordinary differential equation is rewrited as n coupled linear ordinary differential equations system, that is,

$$\frac{\mathrm{d}}{\mathrm{d}x}\boldsymbol{Y} = \mathsf{C}\boldsymbol{Y}, \tag{E.2}$$

where $\boldsymbol{Y} = (y_1, y_2, y_3, ...)^T$ (for example, $y_1 = f(x)$, $y_2 = \mathrm{d}f/\mathrm{d}x$, and $y_3 = \mathrm{d}^2f/\mathrm{d}x^2$,...), and $\mathbf{C}$ is coefficient matrix containing eigenvalue Λ. We assume integral range as $0 \leq x \leq 1$, and integrate from $x = 0$ to $x = 1$ under suitable boundary conditions.

We divide integral range by N, and define i-th quantities as x_i and $\mathbf{C}_i$ etc ($i = 0, 1, 2, 3, ..., N$). For above coupled ordinary differential equation we carry out integrable discretization as follows:

$$\frac{Y_j^{i+1} - Y_j^i}{x_{i+1} - x_i} = u\mathbf{C}_{i+1}Y_j^{i+1} + (1-u)\mathbf{C}_i Y_j^i, \tag{E.3}$$

where u is an arbitrary constant ($0 \leq u \leq 1$), and we assume $u = 0.5$. Then, above equation is written as

$$\begin{pmatrix} -1 - 0.5C_{11}^i \mathrm{d}x & -0.5C_{12}^i \mathrm{d}x & -0.5C_{13}^i \mathrm{d}x & \cdots \\ -0.5C_{21}^i \mathrm{d}x & -1 - 0.5C_{22}^i \mathrm{d}x & -0.5C_{23}^i \mathrm{d}x & \cdots \\ -0.5C_{31}^i \mathrm{d}x & -1 - 0.5C_{32}^i \mathrm{d}x & -1 - 0.5C_{33}^i \mathrm{d}x & \cdots \\ \vdots & \vdots & \vdots & \ddots \end{pmatrix} \begin{pmatrix} y_1^i \\ y_2^i \\ y_3^i \\ \vdots \end{pmatrix}$$

$$+ \begin{pmatrix} 1 - 0.5C_{11}^{i+1} \mathrm{d}x & -0.5C_{12}^{i+1} \mathrm{d}x & -0.5C_{13}^{i+1} \mathrm{d}x & \cdots \\ -0.5C_{21}^{i+1} \mathrm{d}x & 1 - 0.5C_{22}^{i+1} \mathrm{d}x & -0.5C_{23}^{i+1} \mathrm{d}x & \cdots \\ -0.5C_{31}^{i+1} \mathrm{d}x & -0.5C_{32}^{i+1} \mathrm{d}x & 1 - 0.5C_{33}^{i+1} \mathrm{d}x & \cdots \\ \vdots & \vdots & \vdots & \ddots \end{pmatrix} \begin{pmatrix} y_1^{i+1} \\ y_2^{i+1} \\ y_3^{i+1} \\ \vdots \end{pmatrix} = \begin{pmatrix} 0 \\ 0 \\ 0 \\ \vdots \end{pmatrix}, \tag{E.4}$$

where C_{ij} denotes the ij-components of coefficient matrix $\mathbf{C}$, and $\mathrm{d}x \equiv x_{i+1} - x_i$. We summarize equation (E.4) as following matrix form

$$\mathbf{T}_i \boldsymbol{Y}_i + \mathbf{S}_i \boldsymbol{Y}_{i+1} = \mathbf{0}. \tag{E.5}$$

We give boudary conditions at $x_0 (= 0)$ and $x_N (= 1)$ as following forms

$$\mathbf{L}_0 \boldsymbol{Y}_0 = \mathbf{0}, \quad \mathbf{L}_N \boldsymbol{Y}_N = \mathbf{0}, \tag{E.6}$$

and define normalization condition at x_N as

$$\mathbf{M}_N \boldsymbol{Y}_N = 1, \tag{E.7}$$

where $\mathbf{L}_i$ ($i = 0$ and N) and $\mathbf{M}_N$ are matrices containing boundary and normalization conditions. Using these relations, we obtain following matrix form

$$\begin{pmatrix} \mathbf{L}_0 & \mathbf{0} & \mathbf{0} & \mathbf{0} & \cdots & \mathbf{0} \\ \mathbf{T}_0 & \mathbf{S}_0 & \mathbf{0} & \mathbf{0} & \cdots & \mathbf{0} \\ \mathbf{0} & \mathbf{T}_1 & \mathbf{S}_1 & \mathbf{0} & \cdots & \mathbf{0} \\ \vdots & \vdots & & \ddots & & \vdots \\ & & & & \mathbf{T}_{N-1} & \mathbf{S}_{N-1} \\ \mathbf{0} & \cdots & & & \mathbf{0} & \mathbf{M}_N \end{pmatrix} \begin{pmatrix} \boldsymbol{Y}_0 \\ \boldsymbol{Y}_1 \\ \boldsymbol{Y}_2 \\ \vdots \\ \boldsymbol{Y}_{N-1} \\ \boldsymbol{Y}_N \end{pmatrix} = \begin{pmatrix} 0 \\ 0 \\ 0 \\ 0 \\ \vdots \\ 1 \end{pmatrix}. \tag{E.8}$$

Therefore, we can obtain eigenfunctions $\boldsymbol{Y}_i$ by calculating inverse matrix of left-hand side of equation (E.8).

In order to calculate inverse matrix, we carry out following manupulations. First, we define small size matrices given by

$$\mathbf{Q}_0 \equiv \begin{pmatrix} \mathbf{L}_0 \\ \mathbf{T}_0^U \end{pmatrix}, \quad \mathbf{Q}_i = \begin{pmatrix} \mathbf{S}_{i-1}^L \\ \mathbf{T}_i^U \end{pmatrix} \quad (1 \leq i \leq N-1), \quad \mathbf{Q}_N = \begin{pmatrix} \mathbf{S}_{N-1}^L \\ \mathbf{M}_N \end{pmatrix}, \tag{E.9}$$

$$\mathbf{P}_i = \begin{pmatrix} \mathbf{T}_{i-1}^{L} \\ \mathbf{0} \end{pmatrix} \quad (1 \leq i \leq N), \tag{E.10}$$

$$\mathbf{R}_i = \begin{pmatrix} \mathbf{0} \\ \mathbf{S}_i^{U} \end{pmatrix} \quad (0 \leq i \leq N-1), \tag{E.11}$$

where subscripts U and L mean upper and lower half of the matrix, respectively. Using these small matrices, we rewrite equation (E.8) as

$$\begin{pmatrix} \mathbf{Q}_0 & \mathbf{R}_0 & \mathbf{0} & \mathbf{0} & \mathbf{0} & \mathbf{0} & \cdots & \mathbf{0} \\ \mathbf{P}_1 & \mathbf{Q}_1 & \mathbf{R}_1 & \mathbf{0} & \mathbf{0} & \mathbf{0} & \cdots & \mathbf{0} \\ \mathbf{0} & \mathbf{P}_2 & \mathbf{Q}_2 & \mathbf{R}_2 & \mathbf{0} & \mathbf{0} & \cdots & \mathbf{0} \\ \mathbf{0} & \mathbf{0} & \mathbf{P}_3 & \mathbf{Q}_3 & \mathbf{R}_3 & \mathbf{0} & \cdots & \mathbf{0} \\ \vdots & & \ddots & & & & & \vdots \\ \vdots & & & \ddots & & & & \vdots \\ \mathbf{0} & & \cdots & & & \mathbf{P}_{N-1} & \mathbf{Q}_{N-1} & \mathbf{R}_{N-1} \\ \mathbf{0} & & \cdots & & & \mathbf{0} & \mathbf{P}_N & \mathbf{Q}_N \end{pmatrix} \begin{pmatrix} \boldsymbol{Y}_0 \\ \boldsymbol{Y}_1 \\ \boldsymbol{Y}_2 \\ \boldsymbol{Y}_3 \\ \vdots \\ \vdots \\ \boldsymbol{Y}_{N-1} \\ \boldsymbol{Y}_N \end{pmatrix} = \begin{pmatrix} \boldsymbol{d}_0 \\ \boldsymbol{d}_1 \\ \boldsymbol{d}_2 \\ \boldsymbol{d}_3 \\ \vdots \\ \vdots \\ \boldsymbol{d}_{N-1} \\ \boldsymbol{d}_N \end{pmatrix}, \tag{E.12}$$

where $\boldsymbol{d}_i = (0, 0, 0, ..., 0)^T$ $(0 \leq i \leq N-1)$ and $\boldsymbol{d}_N = (1, 0, 0, ..., 0)^T$. We calculate inverse matrix of left-hand side of equation (E.12) using recurrence formula method.

From equation (E.12), we obtain following recurrence formula

$$\mathbf{Q}_0 \boldsymbol{Y}_0 + \mathbf{R}_0 \boldsymbol{Y}_1 = \boldsymbol{d}_0, \tag{E.13}$$

$$\mathbf{P}_1 \boldsymbol{Y}_0 + \mathbf{Q}_1 \boldsymbol{Y}_1 + \mathbf{R}_1 \boldsymbol{Y}_2 = \boldsymbol{d}_1, \tag{E.14}$$

$$\vdots$$

$$\mathbf{P}_{N-1} \boldsymbol{Y}_{N-2} + \mathbf{Q}_{N-1} \boldsymbol{Y}_{N-1} + \mathbf{R}_{N-1} \boldsymbol{Y}_N = \boldsymbol{d}_{N-1}, \tag{E.15}$$

$$\mathbf{P}_N \boldsymbol{Y}_{N-1} + \mathbf{Q}_N \boldsymbol{Y}_N = \boldsymbol{d}_N. \tag{E.16}$$

Using equations (E.13) and (E.14), and eliminating $\boldsymbol{Y}_0$, we obtain

$$\left(\mathbf{Q}_1 - \mathbf{P}_1 \mathbf{Q}_0^{-1} \mathbf{R}_0\right) \boldsymbol{Y}_1 + \mathbf{R}_1 \boldsymbol{Y}_2 = \boldsymbol{d}_1 - \mathbf{P}_1 \mathbf{Q}_0^{-1} \boldsymbol{d}_0. \tag{E.17}$$

We define new matrix $\tilde{\mathbf{Q}}_1 \equiv \mathbf{Q}_1 - \mathbf{P}_1 \mathbf{Q}_0^{-1} \mathbf{R}_0$ and new vector $\tilde{\boldsymbol{d}}_1 \equiv \boldsymbol{d}_1 - \mathbf{P}_1 \mathbf{Q}_0^{-1} \boldsymbol{d}_0$. Then, equation (E.17) is rewritten by

$$\tilde{\mathbf{Q}}_1 \boldsymbol{Y}_1 + \mathbf{R}_1 \boldsymbol{Y}_2 = \tilde{\boldsymbol{d}}_1. \tag{E.18}$$

Therefore, we obtain

$$\tilde{\mathbf{Q}}_i \boldsymbol{Y}_i + \mathbf{R}_i \boldsymbol{Y}_{i+1} = \tilde{\boldsymbol{d}}_i \quad (0 \leq i \leq N-1). \tag{E.19}$$

Using equations (E.15) and (E.16), and eliminating $\boldsymbol{Y}_{N-1}$, we obtain

$$\boldsymbol{Y}_N = \tilde{\mathbf{Q}}_N^{-1} \tilde{\boldsymbol{d}}_N, \tag{E.20}$$

where

$$\tilde{\mathbf{Q}}_0 = \mathbf{Q}_0, \quad \tilde{\mathbf{Q}}_i = \mathbf{Q}_i - \mathbf{P}_i \tilde{\mathbf{Q}}_{i-1}^{-1} \mathbf{R}_{i-1} \quad (1 \leq i \leq N), \tag{E.21}$$

$$\tilde{\boldsymbol{d}}_0 = \boldsymbol{d}_0, \quad \tilde{\boldsymbol{d}}_i = \boldsymbol{d}_i - \mathbf{P}_i \tilde{\mathbf{Q}}_{i-1}^{-1} \tilde{\boldsymbol{d}}_{i-1} \quad (1 \leq i \leq N). \tag{E.22}$$

Using equations (E.19) and (E.20), we obtain $\boldsymbol{Y}_i$ $(0 \leq i \leq N-1)$

$$\boldsymbol{Y}_i = \tilde{\mathbf{Q}}_i^{-1} \tilde{\boldsymbol{d}}_i - \tilde{\mathbf{Q}}_i^{-1} \mathbf{R}_i \boldsymbol{Y}_{i+1} \quad (0 \leq i \leq N-1). \tag{E.23}$$

At this point, we obtain eigenfunctions $\boldsymbol{Y}_i$ $(0 \leq i \leq N)$, however, we do not use boundary condition $\mathbf{L}_N \boldsymbol{Y}_N = \mathbf{0}$ (we use normalization condition instead). Thus, eigenfunctions obtained up to this point is not necessarily satisfied with the boundary condition at x_N. In order to obtain eigensolution which is satisfied with boundary condition at x_N, we use constant Λ as a parameter. First, we define following function

$$D(\Lambda) = \boldsymbol{Y}_N(x = 1; \Lambda). \tag{E.24}$$

We need to look for Λ satisfying $D(\Lambda) = 0$. For equation (E.24), we assume $\Lambda = \Lambda_0 + \delta\Lambda$ and expand $D(\Lambda)$ up to order of $\delta\Lambda^1$, that is,

$$D(\Lambda_0 + \delta\Lambda) \approx D(\Lambda_0) + \left.\frac{\mathrm{d}D}{\mathrm{d}\Lambda}\right|_{\Lambda=\Lambda_0} \delta\Lambda = 0, \tag{E.25}$$

where Λ_0 is an initial guess value and $\delta\Lambda$ is small deviation from true value. From euqtion (E.25), we find

$$\delta\Lambda = -\left(\left.\frac{\mathrm{d}D}{\mathrm{d}\Lambda}\right|_{\Lambda=\Lambda_0}\right)^{-1} D(\Lambda_0). \tag{E.26}$$

In our numerical code, we carry out

$$\Lambda_0 + \delta\Lambda = \Lambda_0 - \left(\left.\frac{\mathrm{d}D}{\mathrm{d}\Lambda}\right|_{\Lambda=\Lambda_0}\right)^{-1} D(\Lambda_0) \to \Lambda_0 \tag{E.27}$$

and calculate $\delta\Lambda$ repeatedly until $|D(\Lambda_0 + \delta\Lambda)| < \epsilon$ for small parameter ϵ. Here, $\mathrm{d}D/\mathrm{d}\Lambda$ is estimated by

$$\left.\frac{\mathrm{d}D}{\mathrm{d}\Lambda}\right|_{\Lambda=\Lambda_0} = \frac{D(\Lambda_0 + \Delta) - D(\Lambda_0)}{\Delta}, \tag{E.28}$$

where Δ is a small parameter.

Finally, we can obtain eigenfunctions $\boldsymbol{Y}_i$ satisfying boundary conditions at x_0 and x_N and normalization condition, and corresponding eigenvalue Λ.

APPENDIX: F Inner mechanical boundary conditions

In this Appendix we briefly discuss inner boundary conditions imposed at center of the star. Now master equations of magnetized stars are summarized as

$$a\frac{\mathrm{d}}{\mathrm{d}a}\boldsymbol{Y} = \boldsymbol{\mathcal{F}}\boldsymbol{Y}$$

for purely toroidal magnetic field, and

$$r\frac{\mathrm{d}}{\mathrm{d}r}\boldsymbol{Y} = \boldsymbol{\mathcal{M}}\boldsymbol{Y} \tag{F.1}$$

for purely poloidal magnetic field.

To determine regularity conditions of eigenfunctions, we generally assume following form near the center of the star

$$\boldsymbol{Y} = r^{\gamma}\boldsymbol{Y}_0, \tag{F.2}$$

where γ is arbitrary constant, and $\boldsymbol{Y}_0$ is constant vector near the center of the star. For examples, substituting (F.2) into (F.1), we obtain

$$\boldsymbol{\mathcal{M}}\boldsymbol{Y}_0 = \gamma\boldsymbol{Y}_0. \tag{F.3}$$

This relation means γ is eigenvalue of matrix $\boldsymbol{\mathcal{M}}$, and $\boldsymbol{Y}_0$ is corresponding to eigen vector near the center of the star. Therefore, we need to solve following characteristic equation to determine γ and $\boldsymbol{Y}_0$

$$|\boldsymbol{\mathcal{M}} - \gamma\mathsf{I}| = 0. \tag{F.4}$$

Since all eigenvectors obtained from above relation become linear independent basis vetors, respectively, we can express eigen solutions near the center of the star as follows:

$$\boldsymbol{Y} = \sum_{i=1}^{N} a_i r^{\gamma_i}\boldsymbol{Y}_0^i, \tag{F.5}$$

where γ_i and $\boldsymbol{Y}_0^i$ denote i-th eigenvalue and eigenvector ($i = 1, 2, 3, ..., N$), and a_i is constant. We note that $N = 2j_{\max}$ for purely toroidal magentic field, and $N = 6j_{\max}$ for purely poloidal magnetic field. For regularity conditions, we select M positive eigenvalues ($\gamma^i \geq 0$), and in general, we can obtain $M = N/2$ positive eigenvalues. Now we classified expression (F.5) into explessions of upper half and lower half as

$$\boldsymbol{Y}^U = \sum_{i=1}^{M} a_i r^{\gamma_i}\boldsymbol{Y}_{0i}^U \equiv \mathsf{U}\boldsymbol{a}, \tag{F.6}$$

$$\boldsymbol{Y}^L = \sum_{i=1}^{M} a_i r^{\gamma_i}\boldsymbol{Y}_{0i}^L \equiv \mathsf{L}\boldsymbol{a}, \tag{F.7}$$

where $\mathsf{U} = (\boldsymbol{Y}_{01}^U, \boldsymbol{Y}_{02}^U, ..., \boldsymbol{Y}_{0M}^U)$ and $\mathsf{L} = (\boldsymbol{Y}_{01}^L, \boldsymbol{Y}_{02}^L, ..., \boldsymbol{Y}_{0M}^L)$ are matrices composed by upper half and lower half of the eigen vectors corresponding eigenvalues γ_i, and $\boldsymbol{a} = (a_1 r^{\gamma_1}, a_2 r^{\gamma_2}, ..., a_M r^{\gamma_M})^T$. Subscripts U and L denote upper half and lower half of eigenfunctions $\boldsymbol{Y}$, respectively, that is, $\boldsymbol{Y}^U = (\boldsymbol{y}_1)^T$ and $\boldsymbol{Y}^L = (\boldsymbol{y}_2)^T$ for purely toroidal magnetic field, and while $\boldsymbol{Y}^U = (\boldsymbol{y}_1, \boldsymbol{y}_2, \boldsymbol{y}_3)^T$ and $\boldsymbol{Y}^L = (\boldsymbol{y}_4, \boldsymbol{y}_5, \boldsymbol{y}_6)^T$ for purely poloidal magnetic field. Thus, we obtain following relation as inner boundary conditions

$$\mathsf{U}^{-1}\boldsymbol{Y}^U - \mathsf{L}^{-1}\boldsymbol{Y}^L = 0. \tag{F.8}$$